PAUL SCHERRER INSTITUT

10 April, 2018

Two-photon exchange corrections to elastic lepton-proton scattering and atomic spectroscopy

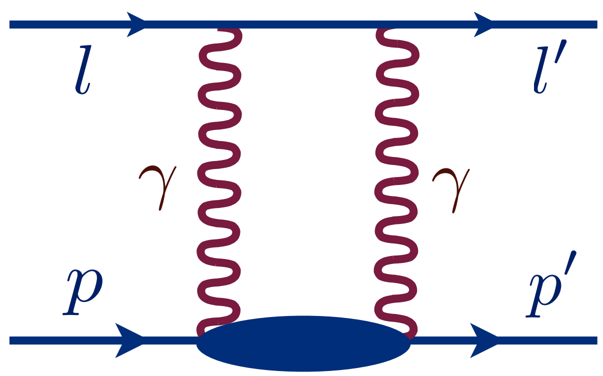

Oleksandr Tomalak

Johannes Gutenberg University,

Mainz, Germany

Muon discrepancies: new physics?

$b \to s\mu^+\mu^-$ ~3-5σ theory vs exp.

$B \to \mu^+\mu^-$ promising channel

Muon discrepancies: new physics?

$b \to s\mu^+\mu^-$

~3-5σ
theory vs exp.

$B \to \mu^+\mu^-$ promising channel

anomalous magnetic moment

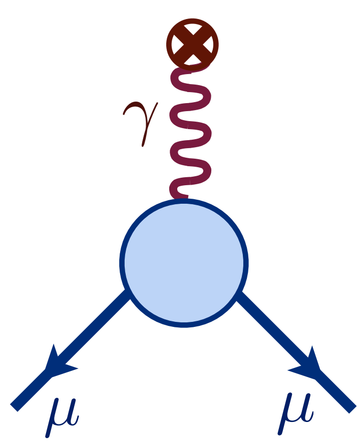

3.6 σ
theory vs exp.

μH Lamb shift

proton size discrepancy

7σ
electron vs muon

hadronic uncertainty is dominant in theory

Muon discrepancies: new physics?

$b \to s\mu^+\mu^-$ ~3-5σ theory vs exp.

$B \to \mu^+\mu^-$ promising channel

anomalous magnetic moment

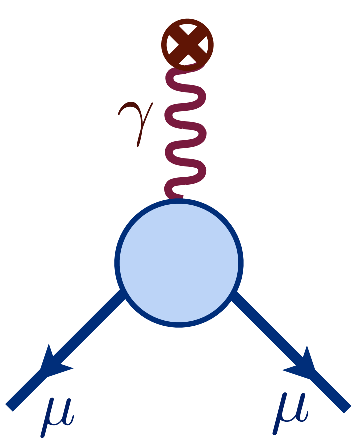

3.6 σ
theory vs exp.

μH Lamb shift

proton size discrepancy

7σ
electron vs muon

hadronic uncertainty is dominant in theory

Tool to explore the proton structure

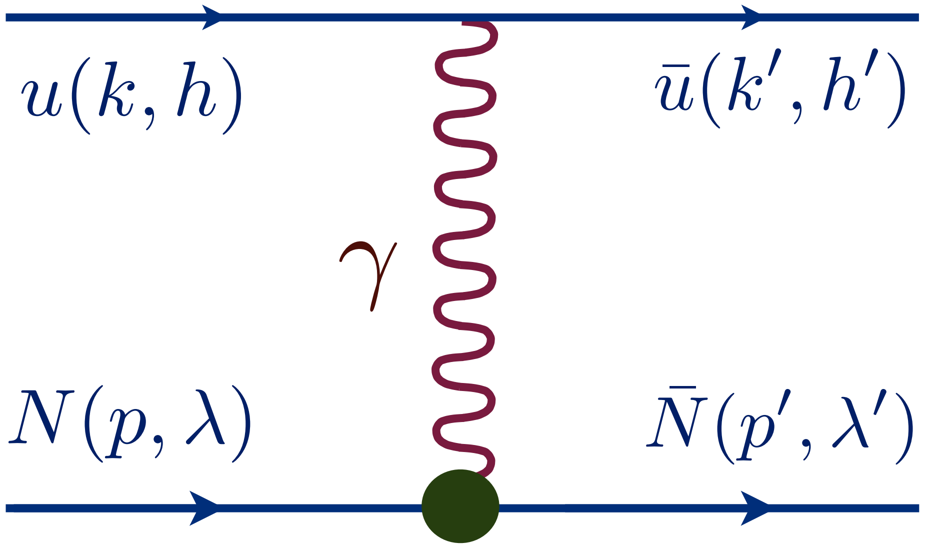

photon-proton vertex

$$\Gamma^{\mu}(Q^2) = \gamma^{\mu} F_D(Q^2) + \frac{i\sigma^{\mu\nu} q_{\nu}}{2M} F_P(Q^2)$$

Dirac and Pauli form factors

lepton energy ω

momentum transfer $Q^2 = -(k - k')^2$

l-p amplitude

$$\boxed{\mathrm{T} = \frac{e^2}{Q^2} \left(\bar{u}\left(k', h'\right) \gamma_{\mu} u\left(k, h\right)\right) \cdot \left(\bar{N}\left(p', \lambda'\right) \Gamma^{\mu}(Q^2) N\left(p, \lambda\right)\right)}$$

Form factors measurement

Sachs electric and magnetic form factors

$$G_E = F_D - \tau F_P \qquad G_M = F_D + F_P$$

Rosenbluth separation

$$\frac{\mathrm{d}\sigma^{\mathrm{unpol}}}{\mathrm{d}\Omega} \sim G_M^2(Q^2) + \frac{\varepsilon}{\tau} G_E^2(Q^2)$$

$\tau \quad \varepsilon$ kinematical variables

$\frac{\mathrm{d}\sigma^{\mathrm{unpol}}}{\mathrm{d}\Omega}$

$G_M^2(Q^2)$

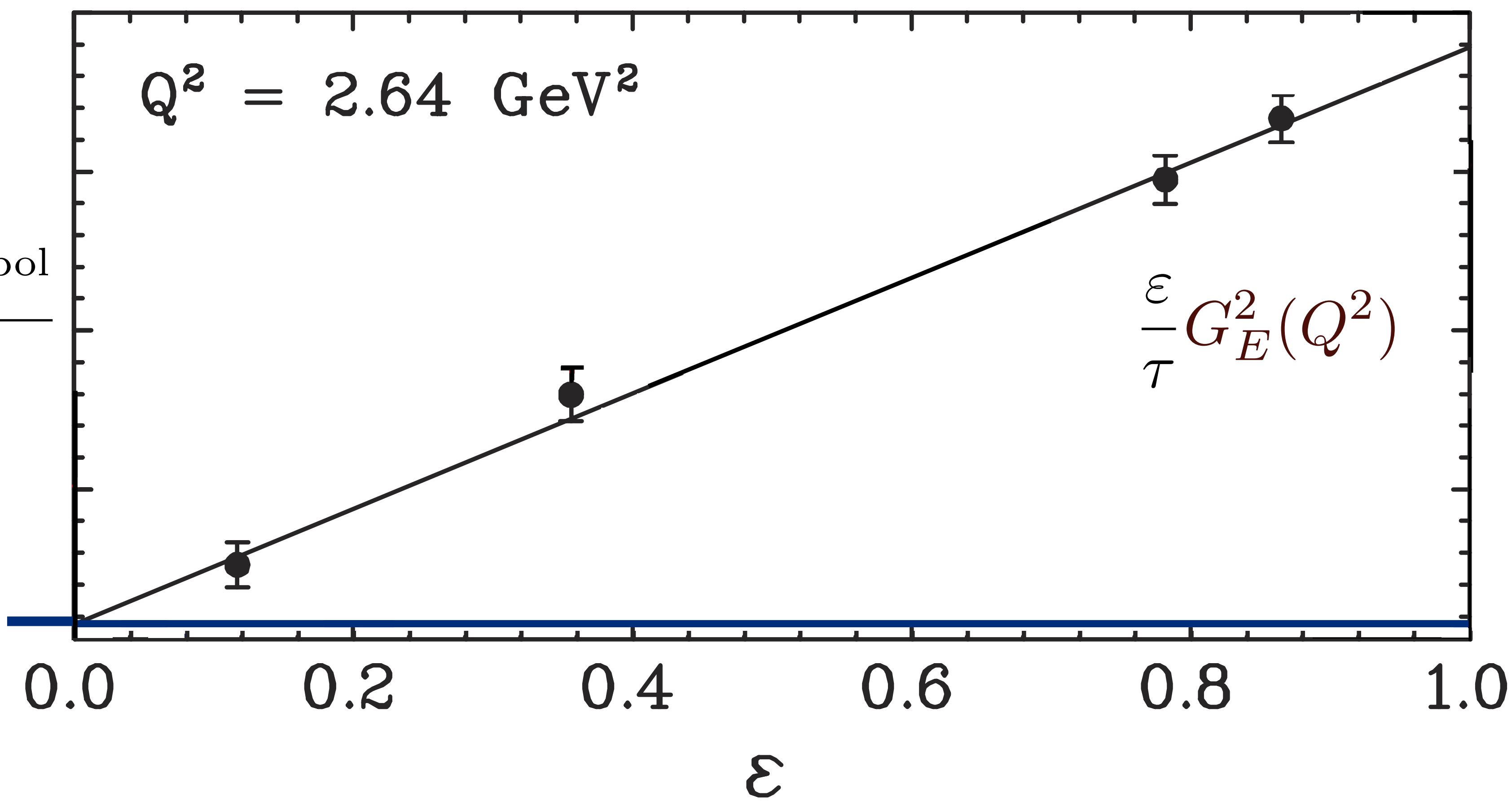

Qattan et al. (2005)

Rosenbluth slope is sensitive to corrections beyond 1γ

Form factors measurement

Sachs electric and magnetic form factors

$$G_E = F_D - \tau F_P \qquad G_M = F_D + F_P$$

Polarization transfer

$\vec{e} + p \to e + \vec{p}$

realized in 2000

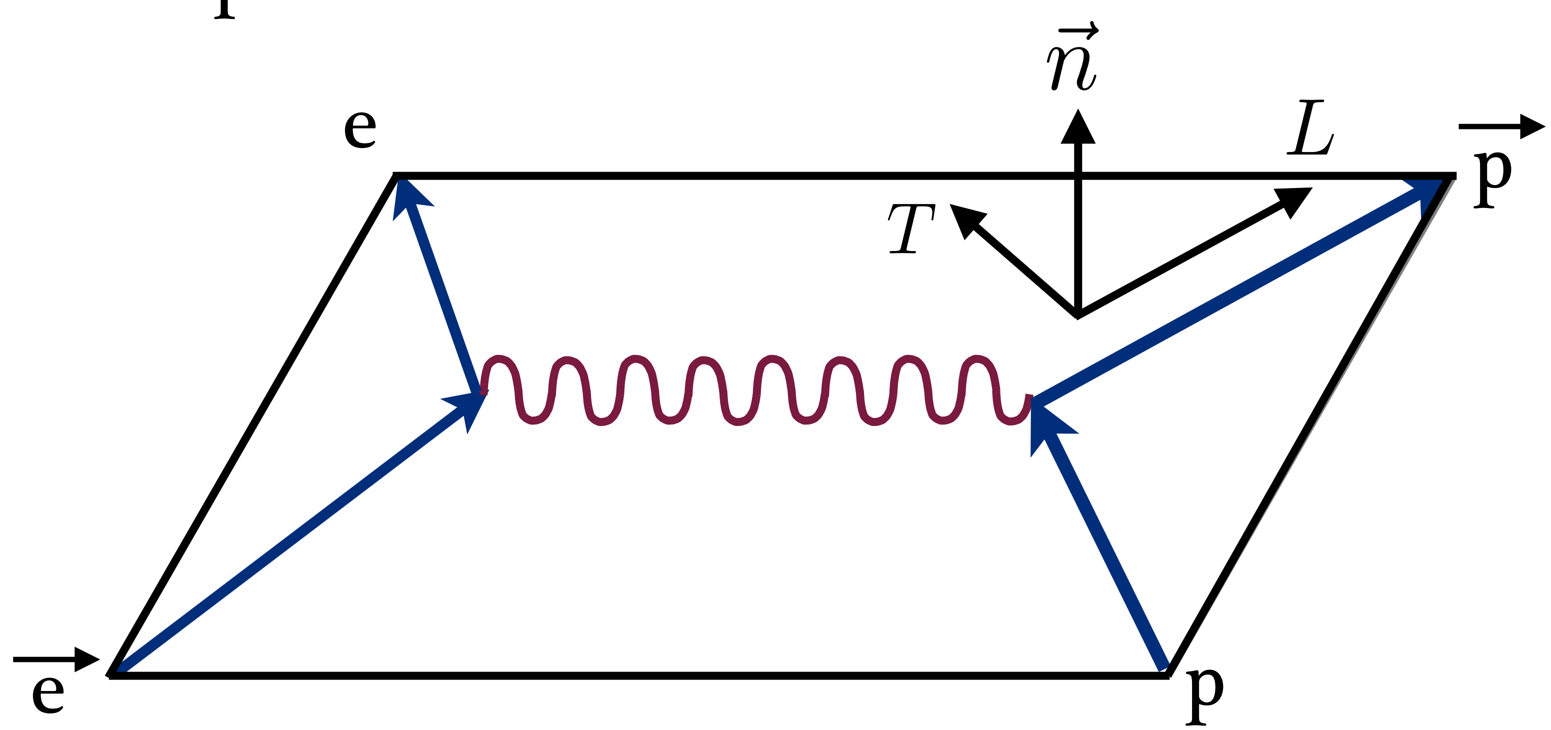

$\mathrm{P_T} \sim G_E(Q^2)G_M(Q^2)$

$\mathrm{P_L} \sim G_M^2(Q^2)$

$$\boxed{\frac{\mathrm{P_T}}{\mathrm{P_L}} \sim \frac{G_E(Q^2)}{G_M(Q^2)}}$$

Proton form factors puzzle

Polarization transfer
JLab (Hall A, C)

vs.

Rosenbluth separation
SLAC, JLab (Hall A, C)

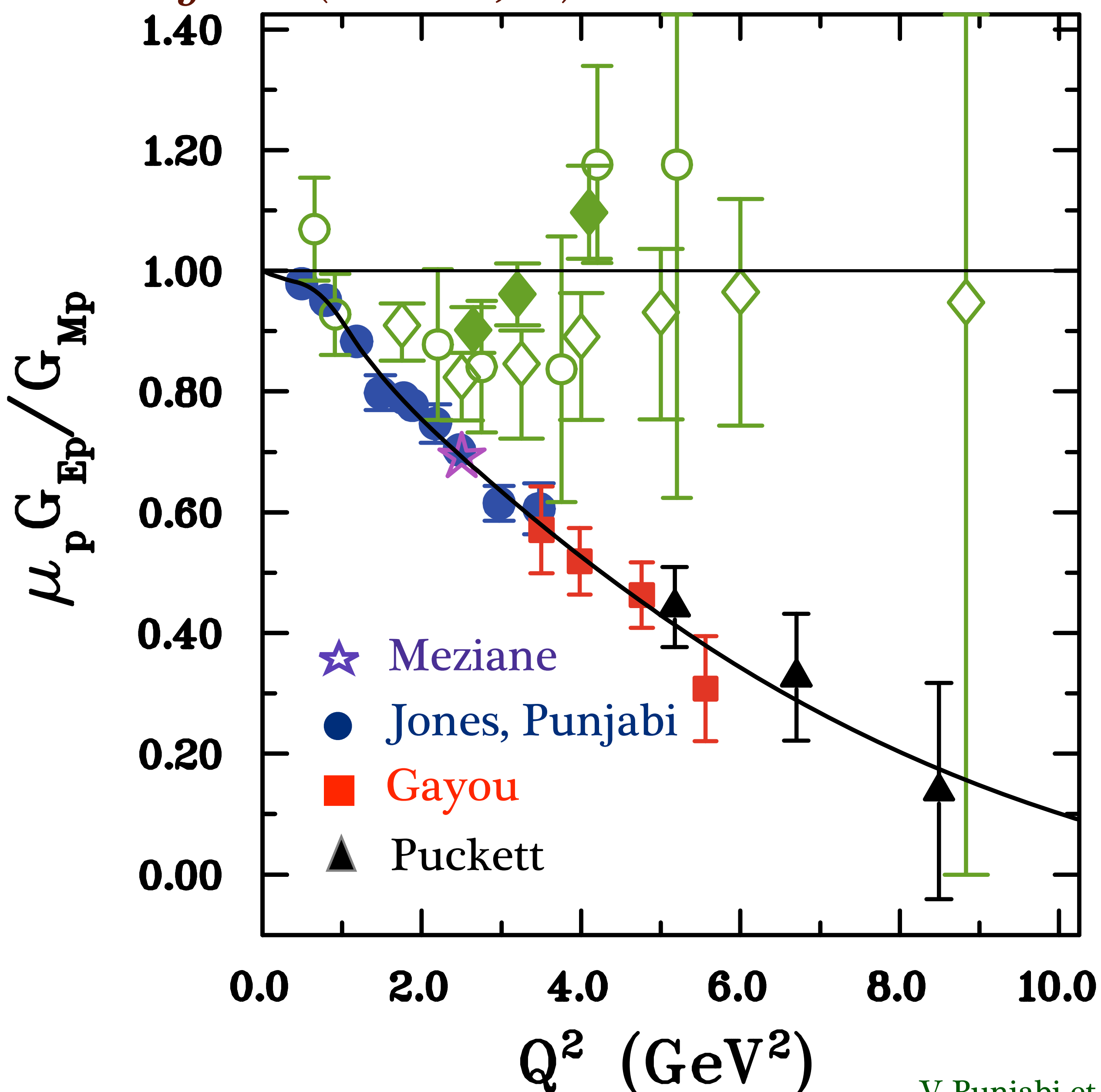

V. Punjabi et al. (2015)

Proton form factors puzzle

Polarization transfer
JLab (Hall A, C)

vs.

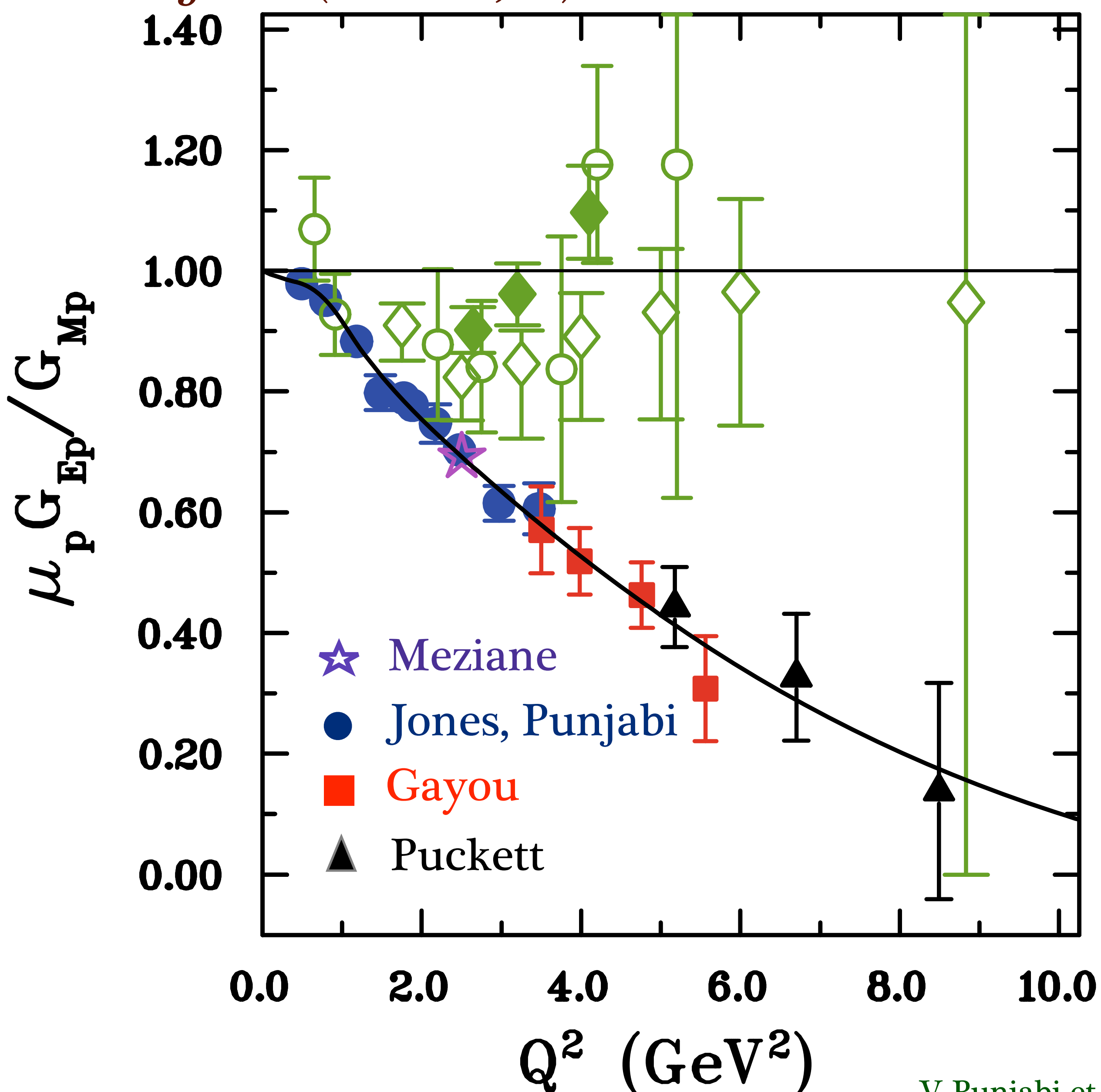

V. Punjabi et al. (2015)

Rosenbluth separation
SLAC, JLab (Hall A, C)

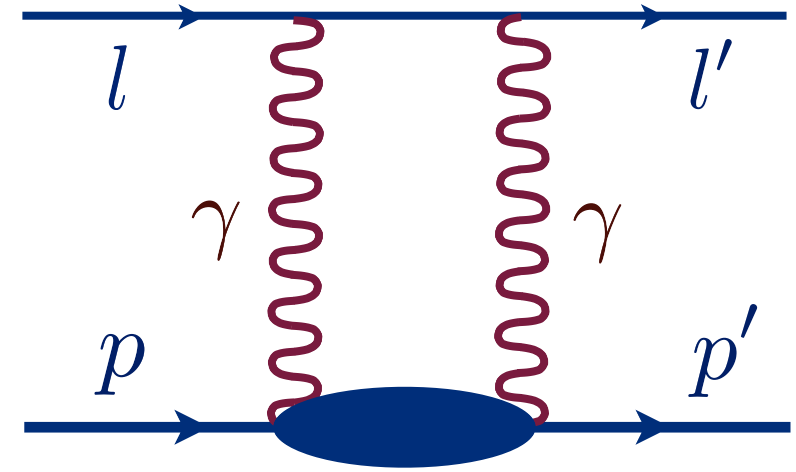

possible explanation
two-photon exchange

Proton form factors puzzle

Polarization transfer
JLab (Hall A, C)

vs.

Rosenbluth separation
SLAC, JLab (Hall A, C)

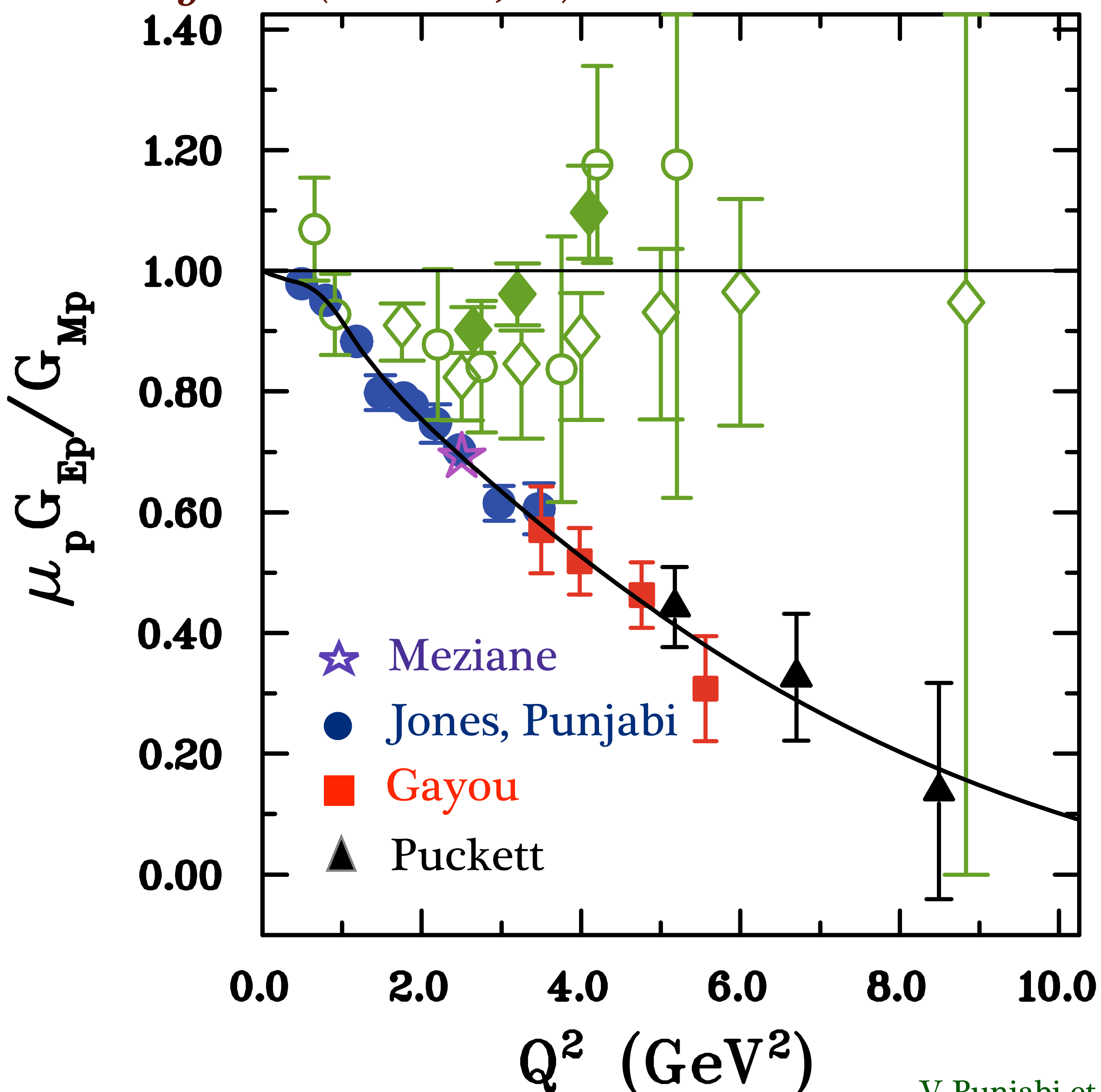

V. Punjabi et al. (2015)

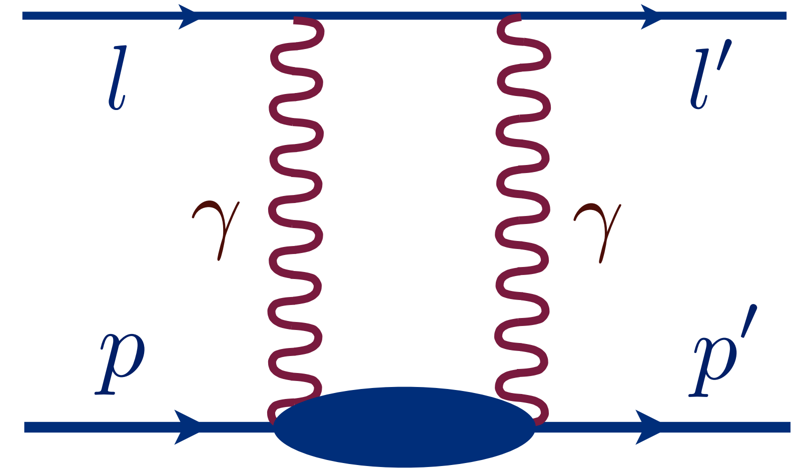

possible explanation
two-photon exchange

new 2ɣ measurements
e^+p/e^-p cross section ratio

$$\mathrm{R} = \frac{\sigma(e^+p)}{\sigma(e^-p)} \approx 1 - 2\delta_{2\gamma}$$

Discrepancy motivates model-independent study of 2ɣ

Proton radius puzzle

electric charge radius

$$< r_E^2 >\equiv -6 \left.\frac{\mathrm{d}G_E(Q^2)}{\mathrm{d}Q^2}\right|_{Q^2=0}$$

- ep elastic scattering

$r_E = 0.879 \pm 0.008$ fm

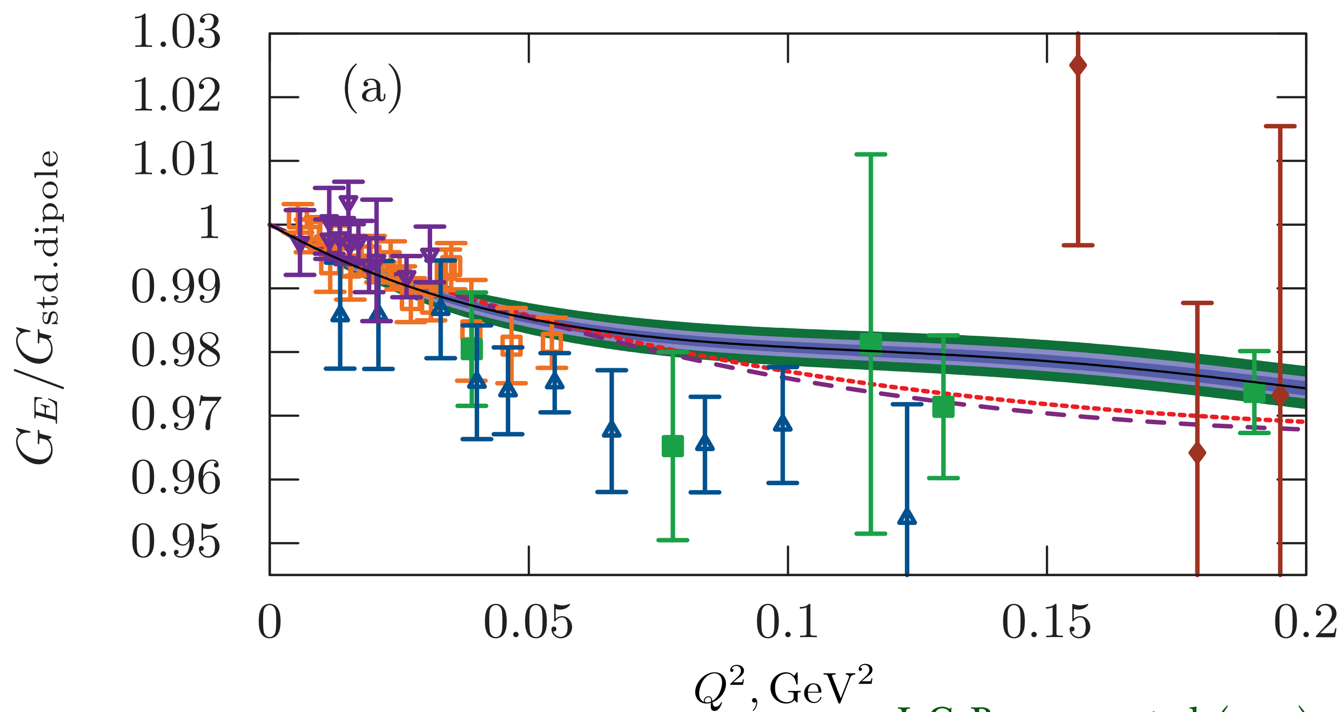

J. C. Bernauer et al. (2014)

Proton radius puzzle

electric charge radius

$$< r_E^2 > \equiv -6 \left. \frac{\mathrm{d}G_E(Q^2)}{\mathrm{d}Q^2} \right|_{Q^2=0}$$

- ep elastic scattering

$r_E = 0.879 \pm 0.008$ fm

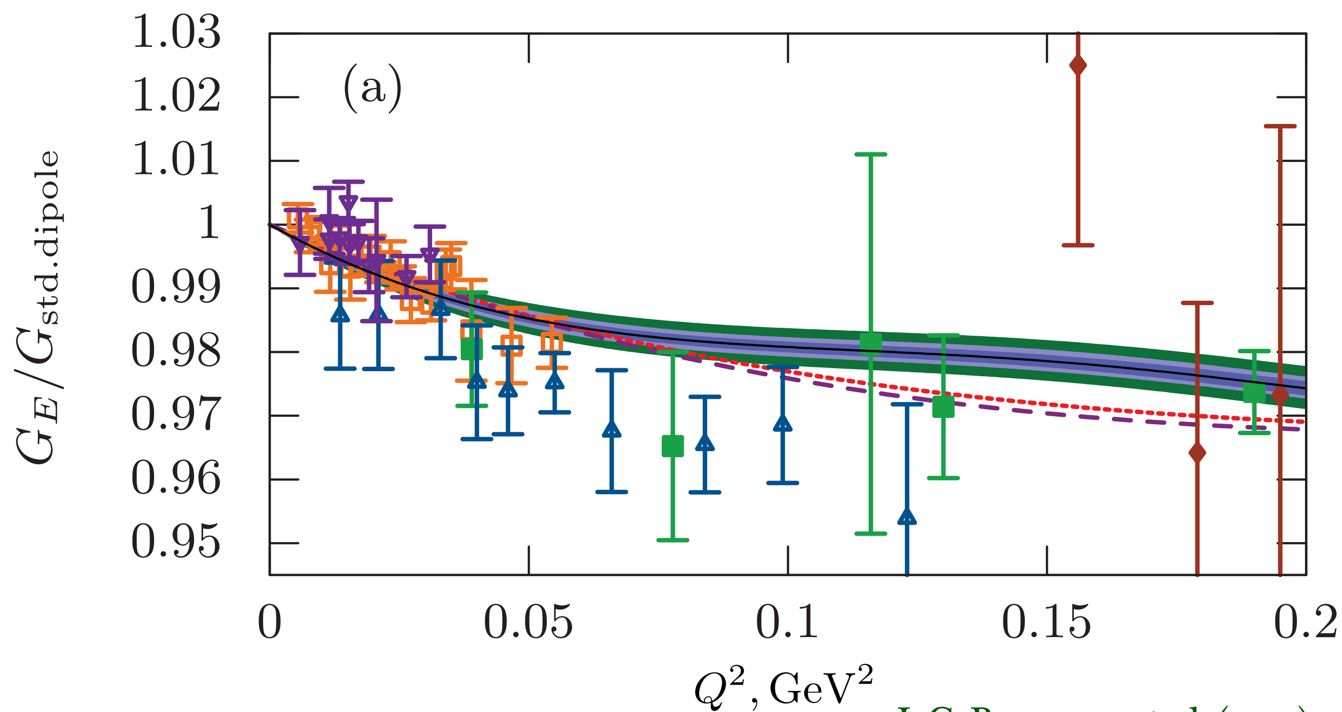

J. C. Bernauer et al. (2014)

- atomic spectroscopy

$$\Delta E_{n\mathrm{S}} \sim m_r^3 < r_E^2 >$$

H, D spectroscopy

$r_E = 0.8758 \pm 0.0077$ fm

CODATA 2010

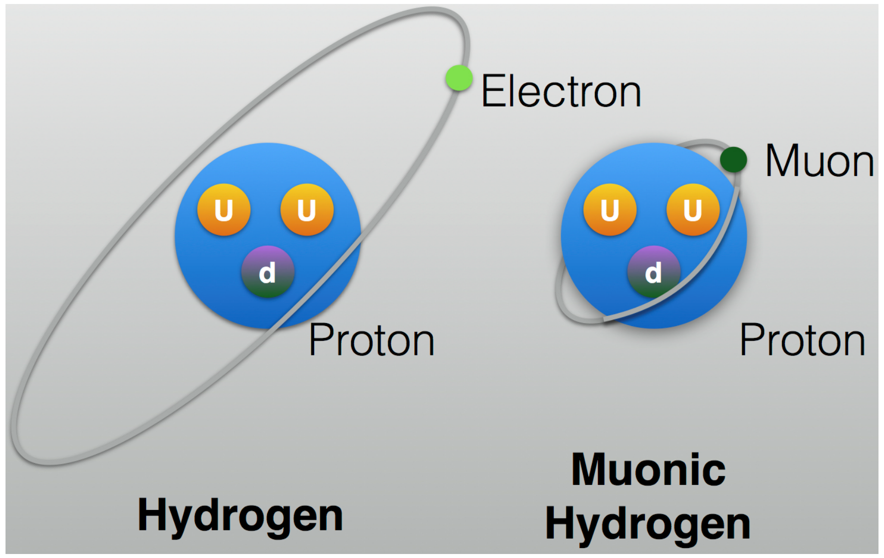

μH Lamb shift

$r_E = 0.8409 \pm 0.0004$ fm

CREMA (2010, 2013)

Proton radius puzzle

electric charge radius

$$< r_E^2 > \equiv -6 \left. \frac{dG_E(Q^2)}{dQ^2} \right|_{Q^2=0}$$

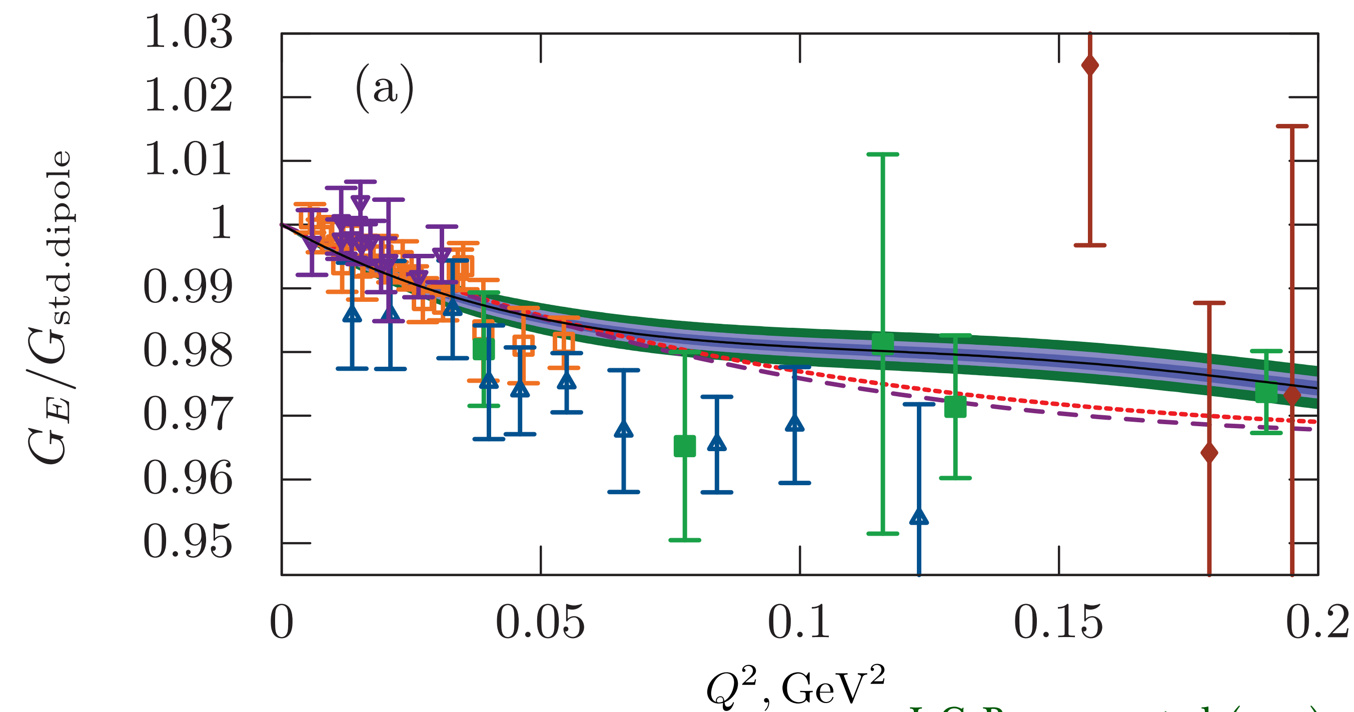

J. C. Bernauer et al. (2014)

- ep elastic scattering

$$r_E = 0.879 \pm 0.008 \text{ fm}$$

- atomic spectroscopy

$$\Delta E_{nS} \sim m_r^3 < r_E^2 >$$

H, D spectroscopy

$$r_E = 0.8758 \pm 0.0077 \text{ fm}$$

CODATA 2010

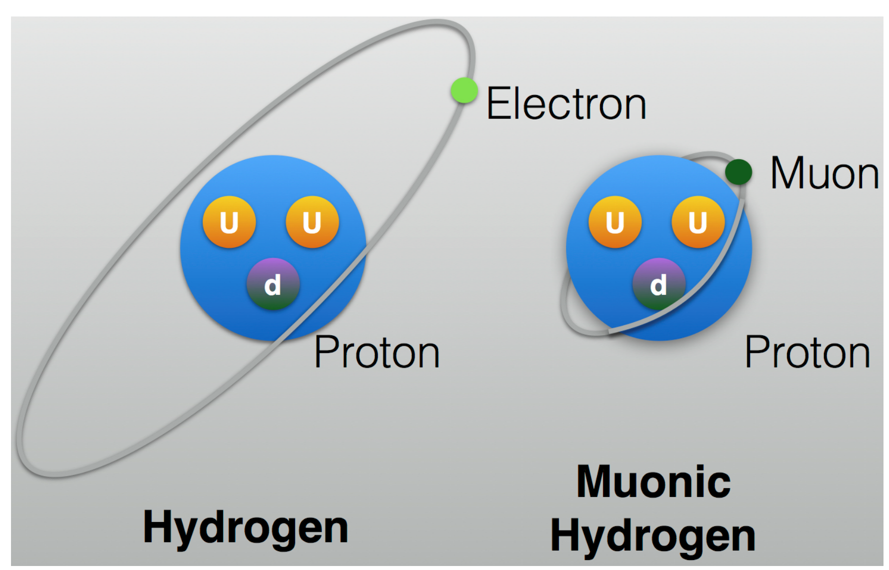

μH Lamb shift

$$r_E = 0.8409 \pm 0.0004 \text{ fm}$$

CREMA (2010, 2013)

7 σ difference !

Proton radius puzzle

electric charge radius

$$< r_E^2 > \equiv -6 \left. \frac{dG_E(Q^2)}{dQ^2} \right|_{Q^2=0}$$

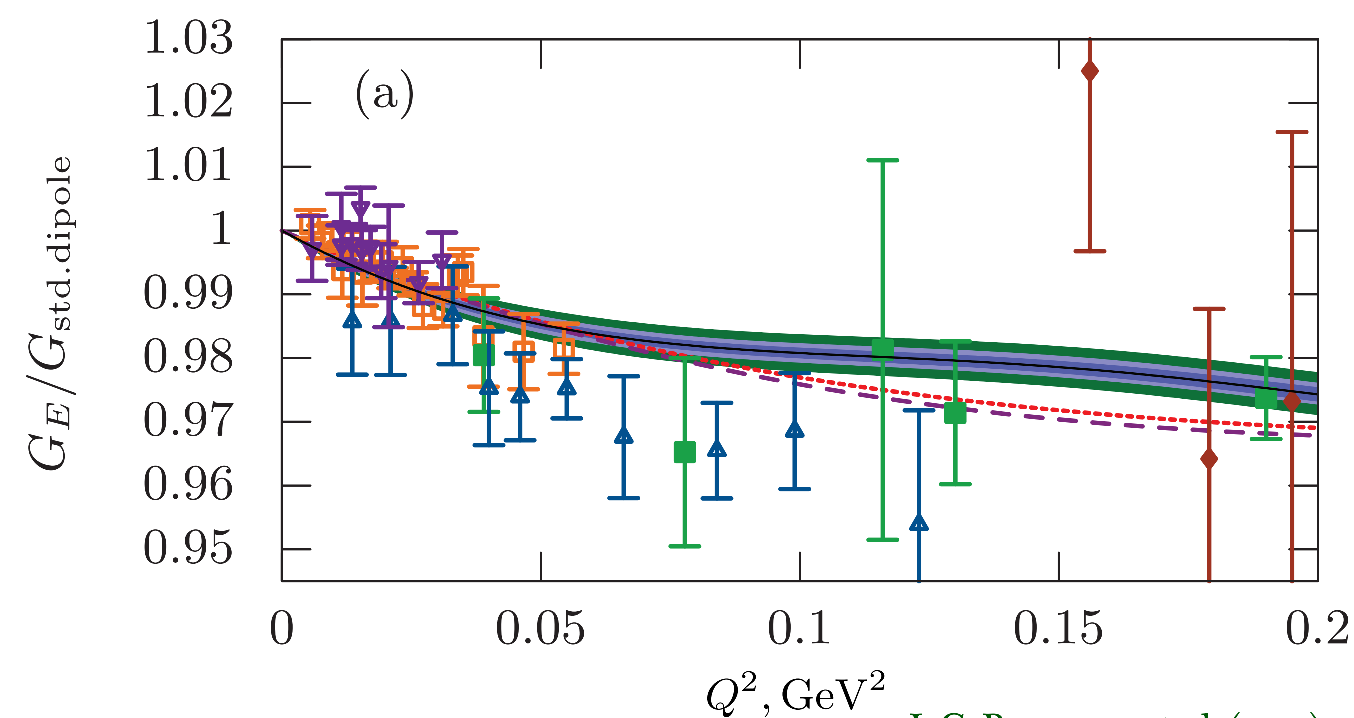

J. C. Bernauer et al. (2014)

- ep elastic scattering

$r_E = 0.879 \pm 0.008$ fm ?

- atomic spectroscopy $\Delta E_{\rm nS} \sim m_r^3 < r_E^2 >$

H, D spectroscopy

$r_E = 0.8758 \pm 0.0077$ fm

CODATA 2010

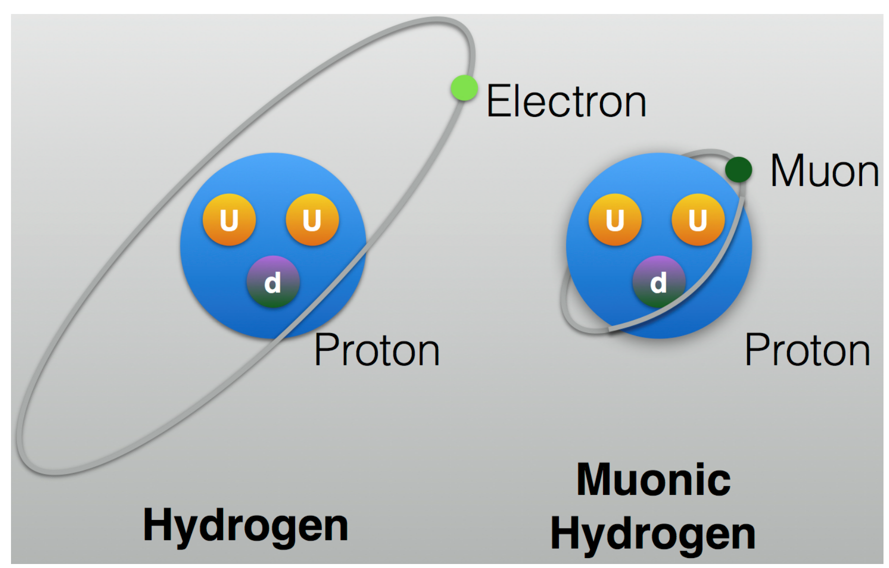

μH Lamb shift

$r_E = 0.8409 \pm 0.0004$ fm

CREMA (2010, 2013)

7 σ difference !

Proton radius puzzle

electric charge radius

$$< r_E^2 > \equiv -6 \left. \frac{\mathrm{d}G_E(Q^2)}{\mathrm{d}Q^2} \right|_{Q^2=0}$$

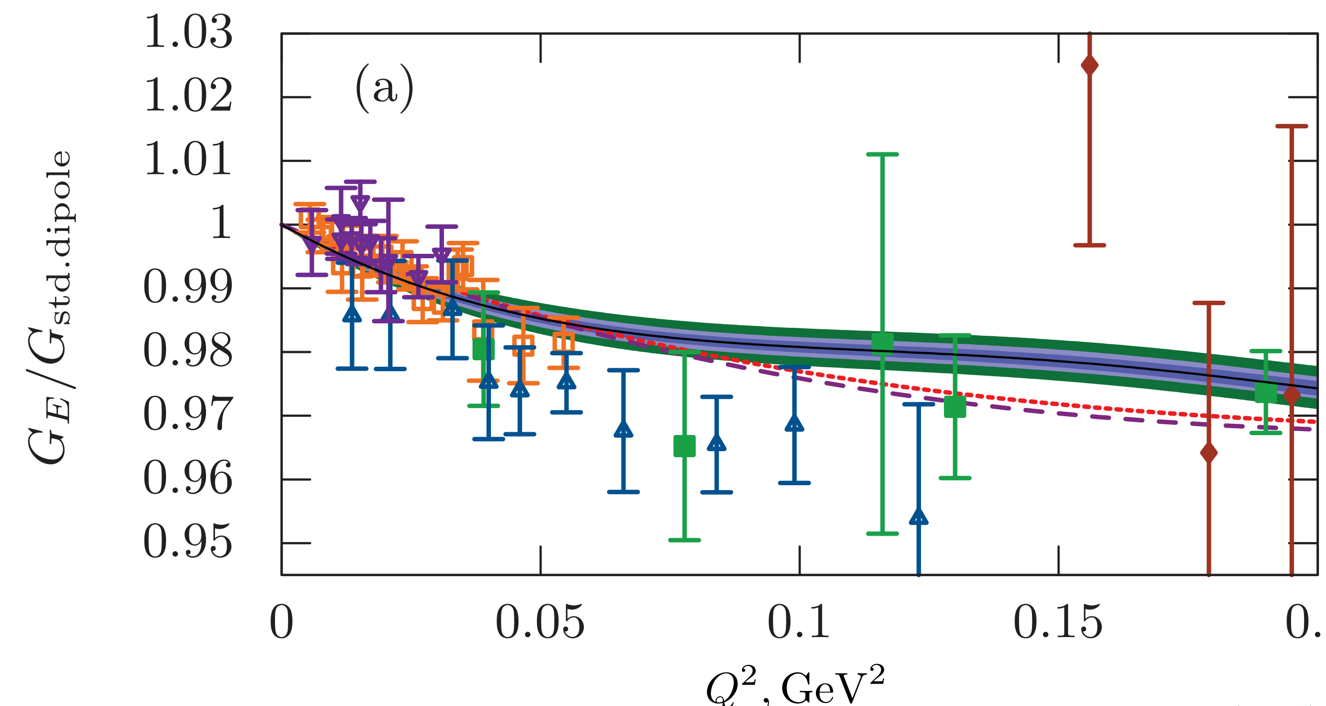

J. C. Bernauer et al. (2014)

- ep elastic scattering

$$r_E = 0.879 \pm 0.008 \text{ fm}$$

- atomic spectroscopy

$$\Delta E_{n\mathrm{S}} \sim m_r^3 < r_E^2 >$$

H, D spectroscopy

$$r_E = 0.8758 \pm 0.0077 \text{ fm}$$

CODATA 2010

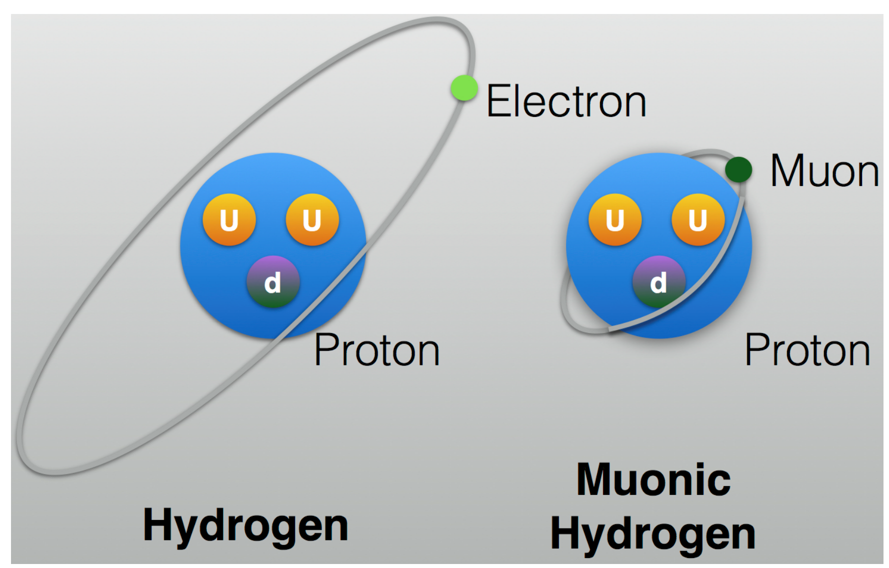

μH Lamb shift

$$r_E = 0.8409 \pm 0.0004 \text{ fm}$$

CREMA (2010, 2013)

eH 2S-4P (2017)

7 σ difference !

Proton radius puzzle

electric charge radius

$$< r_E^2 > \equiv -6 \left. \frac{dG_E(Q^2)}{dQ^2} \right|_{Q^2=0}$$

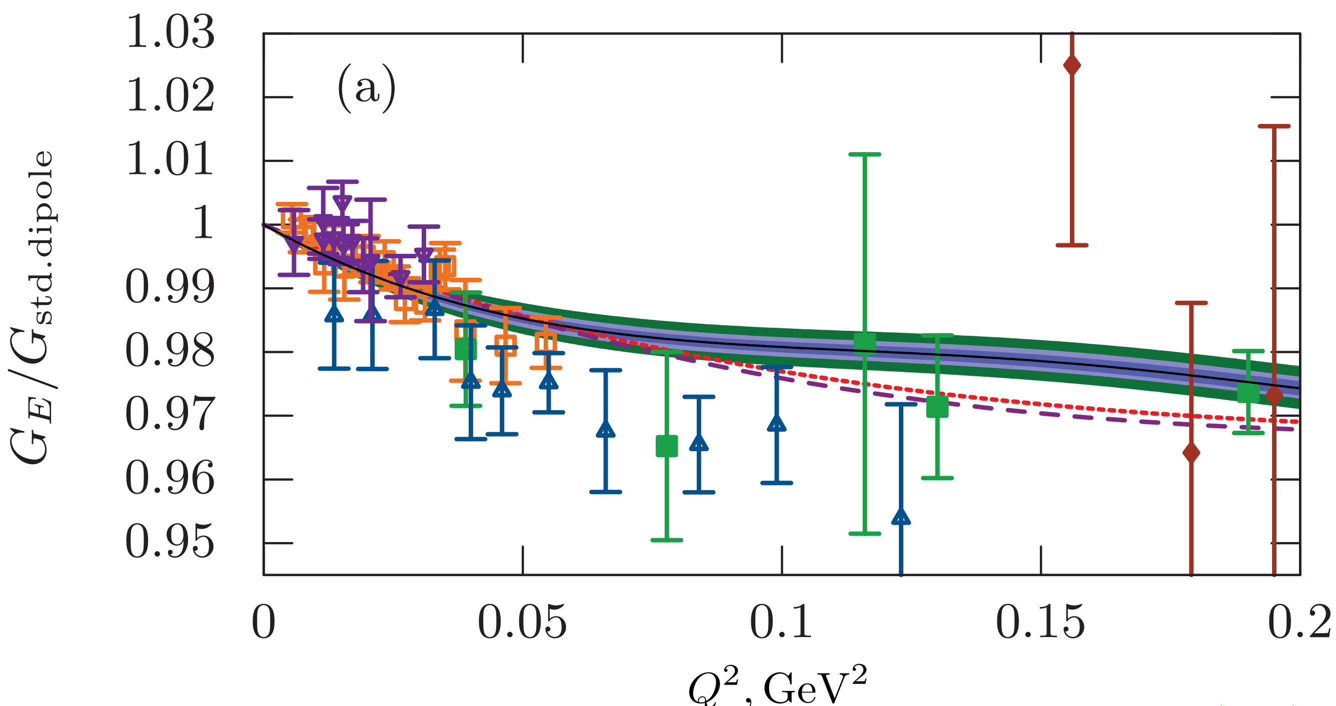

J. C. Bernauer et al. (2014)

- ep elastic scattering

$r_E = 0.879 \pm 0.008$ fm

- atomic spectroscopy

$$\Delta E_{nS} \sim m_r^3 < r_E^2 >$$

H, D spectroscopy

$r_E = 0.8758 \pm 0.0077$ fm

CODATA 2010

eH 1S-3S (2018)

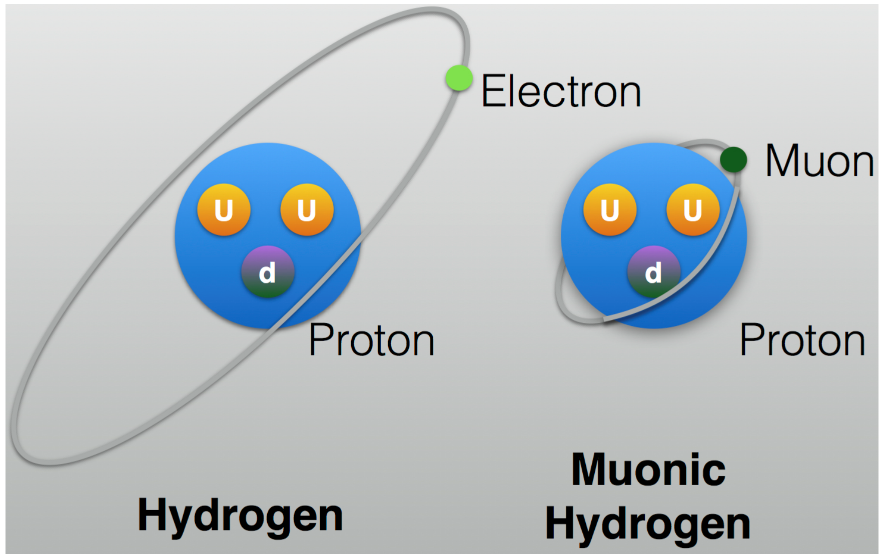

μH Lamb shift

$r_E = 0.8409 \pm 0.0004$ fm

CREMA (2010, 2013)

eH 2S-4P (2017)

7 σ difference !

Proton radius puzzle

electric charge radius

$$< r_E^2 > \equiv -6 \left. \frac{dG_E(Q^2)}{dQ^2} \right|_{Q^2=0}$$

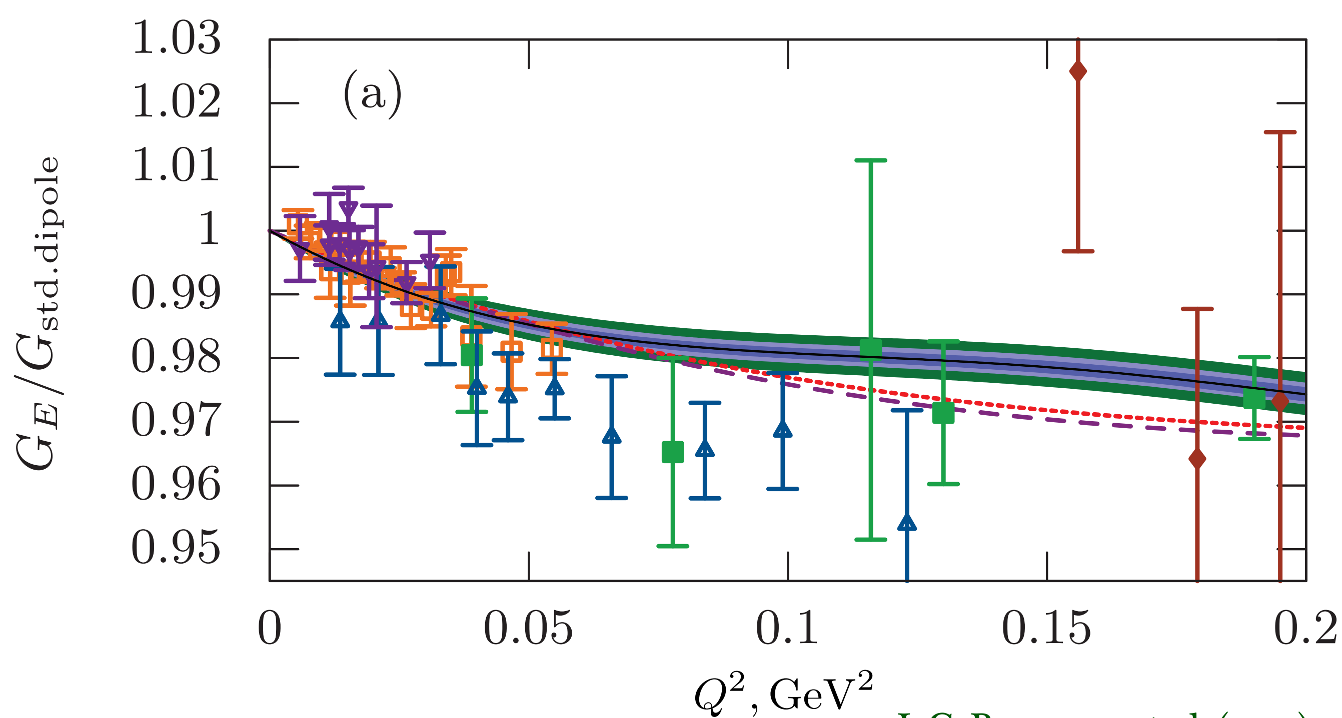

J. C. Bernauer et al. (2014)

- ep elastic scattering

$r_E = 0.879 \pm 0.008$ fm

- atomic spectroscopy

$\Delta E_{nS} \sim m_r^3 < r_E^2 >$

H, D spectroscopy

$r_E = 0.8758 \pm 0.0077$ fm

CODATA 2010

eH 1S-3S (2018)

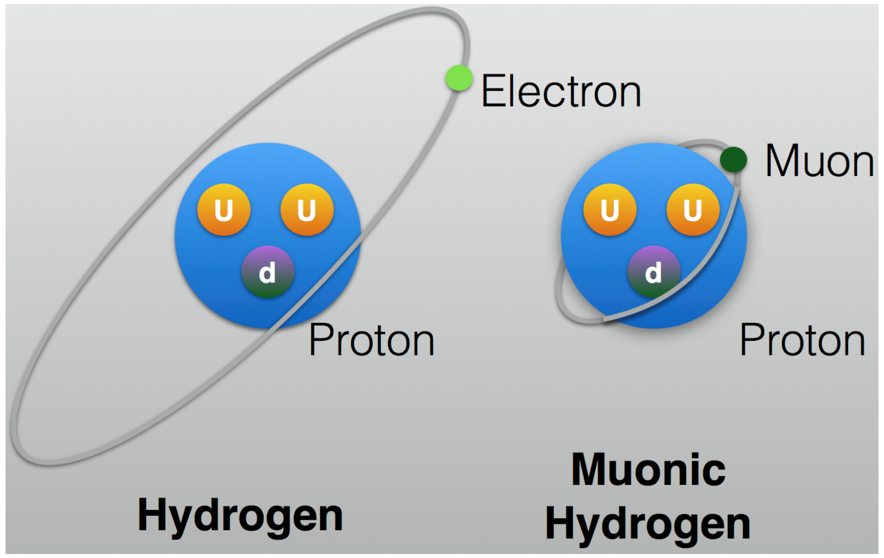

μH, μD Lamb shift

$r_E = 0.8409 \pm 0.0004$ fm

CREMA (2010, 2013)

eH 2S-4P (2017)

7 σ difference !

Scattering experiments and 2ɣ

- charge radius extractions:

eH, eD spectroscopy	ep scattering
μH, μD spectroscopy	μp scattering ????

- μp elastic scattering is planned by MUSE@PSI(2018-19)
  measure with both electron/muon charges

- three nominal beam energies: 115, 153, 210 MeV, $Q^2 < 0.1$ GeV^2

- 2ɣ correction in MUSE ?

Scattering experiments and 2ɣ

- 2ɣ is not among standard radiative corrections

$$\sigma^{\text{exp}} \equiv \sigma_{1\gamma}(1 + \delta_{\text{rad}} + \delta_{\text{soft}} + \delta_{2\gamma})$$

- soft-photon contribution is included

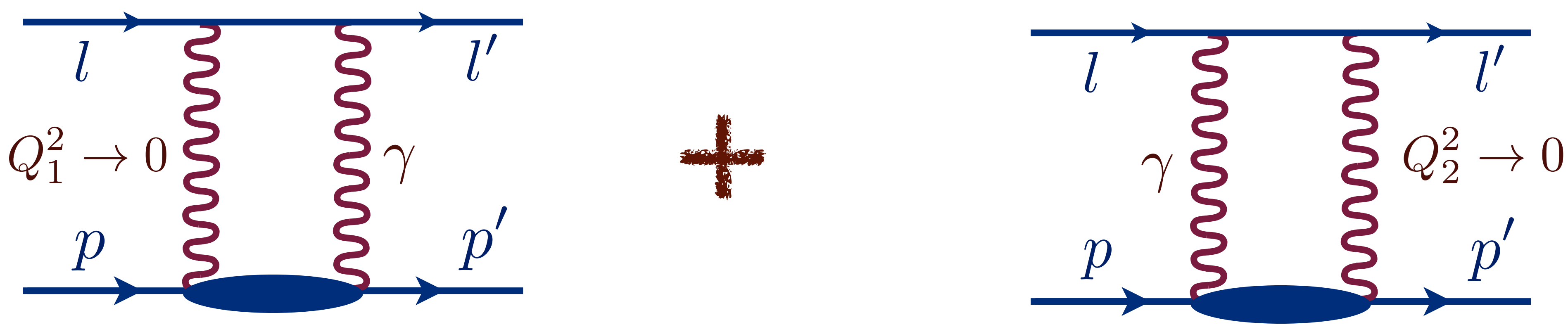

L.C. Maximon and J. A. Tjon (2000)

- hard-photon contribution: Feshbach correction

- charge radius insensitive to 2ɣ model

- magnetic radius depends on 2ɣ model

Elastic muon-proton scattering

and two-photon exchange

Elastic lepton-proton scattering and 2ɣ

momentum transfer

$$Q^2 = -(k-k')^2$$

crossing-symmetric variable

$$\nu = \frac{(k, p+p')}{2}$$

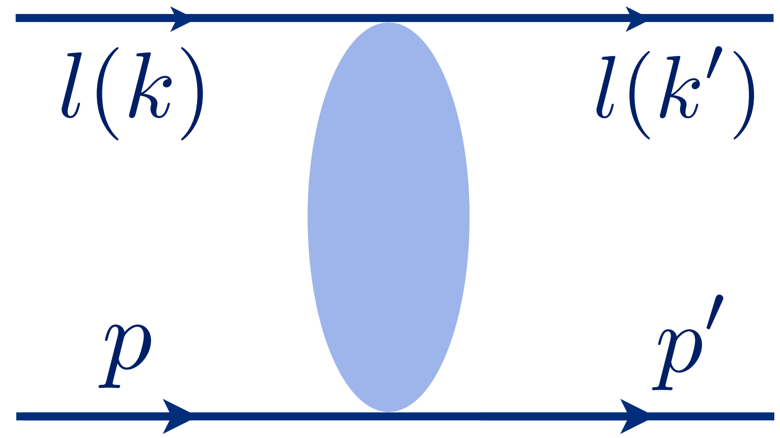

photon polarization parameter

$$\varepsilon, \ \varepsilon_{\mathrm{T}}$$

forward scattering

$$\varepsilon \to 1$$

- leading 2ɣ contribution: interference term

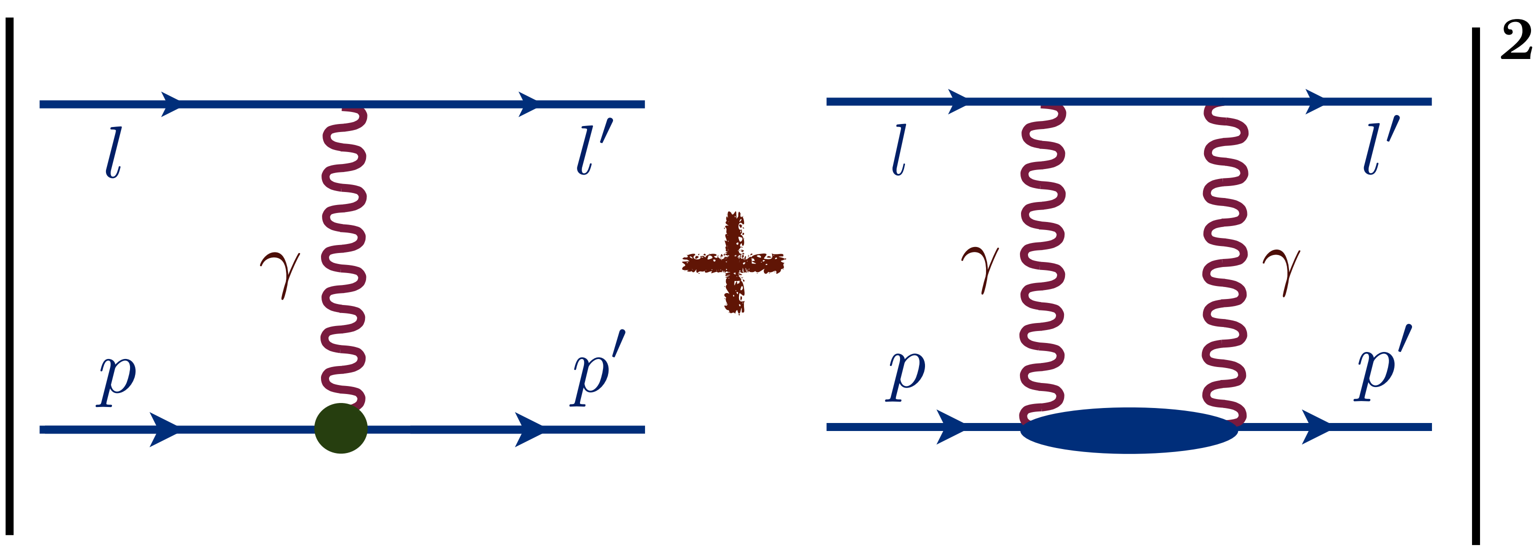

$$\delta_{2\gamma} = \frac{2 \sum\limits_{\text{spin}} T^{1\gamma} \Re T^{2\gamma}}{\sum\limits_{\text{spin}} |T^{1\gamma}|^2}$$

- 2ɣ correction to cross section is given by amplitudes real parts

Elastic lepton-proton scattering and 2ɣ

$$K = \frac{k+k'}{2}$$

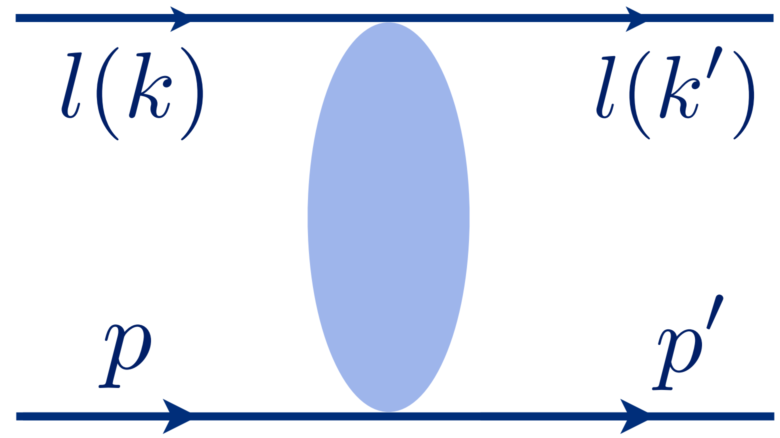

$$P = \frac{p+p'}{2}$$

- electron-proton scattering: 3 structure amplitudes

$$\mathrm{T}^{\mathrm{non-flip}} = \frac{e^2}{Q^2}\bar{l}\gamma_\mu l \cdot \bar{N}\left(\mathcal{G}_M(\nu,Q^2)\gamma^\mu - \mathcal{F}_2(\nu,Q^2)\frac{P^\mu}{M} + \mathcal{F}_3(\nu,Q^2)\frac{\hat{K}P^\mu}{M^2}\right)N$$

P.A.M. Guichon and M. Vanderhaeghen (2003)

- muon-proton scattering: add helicity-flip amplitudes

$$\mathrm{T}^{\mathrm{flip}} = \frac{e^2}{Q^2}\frac{m}{M}\bar{l}l \cdot \bar{N}\left(\mathcal{F}_4(\nu,Q^2) + \mathcal{F}_5(\nu,Q^2)\frac{\hat{K}}{M}\right)N + \frac{e^2}{Q^2}\frac{m}{M}\mathcal{F}_6(\nu,Q^2)\bar{l}\gamma_5 l \cdot \bar{N}\gamma_5 N$$

M. Gorchtein, P.A.M. Guichon and M. Vanderhaeghen (2004)

- 2ɣ correction to cross section is given by amplitudes real parts

Elastic lepton-proton scattering and 2ɣ

kinematical variable

$$\tau = \frac{Q^2}{4M^2}$$

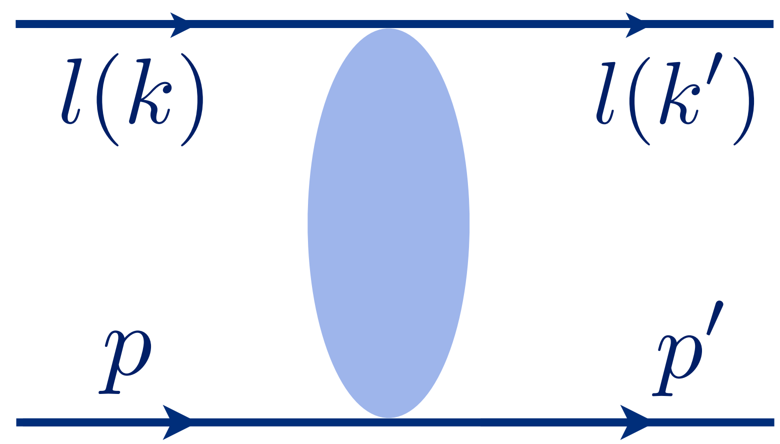

boundary value of ε

$$\varepsilon_0 = \frac{2m^2}{Q^2}$$

- amplitudes entering observables:

$$\mathcal{G}_1 = \mathcal{G}_M + \frac{\nu}{M^2}\mathcal{F}_3 + \frac{m^2}{M^2}\mathcal{F}_5 \qquad \mathcal{G}_3 = \mathcal{G}_1 - \mathcal{G}_M$$

$$\mathcal{G}_2 = \mathcal{G}_M - (1-\tau)\mathcal{F}_2 + \frac{\nu}{M^2}\mathcal{F}_3 \qquad \mathcal{G}_4 = \mathcal{F}_4 + \frac{\nu}{M^2(1+\tau)}\mathcal{F}_5$$

better high-energy behavior

- 2ɣ correction in terms of amplitudes:

$$\boxed{\delta_{2\gamma} = \frac{2}{G_M^2 + \frac{\varepsilon}{\tau}G_E^2}\left\{G_M \Re\mathcal{G}_1^{2\gamma} + \frac{\varepsilon}{\tau}G_E\Re\mathcal{G}_2^{2\gamma} + \frac{1-\varepsilon}{1-\varepsilon_0}\left(\frac{\varepsilon_0}{\tau}\frac{\nu}{M^2}G_E\Re\mathcal{G}_4^{2\gamma} - G_M\Re\mathcal{G}_3^{2\gamma}\right)\right\}}$$

non-forward scattering
at low momentum transfer

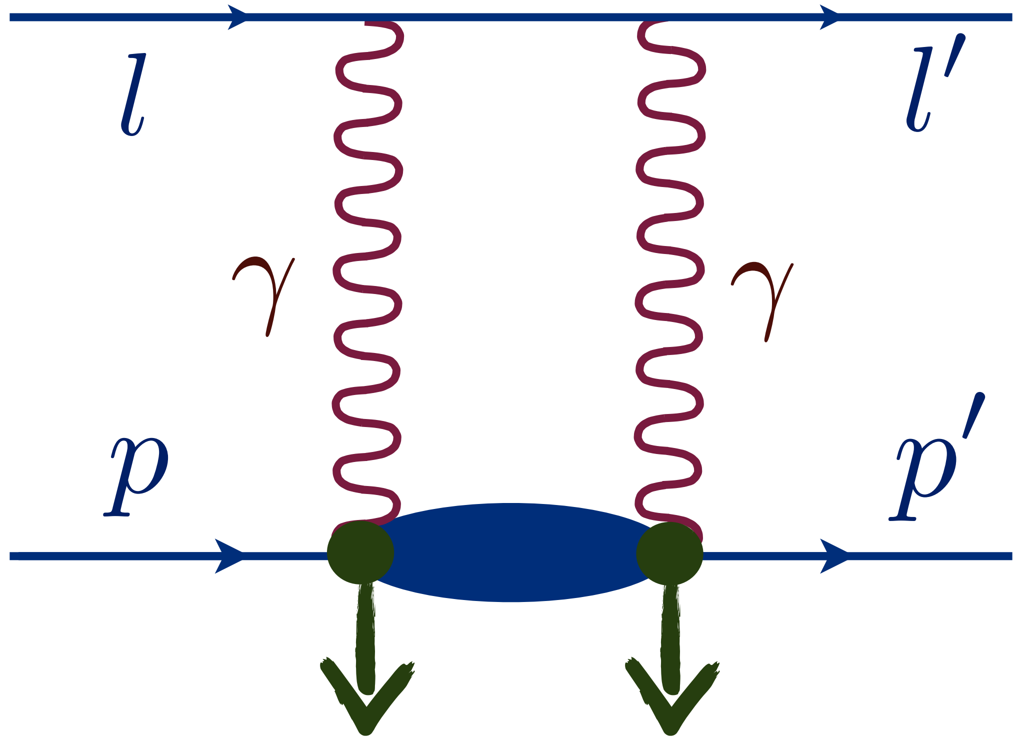

photoproduction vertex or Compton tensor

box diagram

assumption about the vertex

non-forward scattering

at low momentum transfer

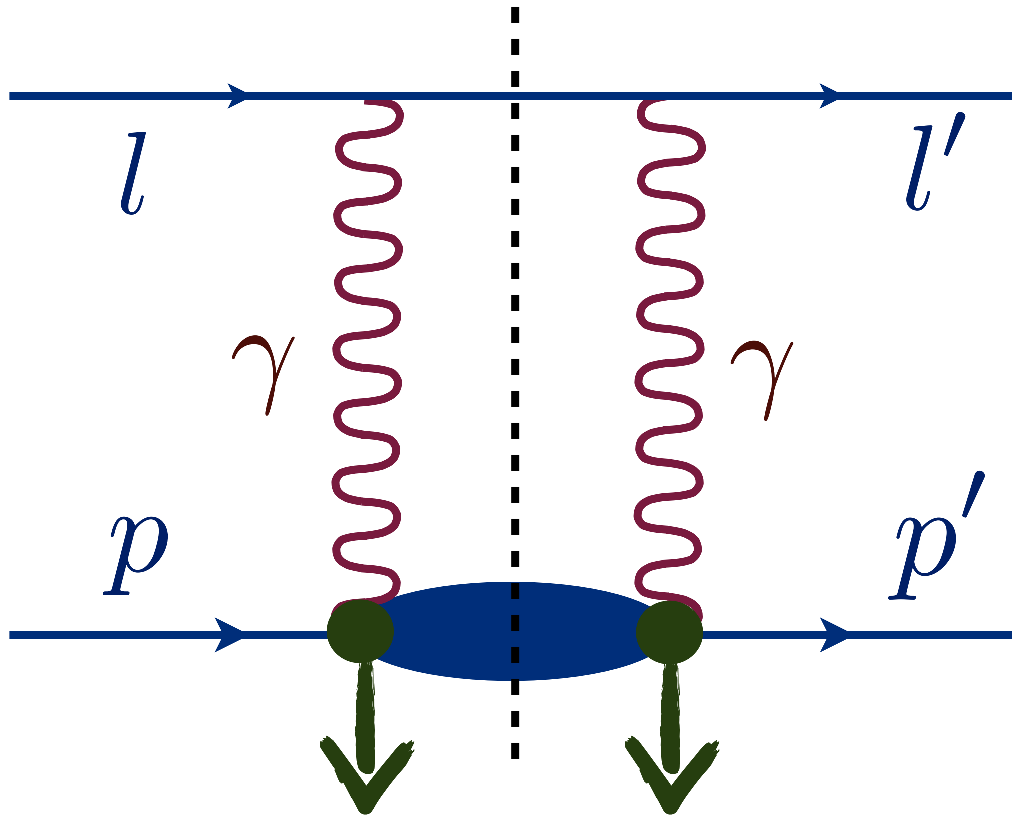

photoproduction vertex or Compton tensor

box diagram

assumption about the vertex

dispersion relations

based on on-shell information

non-forward scattering

proton state

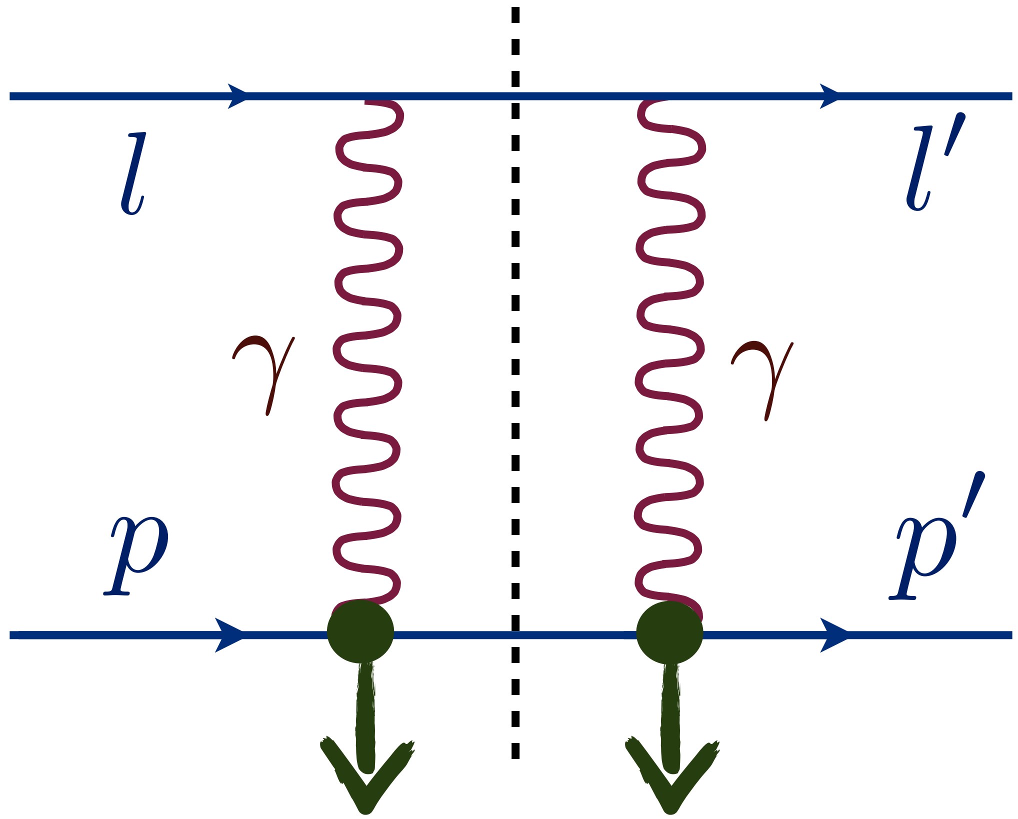

Dirac and Pauli form factors

box diagram

assumption about the vertex

dispersion relations

based on on-shell information

Hadronic model

- one-photon exchange on-shell vertex:

$$\Gamma^\mu(Q^2) = \gamma^\mu F_D(Q^2) + \frac{i\sigma^{\mu\nu}q_\nu}{2M} F_P(Q^2)$$

ep scattering: P. G. Blunden, W. Melnitchouk and J. A. Tjon (2003)

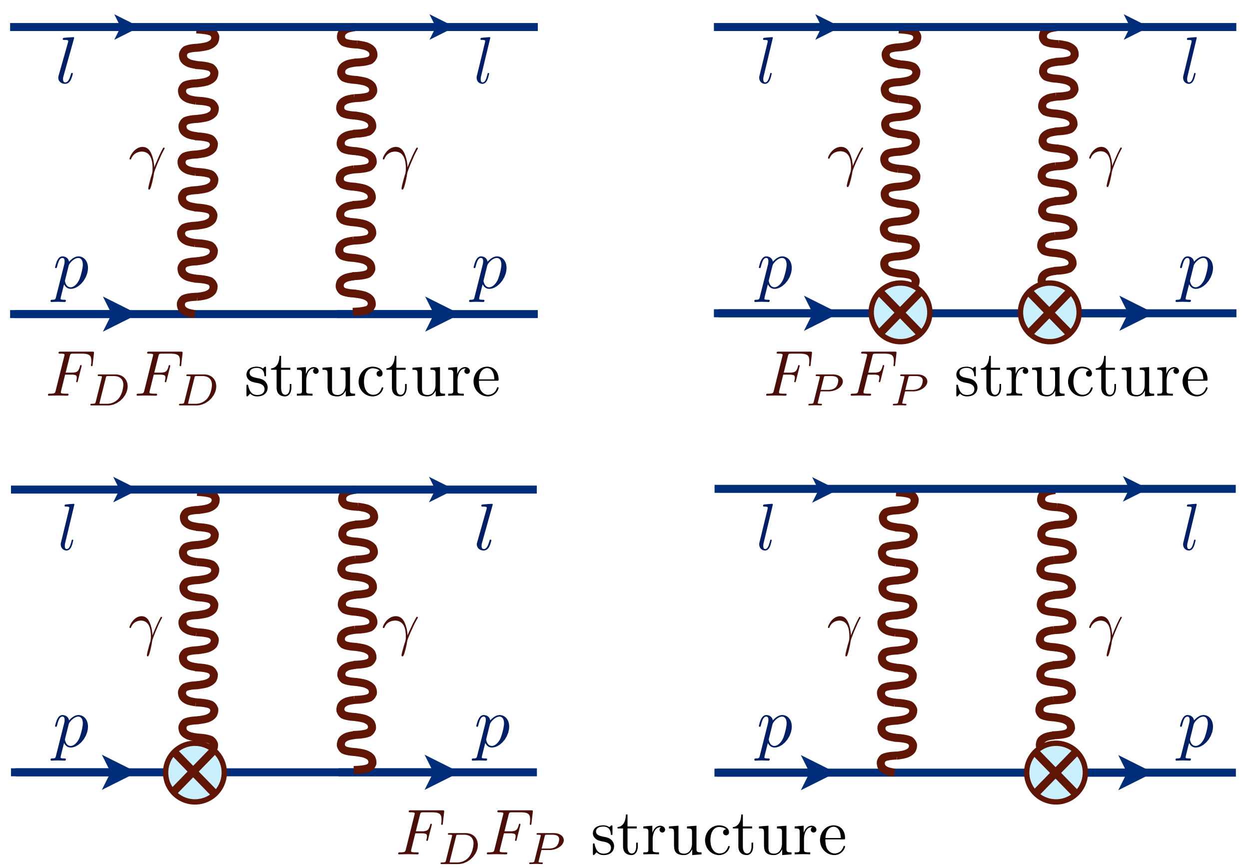

IR divergencies are subtracted

L.C. Maximon and J. A. Tjon (2000)

- dipole electric and magnetic FFs:

$$G_E = F_D - \tau F_P = \frac{1}{(1+Q^2/\Lambda^2)^2} \qquad G_M = F_D + F_P = \frac{\mu_P}{(1+Q^2/\Lambda^2)^2}$$

non-forward scattering

proton state

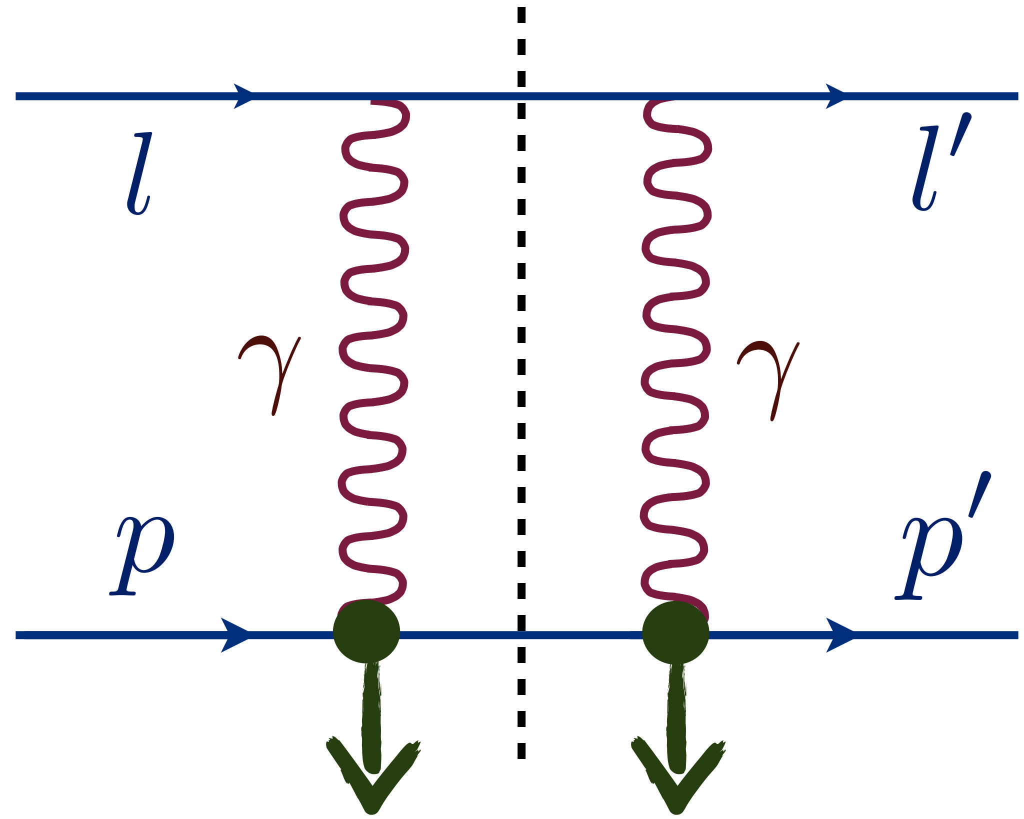

Dirac and Pauli form factors

box diagram

dispersion relations

assumption about the vertex

based on on-shell information

Fixed-Q^2 dispersion relation framework

on-shell 1γ amplitudes

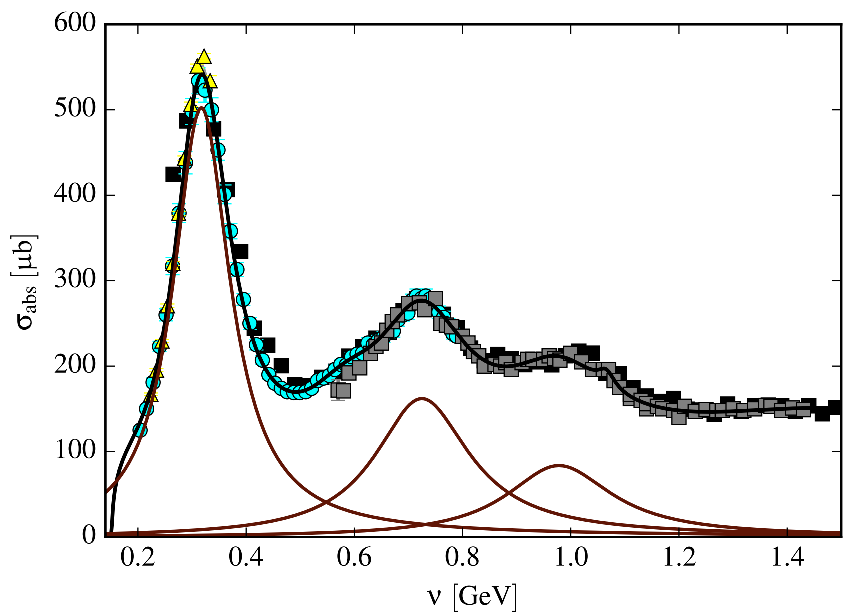

2γ prediction

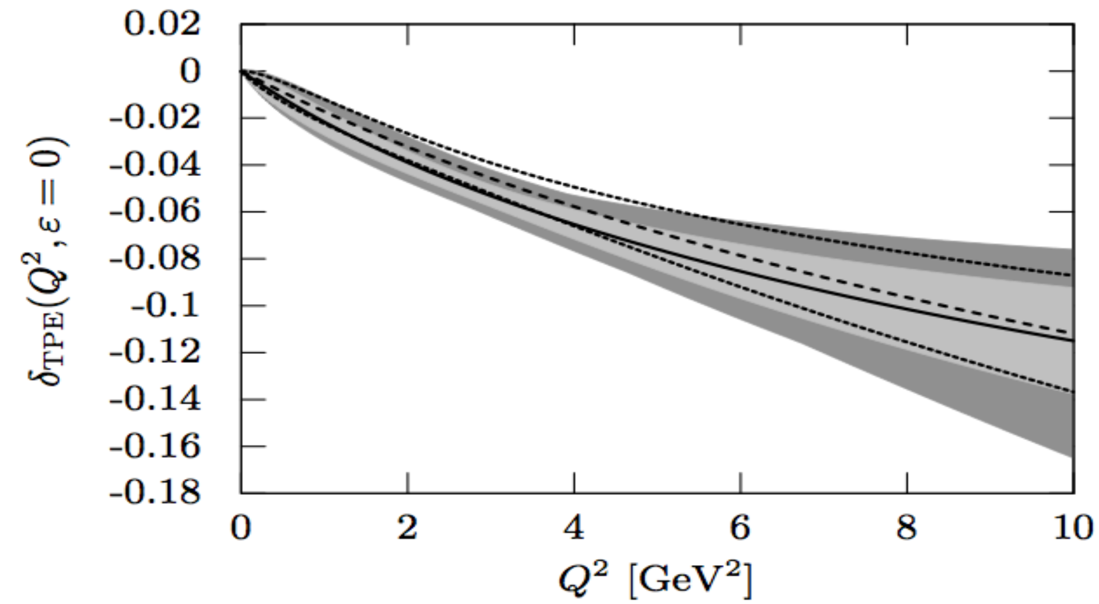

experimental data

cross section correction

unitarity

$$\Re \mathcal{F}(\nu) = \frac{2\nu}{\pi} \mathcal{P} \int_{\nu_{min}}^{\infty} \frac{\Im \mathcal{F}(\nu' + i0)}{\nu'^2 - \nu^2} \mathrm{d}\nu'$$

disp. rel.

2γ imaginary parts

2γ real parts

Mandelstam plot

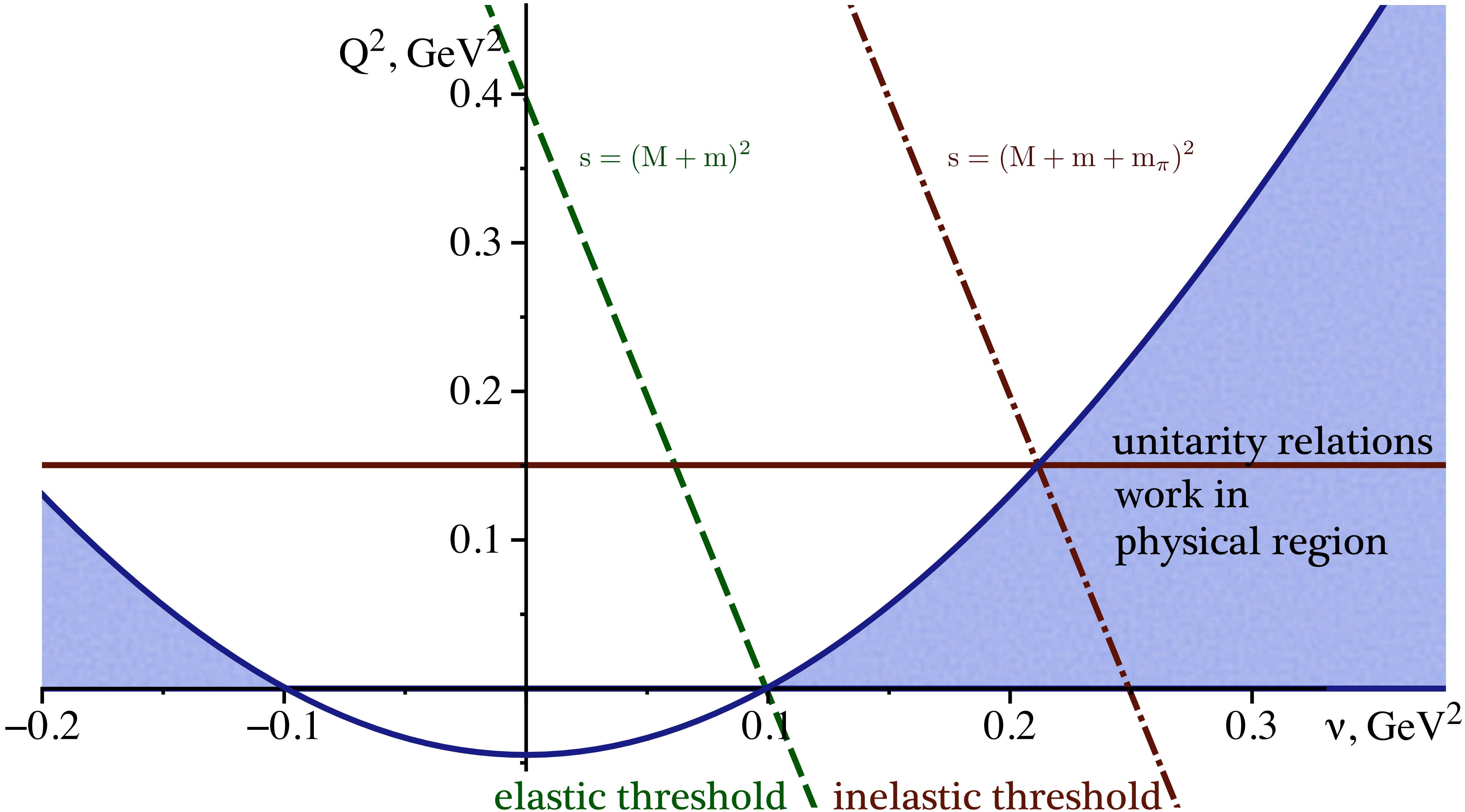

- proton intermediate state is outside physical region for $Q^2 > 0$
- inelastic states are inside physical region for MUSE kinematics

Analytical continuation. Elastic state

- contour deformation method:

$\int d\Omega$ → angular integration to integration on curve in complex plane → deform integration contour keeping poles inside going to unph. region

- analytical continuation reproduces results in unphysical region

$Q^2 = 0.1\ \mathrm{GeV}^2$

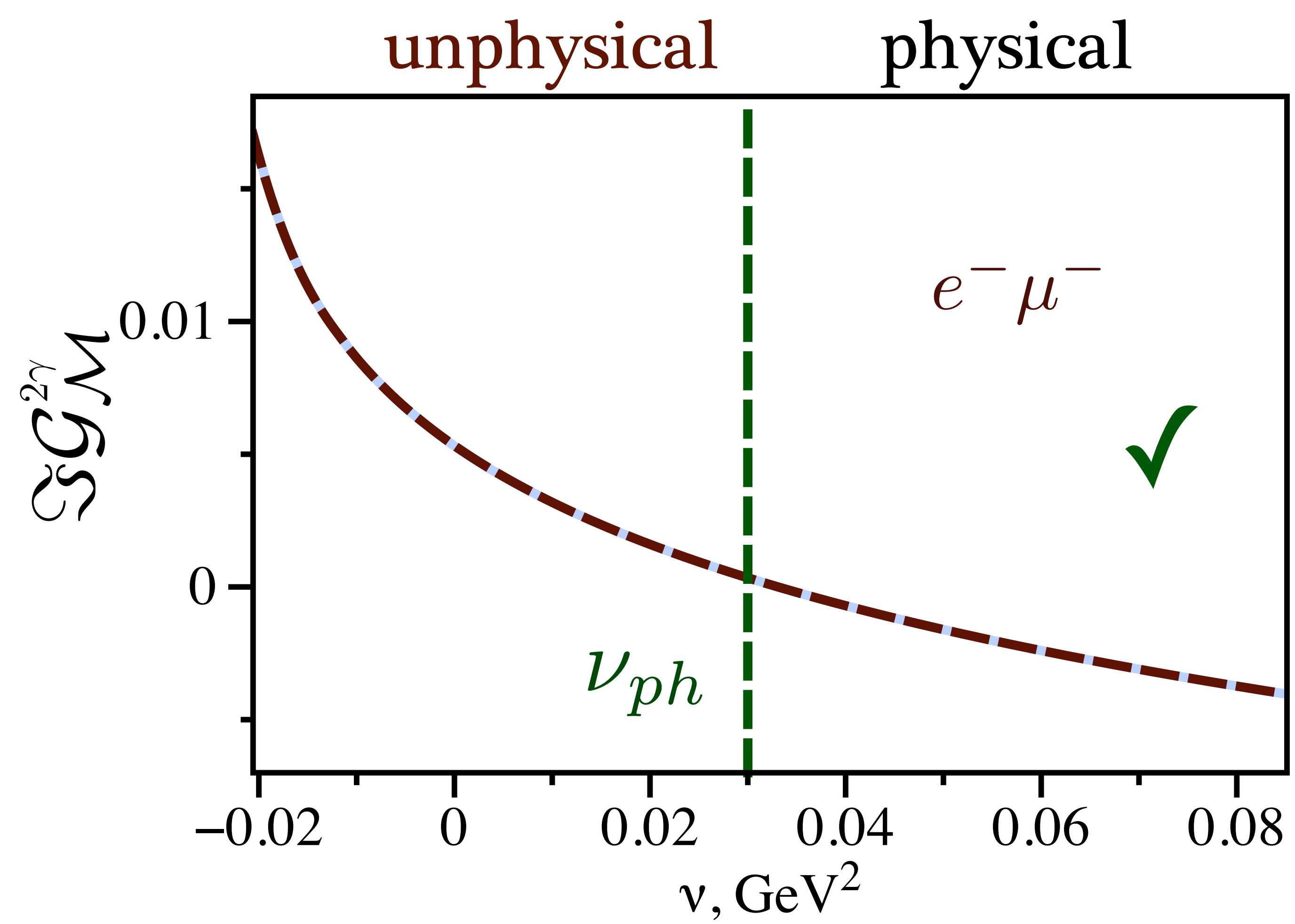

- numerical method of analytical continuation

Hadronic model vs. dispersion relations

- imaginary parts are reproduced for all amplitudes

- real parts are reproduced by unsubtracted disp. relations for

  - $F_D F_D$ amplitudes — all amplitudes

  - $F_D F_P$ amplitudes — $\mathcal{G}_M, \ \mathcal{F}_2, \ \mathcal{F}_3, \ \mathcal{F}_5$

  - $F_P F_P$ amplitudes — $\mathcal{G}_M + \dfrac{\nu}{M^2}\mathcal{F}_3, \ \mathcal{F}_2, \ \mathcal{F}_5$

32

Hadronic model vs. dispersion relations

- imaginary parts are reproduced for all amplitudes

- real parts are reproduced by unsubtracted disp. relations for

  - $F_D F_D$ amplitudes — all amplitudes
  - $F_D F_P$ amplitudes — $\mathcal{G}_M, \ \mathcal{F}_2, \ \mathcal{F}_3, \ \mathcal{F}_5$
  - $F_P F_P$ amplitudes — $\mathcal{G}_M + \frac{\nu}{M^2}\mathcal{F}_3, \ \mathcal{F}_2, \ \mathcal{F}_5$

- fixed-Q^2 subtracted dispersion relation works for all amplitudes

33

Hadronic model vs. dispersion relations

- imaginary parts are reproduced for all amplitudes

- real parts are reproduced by unsubtracted disp. relations for

  - $F_D F_D$ amplitudes — all amplitudes
  - $F_D F_P$ amplitudes — $\mathcal{G}_M, \ \mathcal{F}_2, \ \mathcal{F}_3, \ \mathcal{F}_5$
  - $F_P F_P$ amplitudes — $\mathcal{G}_M + \dfrac{\nu}{M^2}\mathcal{F}_3, \ \mathcal{F}_2, \ \mathcal{F}_5$

- fixed-Q^2 subtracted dispersion relation works for all amplitudes

- Regge analysis: amplitude $\mathcal{F}_4$ can be constant

- hadronic model violates unitarity
- amplitude $\mathcal{F}_4$ could require a subtraction

Low Q² and unsubtracted disp. relations

- amplitudes behaviour at $Q^2 \to 0$:

$$\mathcal{G}_1 \to 0$$
$$\mathcal{G}_2 \to 0$$
$$\mathcal{G}_4 \to 0$$

$$\Rightarrow$$

$$\boxed{\delta_{2\gamma} \to 0}$$

Low Q² and unsubtracted disp. relations

- amplitudes behaviour at $Q^2 \to 0$:

$$\mathcal{G}_1 \to 0 \qquad \mathcal{G}_2 \to 0 \qquad \mathcal{G}_4 \to 0$$

$$\Rightarrow \quad \boxed{\delta_{2\gamma} \to 0}$$

- proton state contribution to 2γ correction:

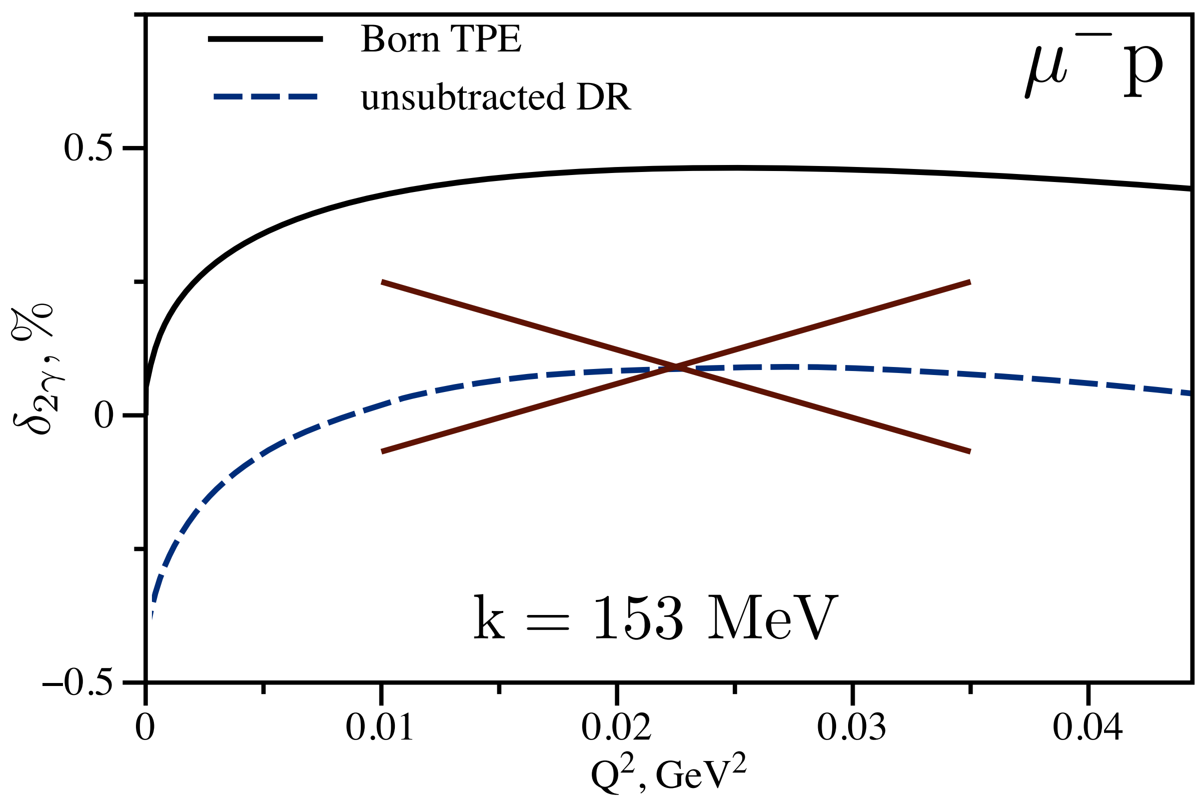

Low Q² and unsubtracted disp. relations

- amplitudes behaviour at $Q^2 \to 0$:

$$\mathcal{G}_1 \to 0$$
$$\mathcal{G}_2 \to 0$$
$$\mathcal{G}_4 \to 0$$

$\Rightarrow$

$$\delta_{2\gamma} \to 0$$

- proton state contribution to 2γ correction:

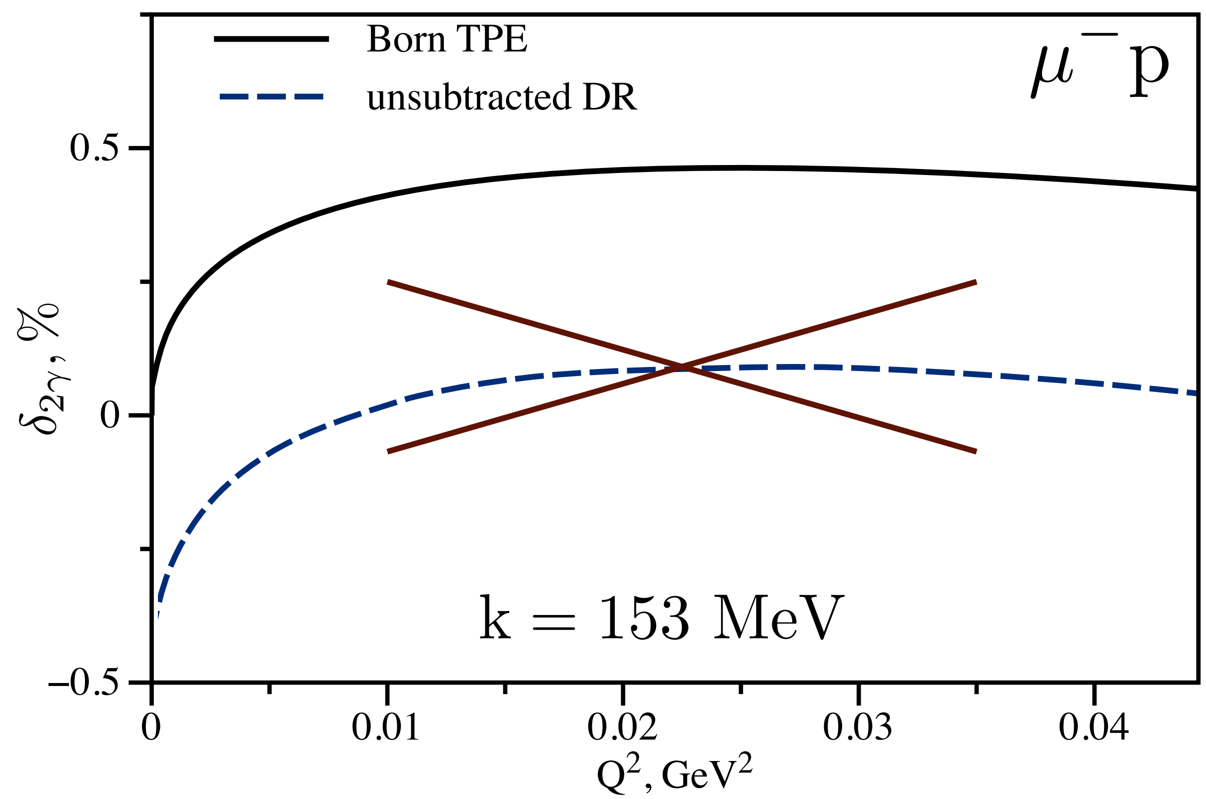

problematic amplitude

$$\mathcal{G}_4 = \mathcal{F}_4 + \frac{\nu}{M^2(1+\tau)}\mathcal{F}_5$$

- dispersion relations approach requires a subtraction

Hadronic model results

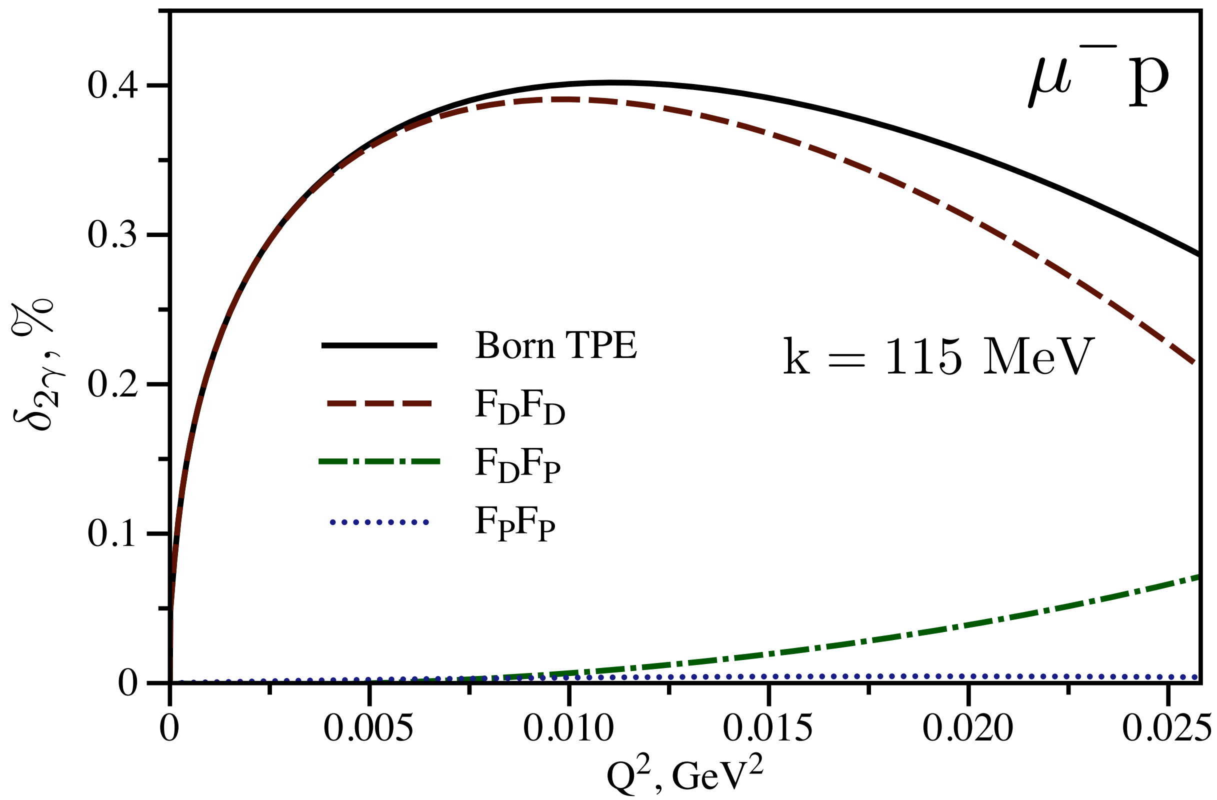

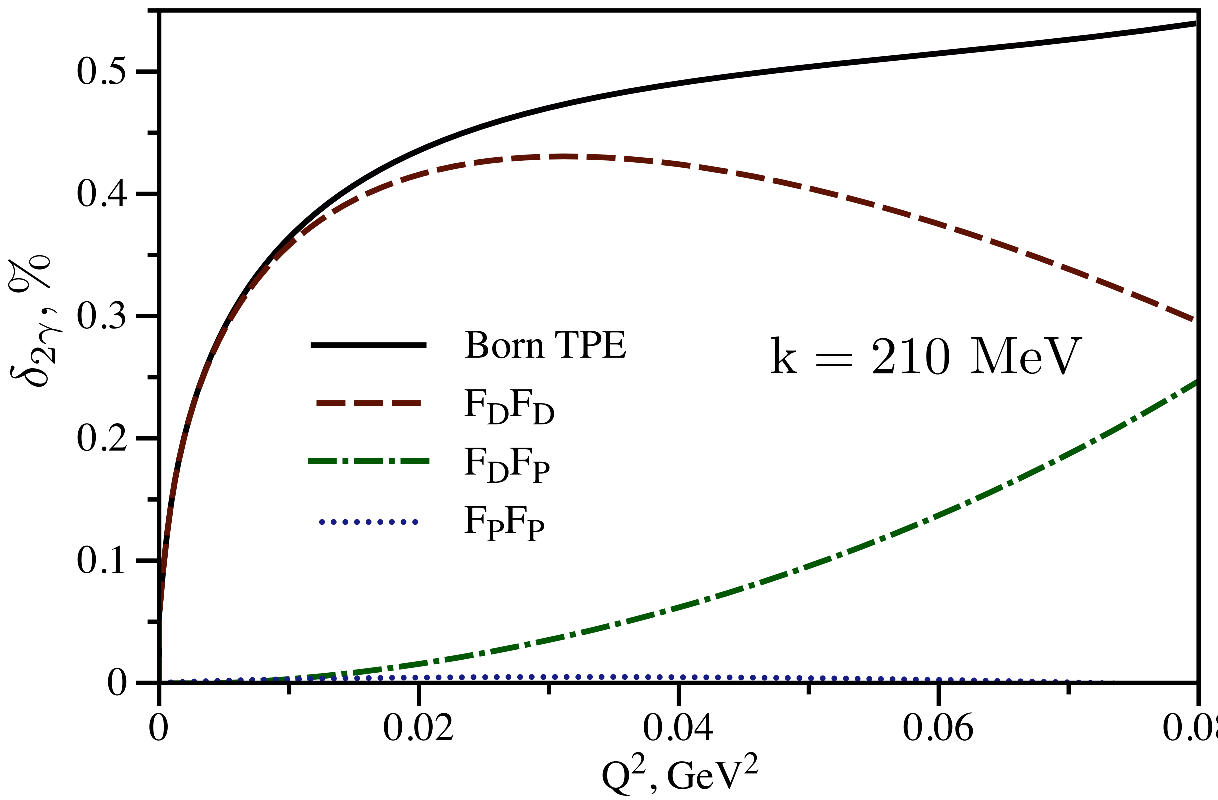

- $F_D F_D$ contribution dominates

Hadronic model results

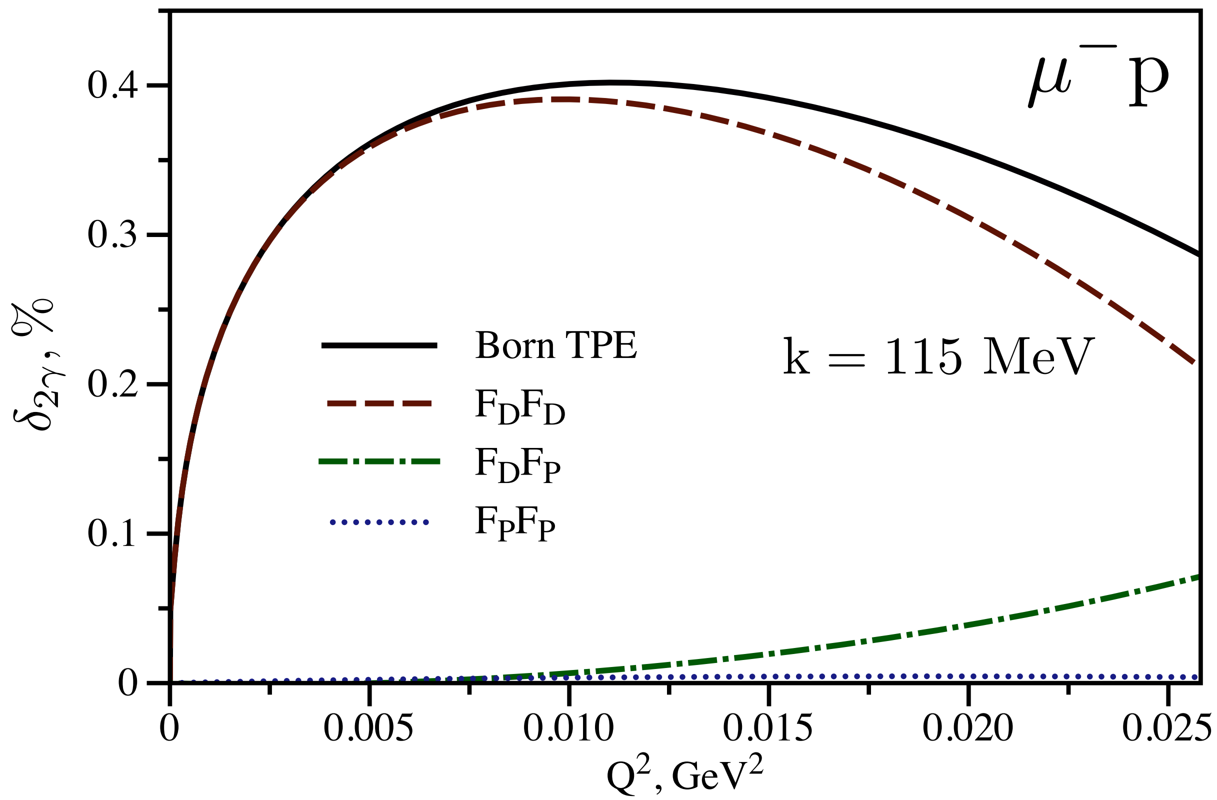

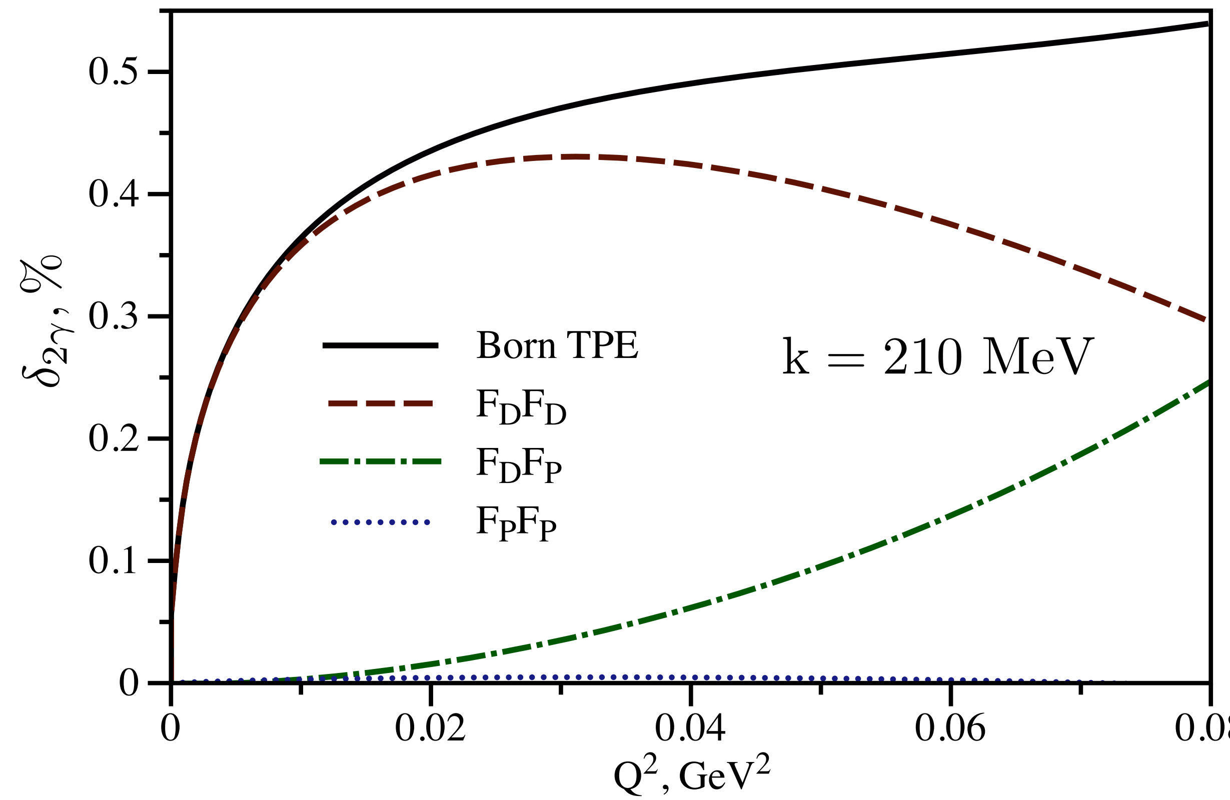

- $F_D F_D$ contribution dominates

expected muon over electron ratio

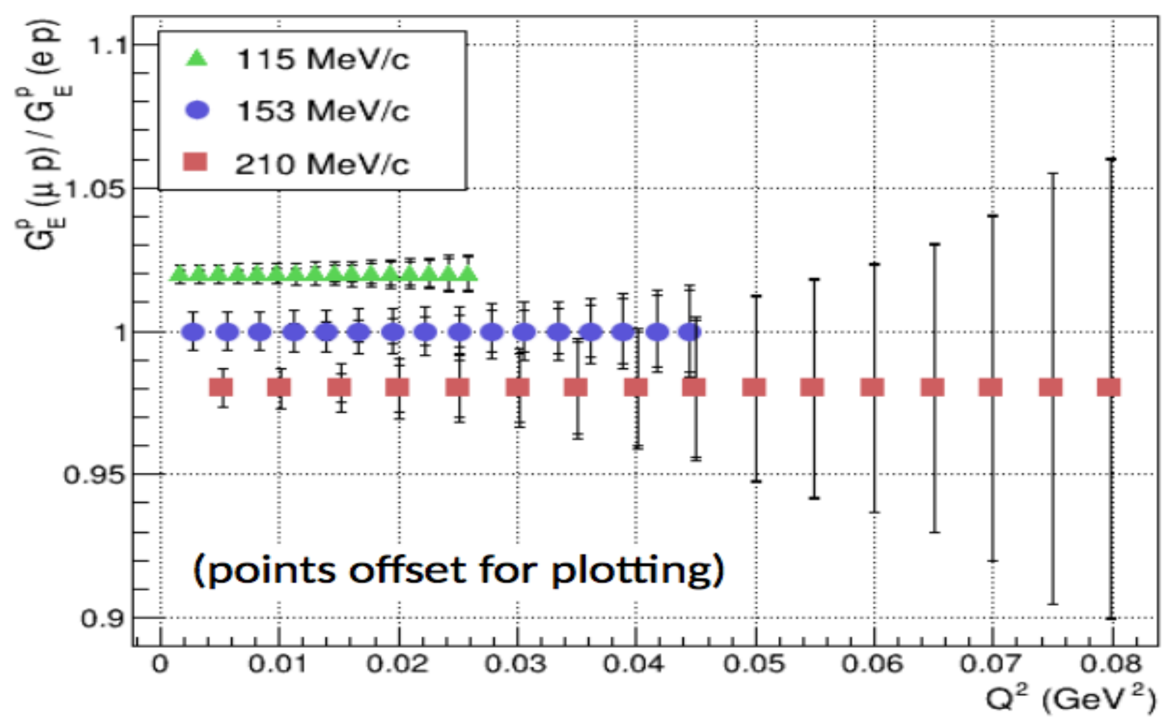

K. Mesick talk (PAVI 2014), MUSE TDR (2016)

- 2γ: experimental accuracy level

Low-Q² inelastic 2ɣ correction

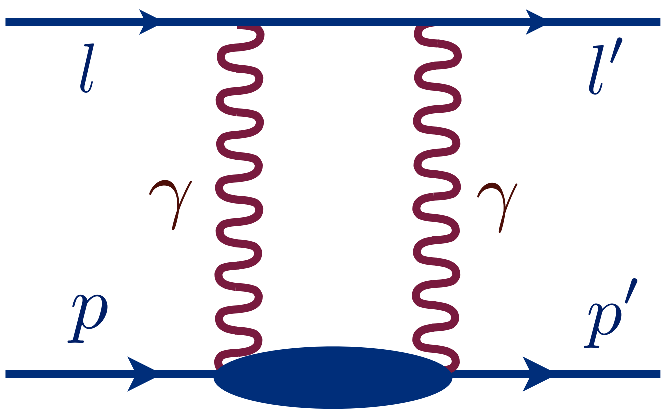

- 2ɣ blob: near-forward virtual Compton scattering

Feshbach inelastic elastic

$$\text{ep}: \quad \delta_{2\gamma} \sim a\,\sqrt{Q^2} + b\,Q^2 \ln Q^2 + c\,Q^2 \ln^2 Q^2$$

R. W. Brown (1970), O. T. and M. Vanderhaeghen (2014-2015)

subtraction function + unpolarized proton structure

M. E. Christy, P. E. Bosted (2010)

$$\delta_{2\gamma} = \int \mathrm{d}\nu_\gamma \mathrm{d}Q^2 (w_1(\nu_\gamma, Q^2) \cdot F_1(\nu_\gamma, Q^2) + w_2(\nu_\gamma, Q^2) \cdot F_2(\nu_\gamma, Q^2))$$

Low-Q² inelastic 2ɣ correction

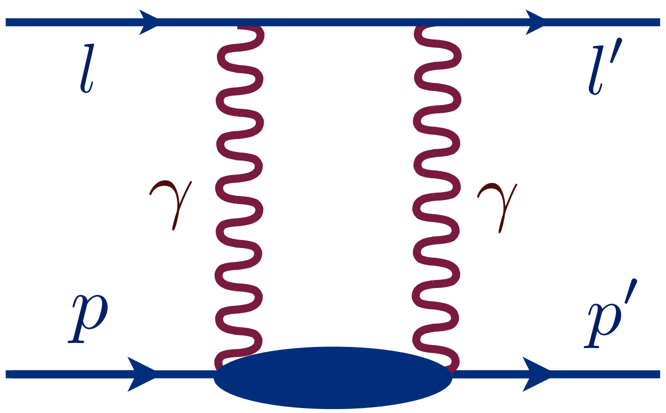

- 2ɣ blob: near-forward virtual Compton scattering

Feshbach inelastic elastic

$$\text{ep}: \quad \delta_{2\gamma} \sim a\,\sqrt{Q^2} + b\,Q^2 \ln Q^2 + c\,Q^2 \ln^2 Q^2$$

R. W. Brown (1970), O. T. and M. Vanderhaeghen (2014-2015)

subtraction function + unpolarized proton structure

M. E. Christy, P. E. Bosted (2010)

$$\delta_{2\gamma} = \int \mathrm{d}\nu_\gamma \mathrm{d}Q^2 (w_1(\nu_\gamma, Q^2) \cdot F_1(\nu_\gamma, Q^2) + w_2(\nu_\gamma, Q^2) \cdot F_2(\nu_\gamma, Q^2))$$

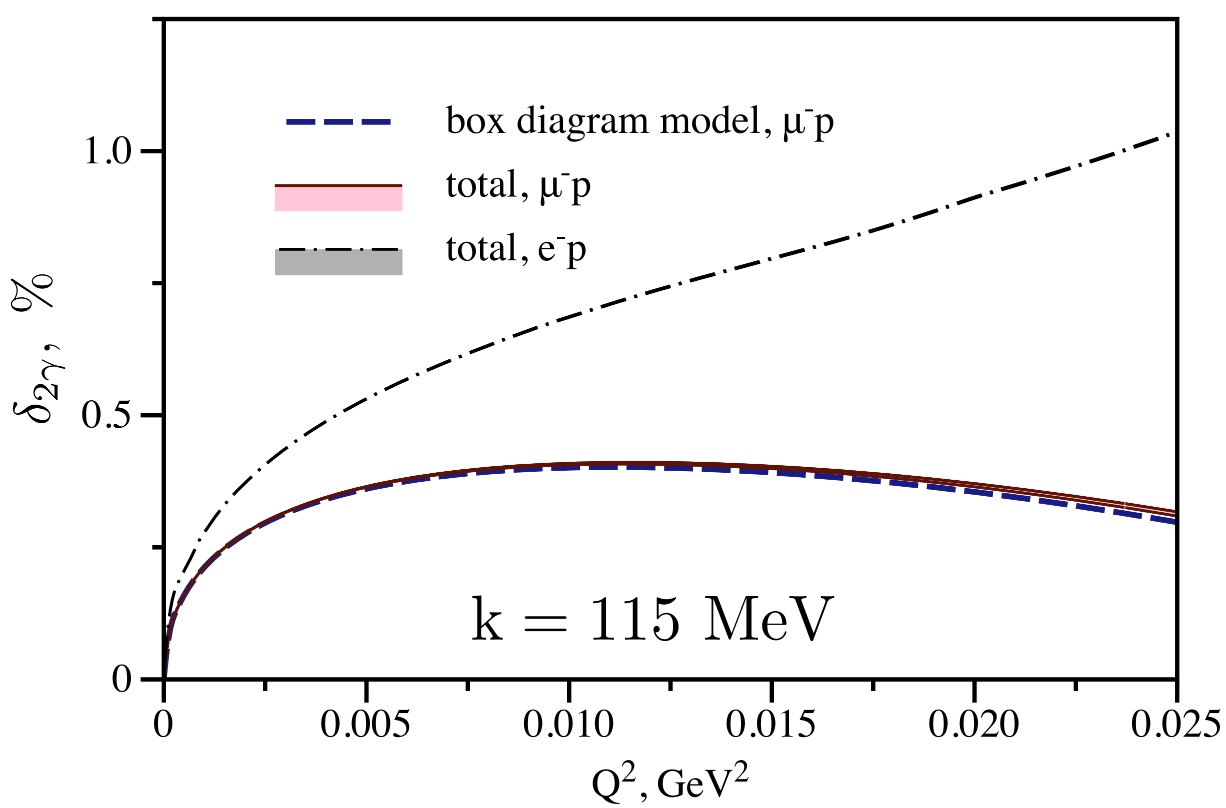

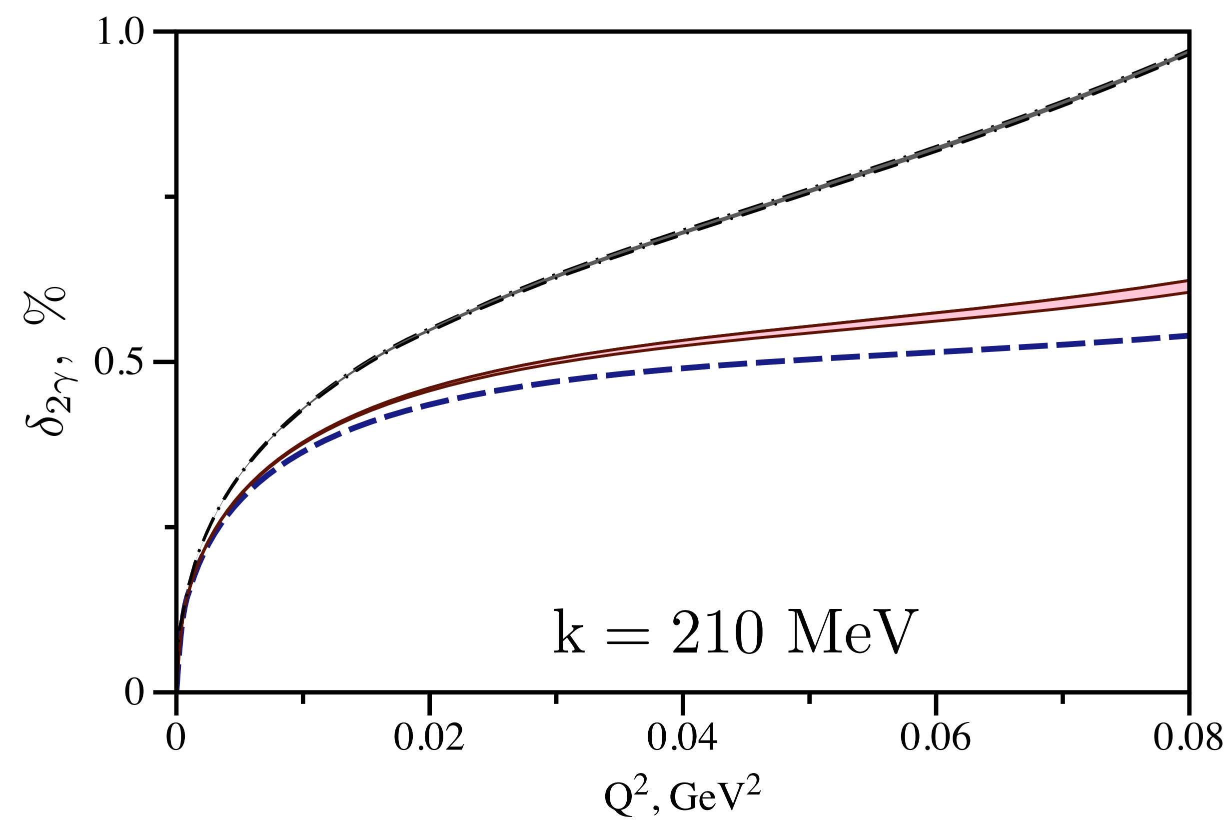

- MUSE can test r_E in one charge channel

Subtracted dispersion relations

- subtraction function in Compton scattering → $\mathcal{F}_4$

- fix subtraction to model estimate

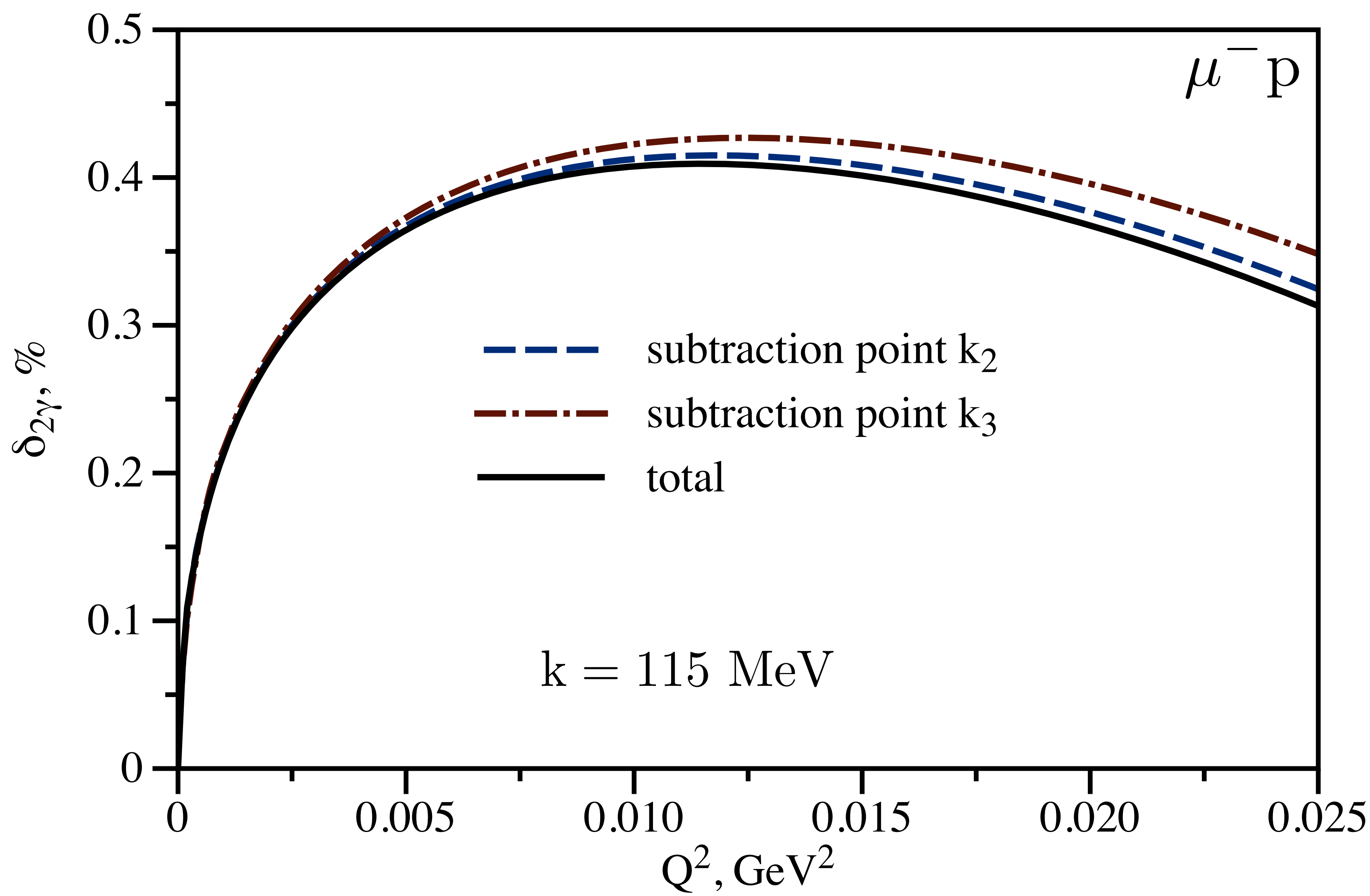

- result is similar to model calculation. Expect data

COMPASS proton radius experiment

- elastic μp scattering at SPS with 100 GeV beam

- measure $\mathrm{G_E^2} + \tau \mathrm{G_M^2}$ at forward angles

- test runs in 2018 and 2021; data taking in 2022

COMPASS proton radius experiment

- elastic μp scattering at SPS with 100 GeV beam

- measure $\mathrm{G_E^2} + \tau \mathrm{G_M^2}$ at forward angles

- test runs in 2018 and 2021; data taking in 2022

2ɣ corrections?

- **$\mathrm{F_D F_D}$** contribution dominates

- Feshbach correction (+ recoil)

$$\delta_{2\gamma} = \frac{\alpha \pi Q}{2\omega}\left(1 + \frac{m}{M}\right) \rightarrow$$ 2 orders lower than MUSE

- inelastic states: kinematically enhanced

- sub per mille level of 2ɣ in COMPASS kinematics

Hyperfine splitting in ordinary and muonic hydrogen

Lamb shift and hyperfine splitting in H

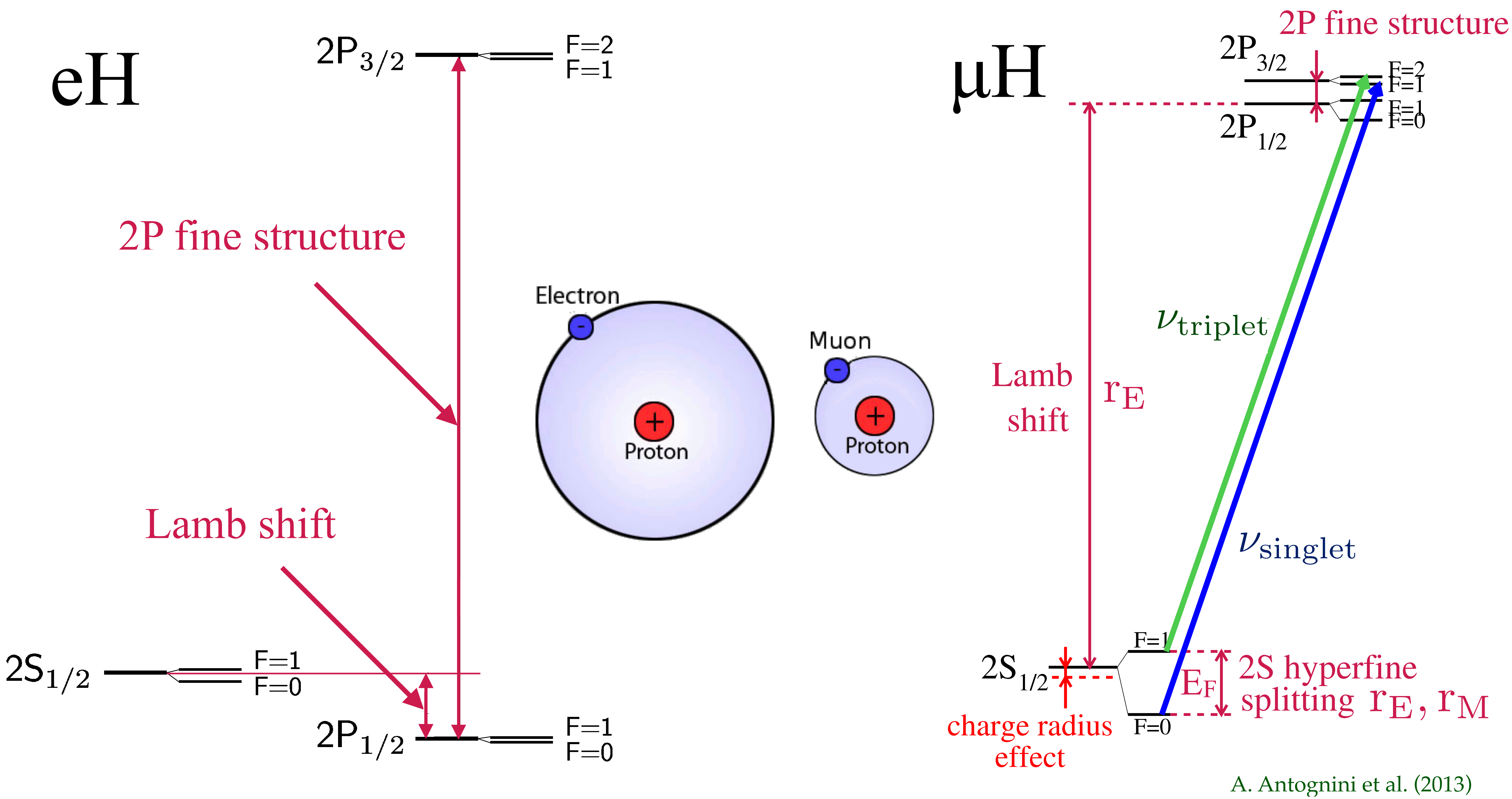

- 1S HFS in μH with 1 ppm accuracy at PSI, J-PARC, RIKEN-RAL

R. Pohl et al. (2016)

2γ correction to μH HFS

$$\delta E^{2\gamma}_{\mathrm{HFS}} = \Delta_{\mathrm{HFS}} E_{\mathrm{F}}$$

$$E_{\mathrm{F}} = \frac{8\alpha^4}{3} \frac{M^2 m^2}{(M+m)^3} \frac{\mu_P}{n^3}$$

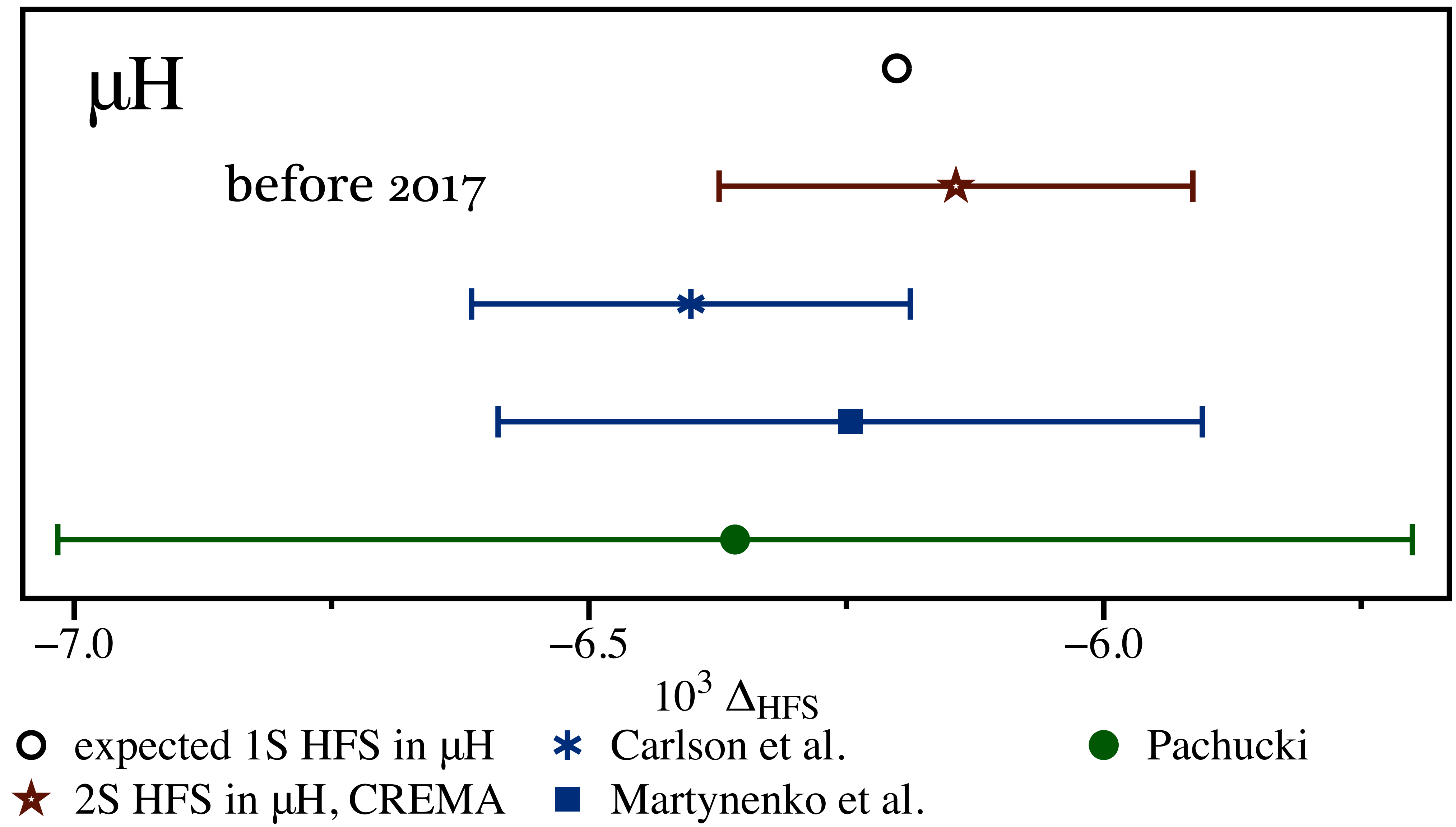

- reduction of uncertainty is needed

Elastic lepton-proton scattering

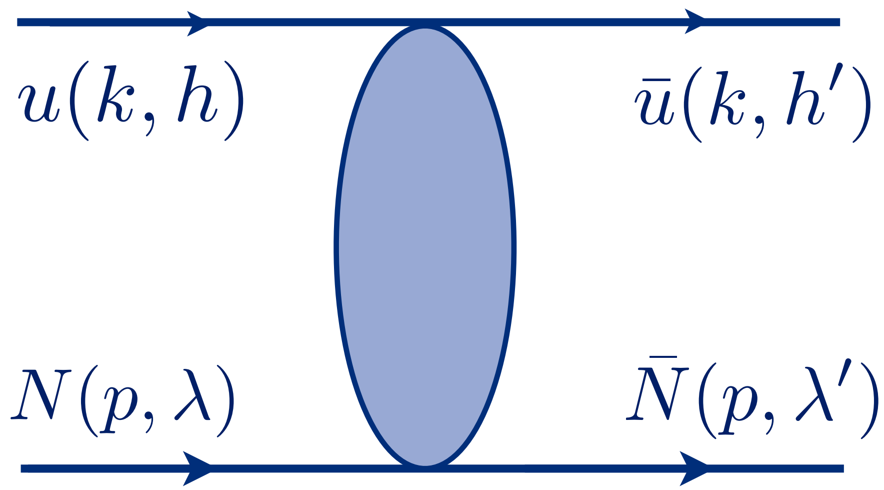

lepton energy

in lab frame

ω

- 3 forward lepton-proton amplitudes:

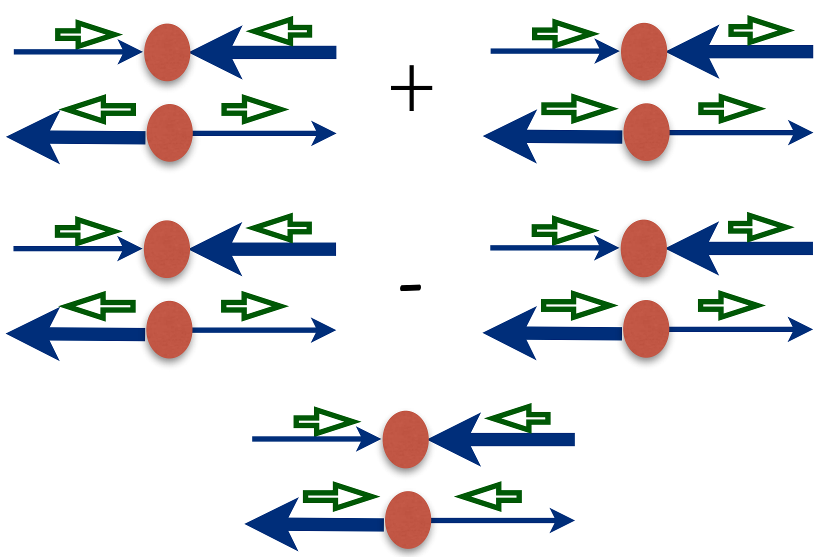

$f_+(\omega)$ unpolarised amplitude

$\left.\begin{array}{l} f_-(\omega) \\ g(\omega) \end{array}\right\}$ polarised amplitudes

Elastic lepton-proton scattering

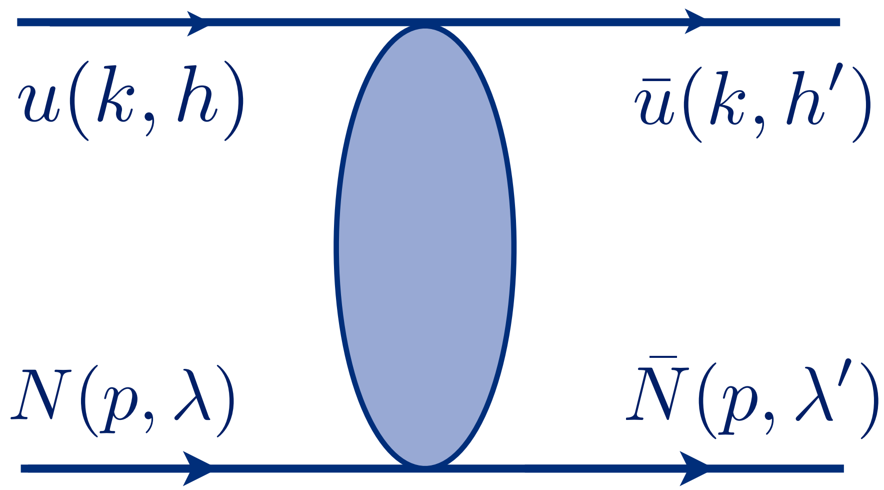

lepton energy

in lab frame

ω

- 3 forward lepton-proton amplitudes:

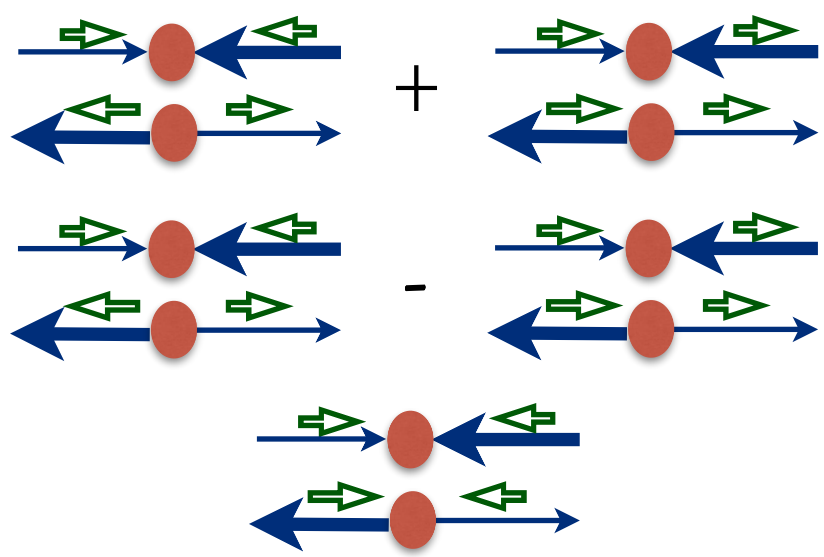

$f_+(\omega)$ unpolarised amplitude

$f_-(\omega)$

$g(\omega)$

polarised amplitudes

- imaginary parts $\leftrightarrow$ cross sections

- 2ɣ correction to energy levels: amplitudes at threshold

Elastic lepton-proton scattering

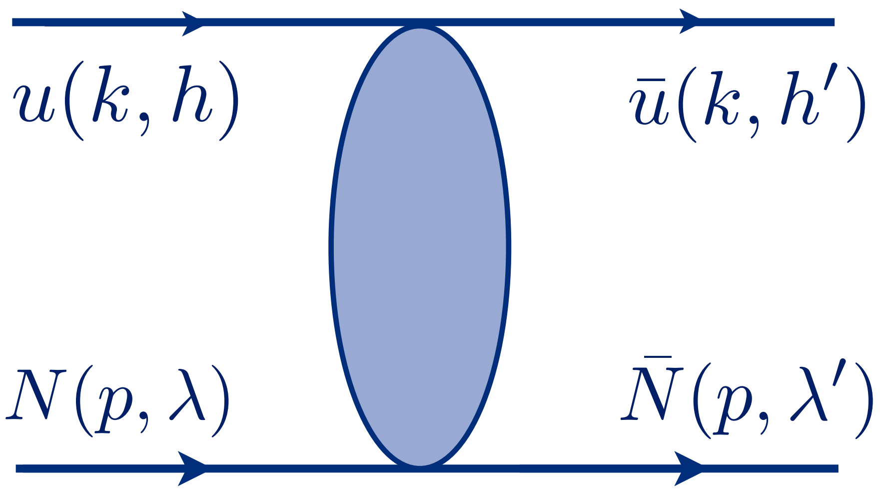

lepton energy

in lab frame

ω

- 3 forward lepton-proton amplitudes:

$$\mathrm{T} = \frac{f_+(\omega)}{4Mm}\,\bar{u}(k,h')u(k,h)\,\bar{N}(p,\lambda')N(p,\lambda)$$

$$-\frac{mf_-(\omega)+\omega g(\omega)}{8M(\omega^2-m^2)}\,\bar{u}(k,h')\gamma^{\mu\nu}u(k,h)\,\bar{N}(p,\lambda')\gamma_{\mu\nu}N(p,\lambda)$$

$$+\frac{\omega f_-(\omega)+mg(\omega)}{4M(\omega^2-m^2)}\,\bar{u}(k,h')\gamma_\mu\gamma_5 u(k,h)\,\bar{N}(p,\lambda')\gamma^\mu\gamma_5 N(p,\lambda)$$

Elastic lepton-proton scattering

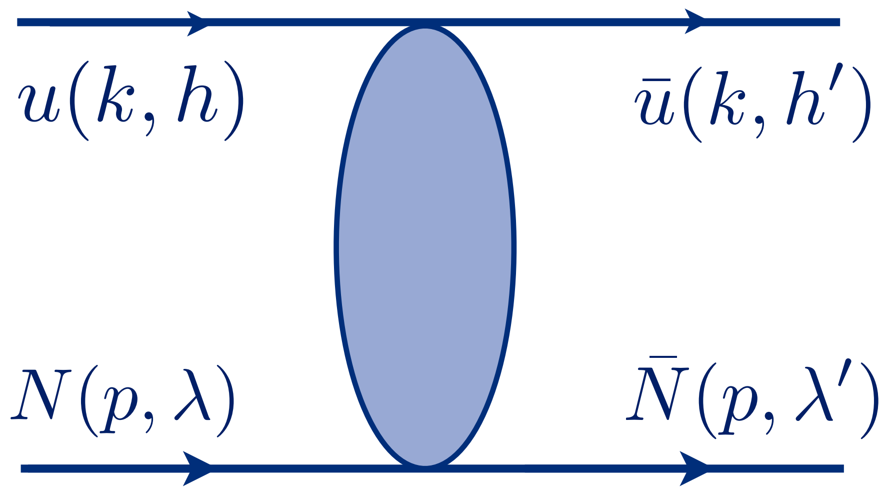

lepton energy

in lab frame

ω

- 3 forward lepton-proton amplitudes:

$$\mathrm{T} = \frac{f_+(\omega)}{4Mm}\,\bar{u}(k,h')u(k,h)\,\bar{N}(p,\lambda')N(p,\lambda)$$

$$-\frac{mf_-(\omega)+\omega g(\omega)}{8M(\omega^2-m^2)}\,\bar{u}(k,h')\gamma^{\mu\nu}u(k,h)\,\bar{N}(p,\lambda')\gamma_{\mu\nu}N(p,\lambda)$$

$$+\frac{\omega f_-(\omega)+mg(\omega)}{4M(\omega^2-m^2)}\,\bar{u}(k,h')\gamma_\mu\gamma_5u(k,h)\,\bar{N}(p,\lambda')\gamma^\mu\gamma_5N(p,\lambda)$$

- relation to non-forward amplitudes:

$$f_+(\omega) = e^2 2M\omega\,\frac{\delta_{2\gamma}(\omega,Q^2)}{Q^2}\bigg|_{Q^2\to 0} \qquad f_-(\omega) = e^2\mathcal{G}_M\left(\omega,Q^2=0\right) \qquad g(\omega) = -e^2\frac{m}{M}\mathcal{F}_6\left(\omega,Q^2=0\right)$$

2γ exchange

- 2γ through experimental input:

Compton amplitudes

Carlson et al. (2008)

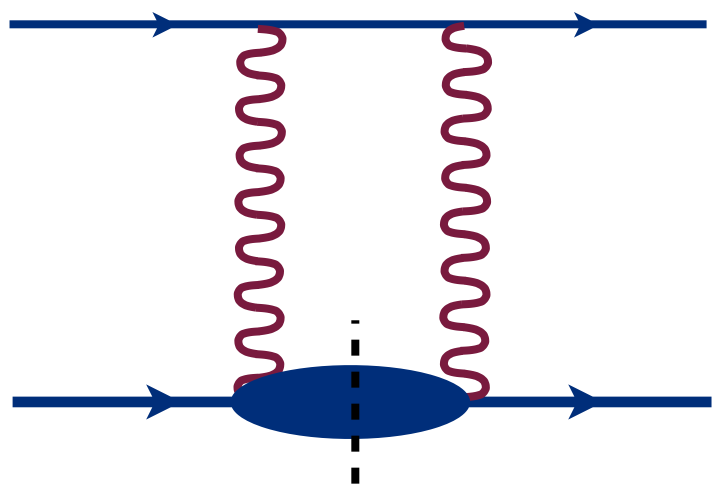

$\stackrel{?}{=}$

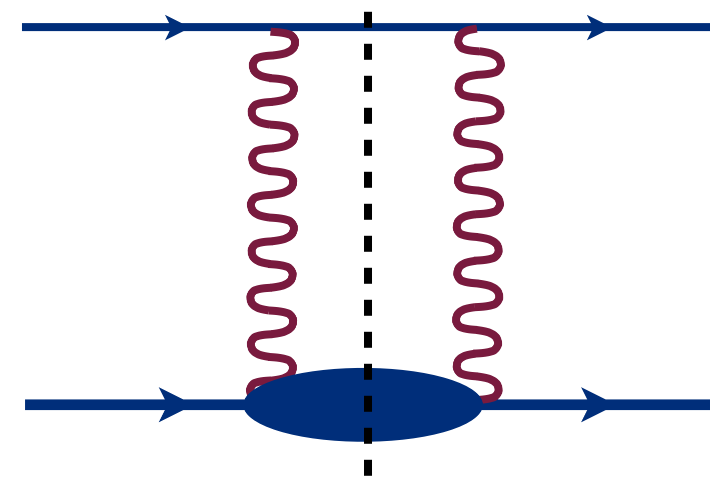

lepton-proton amplitudes

Dispersion relation framework

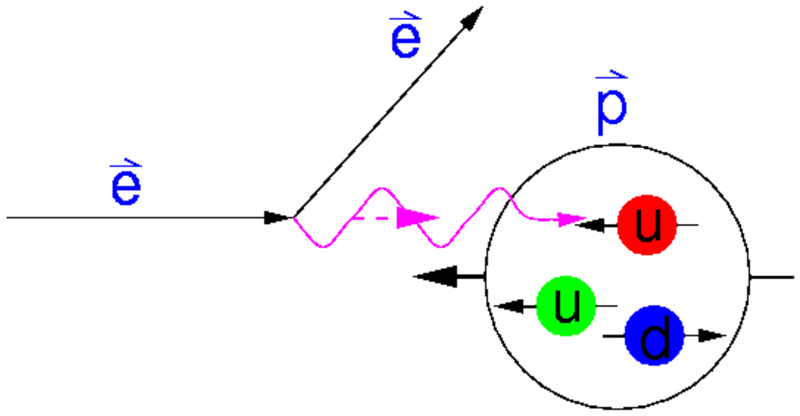

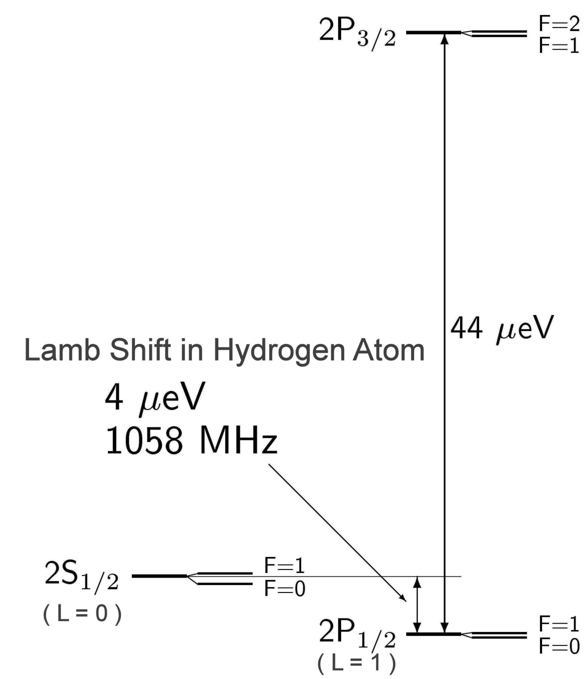

$f(z)$

analyticity

experimental cross sections

energy levels correction

optical theorem

$$\Re\mathcal{F}(\nu) = \frac{2\nu}{\pi}\mathcal{P}\int_{\nu_{th}}^{\infty}\frac{\Im\mathcal{F}(\nu'+i0)}{\nu'^2-\nu^2}\mathrm{d}\nu'$$

DR

amplitudes: imaginary parts

amplitudes: real parts

2γ exchange

- 2γ through experimental input:

Compton amplitudes
Carlson et al. (2008)

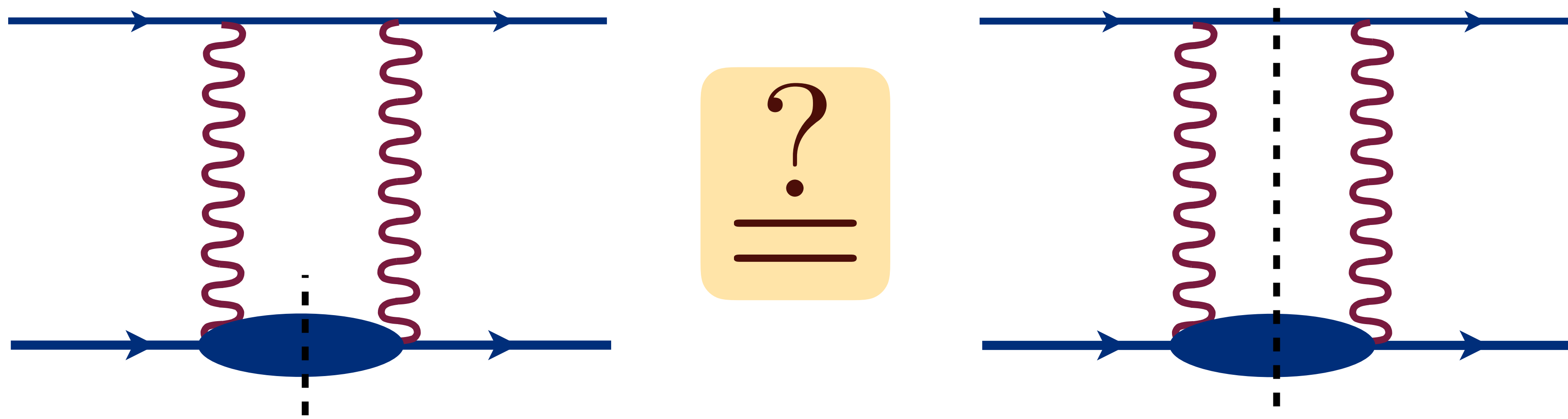

lepton-proton amplitudes

- subtraction is needed for unpolarised amplitude $f_+^{2\gamma}$
- distinct result for polarised amplitude $g^{2\gamma}$
- distinct result for lp $\rightarrow$ lX channel contribution

2γ exchange

- 2γ through experimental input:

Compton amplitudes

Carlson et al. (2008)

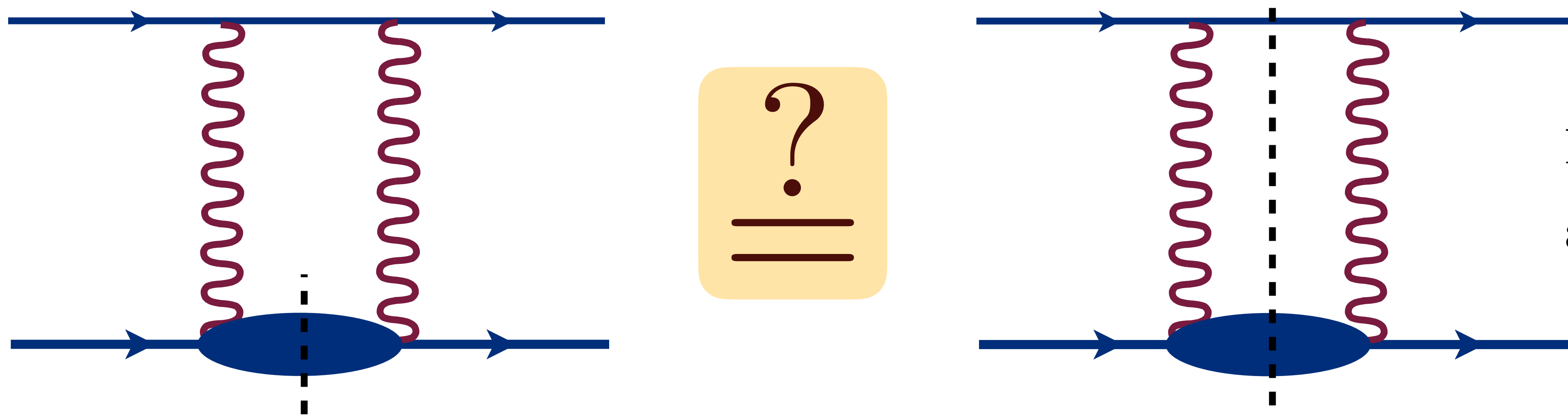

lepton-proton amplitudes

- subtraction is needed for unpolarised amplitude $f_+^{2\gamma}$
- distinct result for polarised amplitude $g^{2\gamma}$
- distinct result for lp $\rightarrow$ lX channel contribution

$$\int_0^1 g_2(x, Q^2)\mathrm{d}x = 0$$

- polarised amplitudes are in agreement
- new derivation of Burkhardt-Cottingham sum rule

Hyperfine splitting correction

- effective Hamiltonian:

$$\mathrm{H} \equiv -f_+^{2\gamma} - 4g^{2\gamma}\vec{\mathrm{S}}\cdot\vec{\mathrm{s}} - 4(f_-^{2\gamma} + g^{2\gamma})(\vec{\mathrm{S}}\cdot\hat{p})(\vec{\mathrm{s}}\cdot\hat{k})$$

Hyperfine splitting correction

$$\int_0^1 g_2(x, Q^2)\mathrm{d}x = 0$$

- effective Hamiltonian:

$$\mathrm{H} \equiv -f_+^{2\gamma} - 4g^{2\gamma}\vec{\mathrm{S}}\cdot\vec{\mathrm{s}} - 4(f_-^{2\gamma} + g^{2\gamma})(\vec{\mathrm{S}}\cdot\hat{p})(\vec{\mathrm{s}}\cdot\hat{k}) = -f_+^{2\gamma} + 4f_-^{2\gamma}\vec{\mathrm{S}}\cdot\vec{\mathrm{s}}$$

Hyperfine splitting correction

$$\int_0^1 g_2(x,Q^2)\,\mathrm{d}x = 0$$

- effective Hamiltonian:

$$\mathrm{H} \equiv -f_+^{2\gamma} - 4g^{2\gamma}\vec{\mathrm{S}}\cdot\vec{\mathrm{s}} - 4(f_-^{2\gamma}+g^{2\gamma})(\vec{\mathrm{S}}\cdot\hat{p})(\vec{\mathrm{s}}\cdot\hat{k}) = -f_+^{2\gamma} + 4f_-^{2\gamma}\vec{\mathrm{S}}\cdot\vec{\mathrm{s}}$$

- amplitude decomposition:

$$\mu_{\mathrm{P}} e^2 \Delta_{\mathrm{HFS}} = -g^{2\gamma}(m) + \frac{1}{2}f_-^{2\gamma}(m) = \frac{3}{2}f_-^{2\gamma}(m)$$

- traditional decomposition:

$$\Delta_{\mathrm{HFS}} = \Delta_{\mathrm{Z}} + \Delta^{\mathrm{R}} + \Delta^{\mathrm{pol}}$$

Zemach term
$\mathrm{G_E},\ \mathrm{G_M}$

recoil correction
$\mathrm{G_E},\ \mathrm{G_M}$

polarizability
$\mathrm{F}_2,\ g_1,\ g_2$

Hyperfine splitting correction

$$\int_0^1 g_2(x,Q^2)\mathrm{d}x = 0$$

- effective Hamiltonian:

$$\mathrm{H} \equiv -f_+^{2\gamma} - 4g^{2\gamma}\vec{\mathrm{S}}\cdot\vec{\mathrm{s}} - 4(f_-^{2\gamma}+g^{2\gamma})(\vec{\mathrm{S}}\cdot\hat{p})(\vec{\mathrm{s}}\cdot\hat{k}) = -f_+^{2\gamma} + 4f_-^{2\gamma}\vec{\mathrm{S}}\cdot\vec{\mathrm{s}}$$

- amplitude decomposition:

$$\mu_{\mathrm{P}} e^2 \Delta_{\mathrm{HFS}} = -g^{2\gamma}(m) + \frac{1}{2}f_-^{2\gamma}(m) = \frac{3}{2}f_-^{2\gamma}(m)$$

- traditional decomposition:

$$\Delta_{\mathrm{HFS}} = \Delta_{\mathrm{Z}} + \Delta^{\mathrm{R}} + \Delta^{\mathrm{pol}}$$

Zemach term
$\mathrm{G_E},\ \mathrm{G_M}$

recoil correction
$\mathrm{G_E},\ \mathrm{G_M}$

polarizability
$\mathrm{F_2},\ g_1,\ g_2$

- uncertainty budget:

> 100 ppm

< 10 ppm

100 ppm

Zemach correction in μH

- **Zemach correction expanding form factors:**

$$\Delta_{\mathrm{Z}} = \frac{8\alpha m_r}{\pi} \int_{Q_0}^{\infty} \frac{\mathrm{d}Q}{Q^2} \left(\frac{\mathrm{G_M}\left(Q^2\right) \mathrm{G_E}\left(Q^2\right)}{\mu_{\mathrm{P}}} - 1 \right) + \frac{4\alpha m_r Q_0}{3\pi} \left(-\mathrm{r_E^2} - \mathrm{r_M^2} + \frac{\mathrm{r_E^2 r_M^2}}{18} Q_0^2 \right)$$

Zemach correction in μH

- Zemach correction expanding form factors:

$$\Delta_{\mathrm{Z}} = \frac{8\alpha m_r}{\pi}\int\limits_{Q_0}^{\infty}\frac{\mathrm{d}Q}{Q^2}\left(\frac{\mathrm{G_M}\left(Q^2\right)\mathrm{G_E}\left(Q^2\right)}{\mu_{\mathrm{P}}}-1\right)+\frac{4\alpha m_r Q_0}{3\pi}\left(-\mathrm{r_E^2}-\mathrm{r_M^2}+\frac{\mathrm{r_E^2 r_M^2}}{18}Q_0^2\right)$$

- dependence on splitting: consistency check

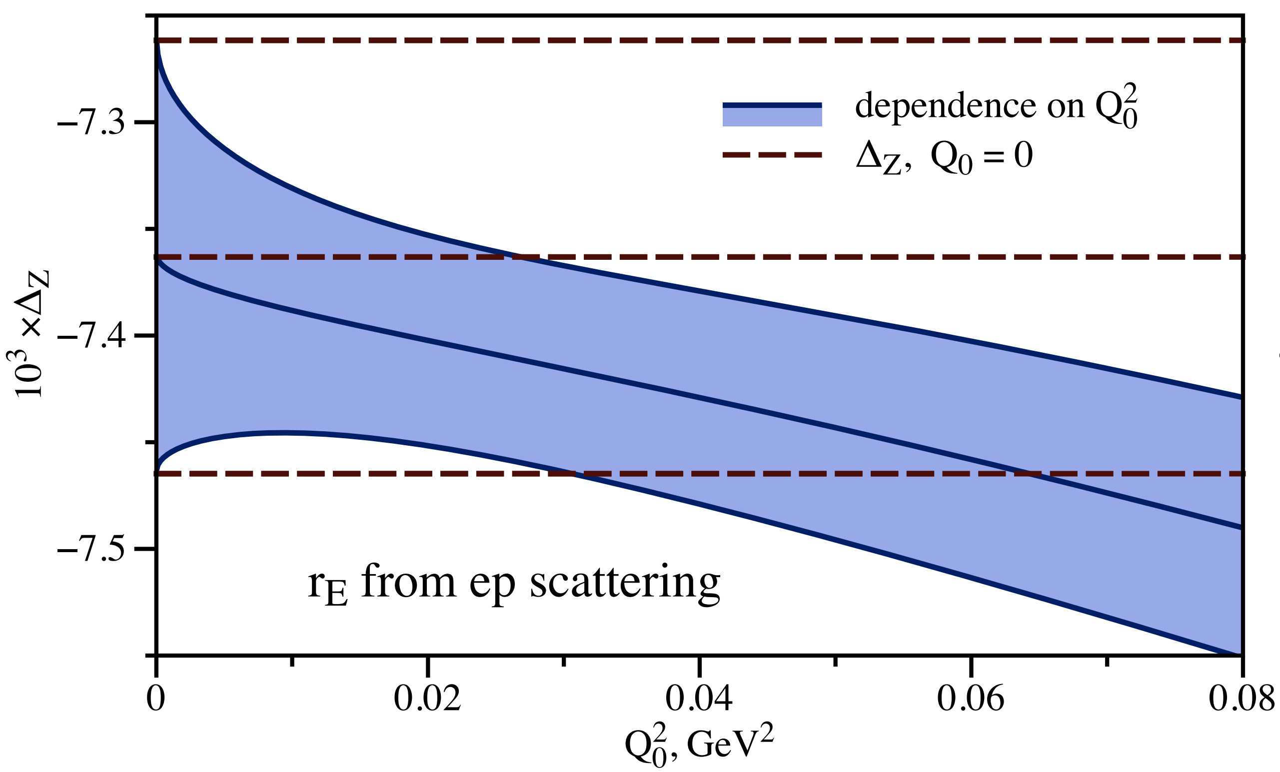

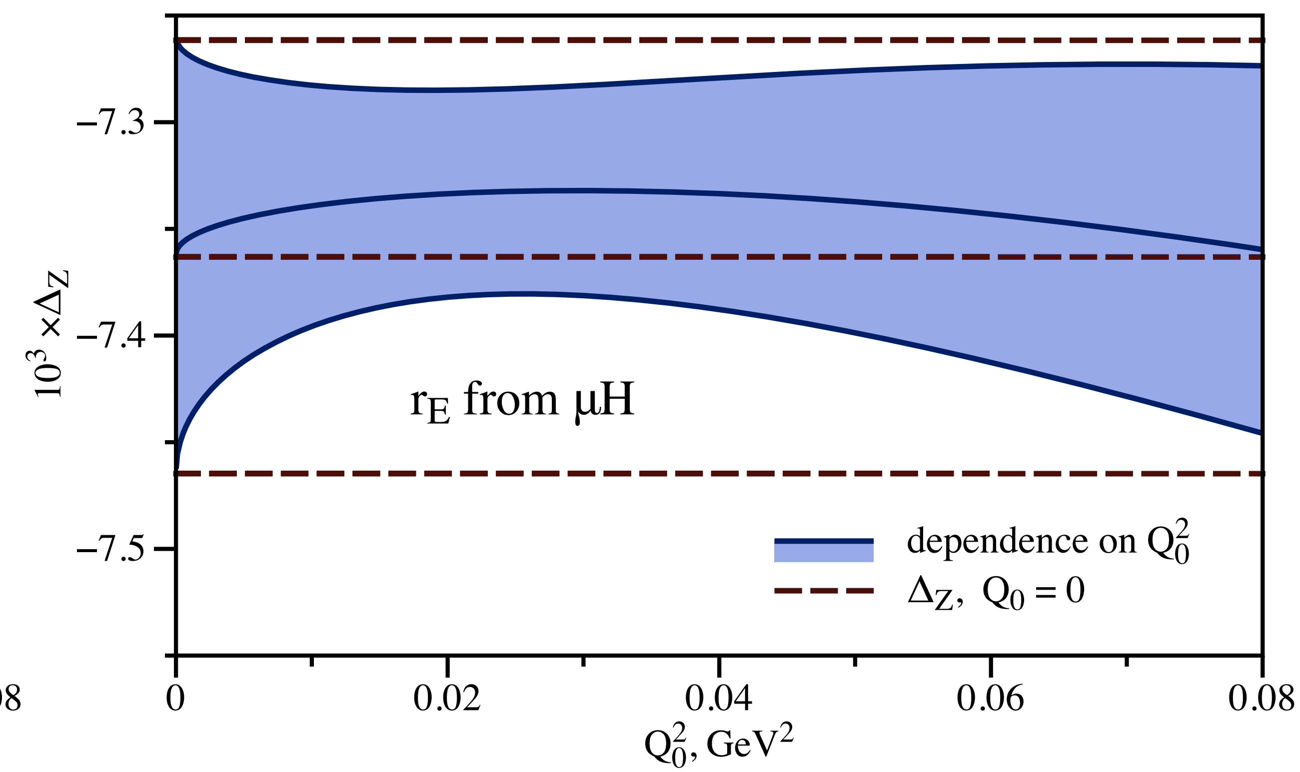

Zemach correction in μH

- Zemach correction expanding form factors:

$$\Delta_Z = \frac{8\alpha m_r}{\pi} \int_{Q_0}^{\infty} \frac{dQ}{Q^2} \left(\frac{G_M(Q^2)\, G_E(Q^2)}{\mu_P} - 1 \right) + \frac{4\alpha m_r Q_0}{3\pi} \left(-r_E^2 - r_M^2 + \frac{r_E^2 r_M^2}{18} Q_0^2 \right)$$

- dependence on splitting: consistency check

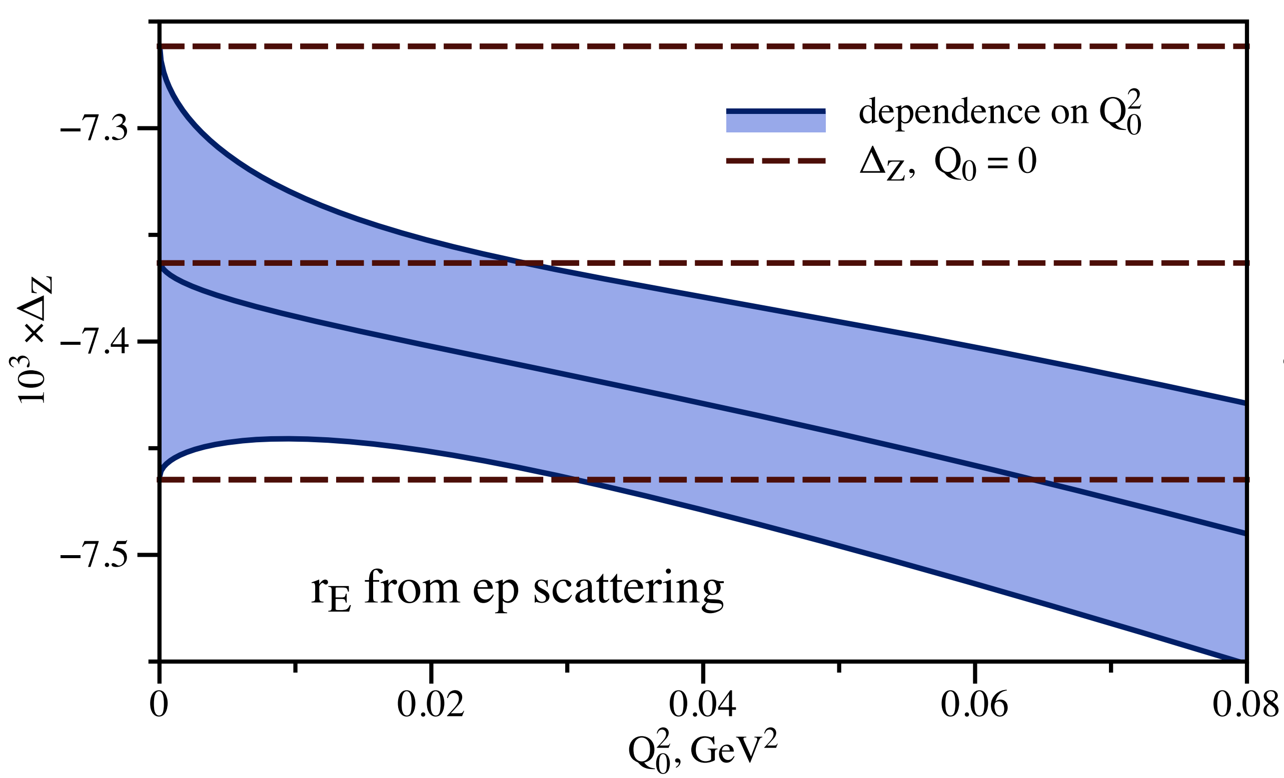

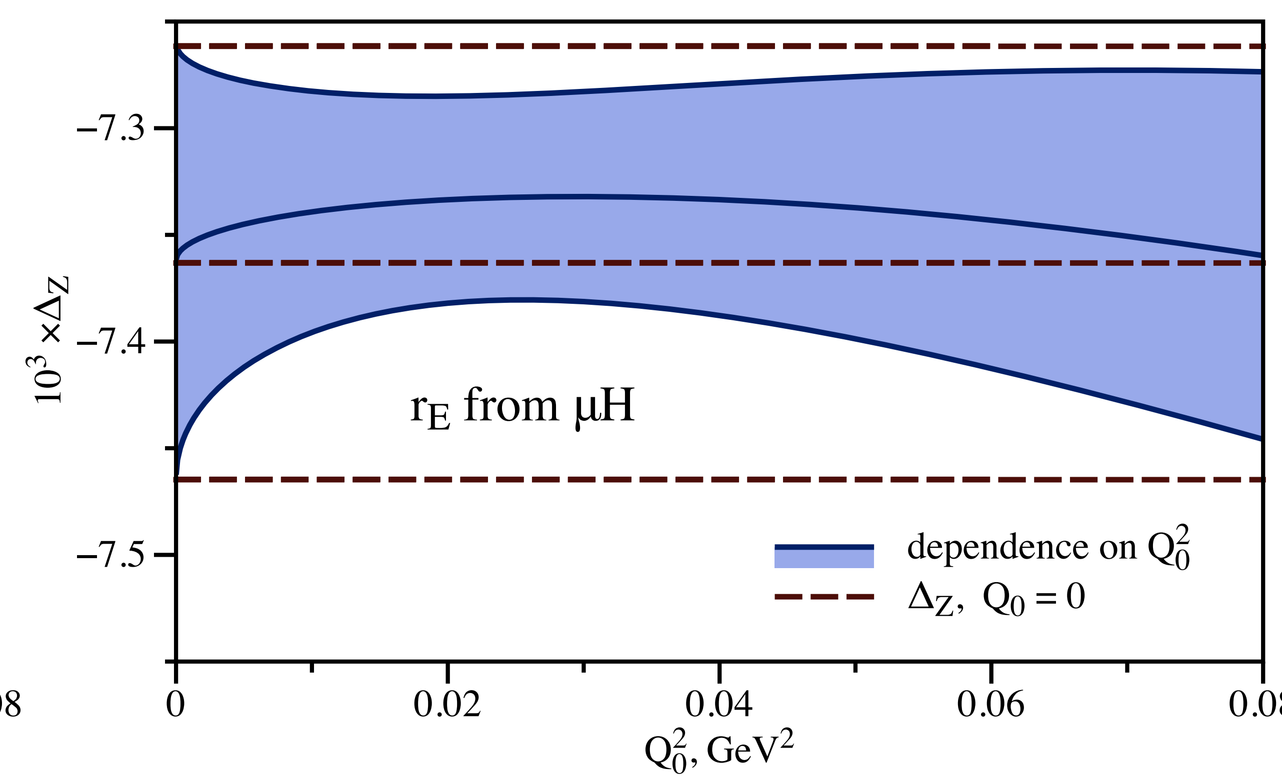

- 95 ppm change for μH and ep radii with $Q_0 = 0.2$ GeV

- 1.5-2 times more precise
- magnetic radius is equally important

2γ correction in eH 1S HFS

- measurements of 1S HFS in eH (21 cm line):

$$\nu_{\rm HFS}(\mathrm{H}) = 1420.4057517667(9)\ \mathrm{MHz} \qquad \text{1970th}$$

2γ correction in eH 1S HFS

- measurements of 1S HFS in eH (21 cm line):

$$\nu_{\mathrm{HFS}}(\mathrm{H}) = 1420.4057517667(9)\ \mathrm{MHz}$$ 1970th

- accuracy 10^{-12} - precise extraction of TPE

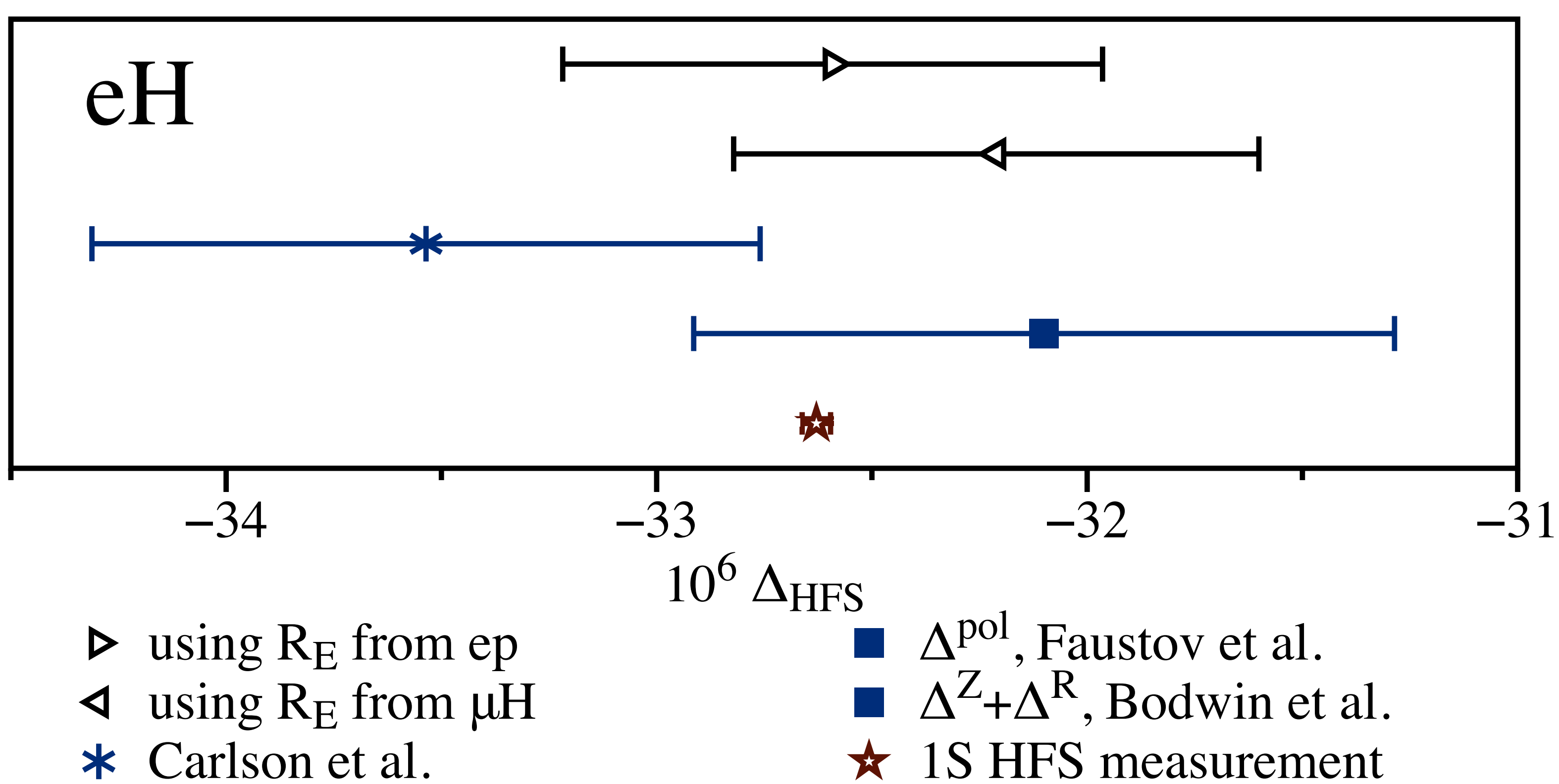

radiative corrections

Eides et al. (2008)
Martynenko et al.

- dispersive evaluation and phenomenological extractions agree

2γ correction in eH 1S HFS

- measurements of 1S HFS in eH (21 cm line):

$$\nu_{\mathrm{HFS}}(\mathrm{H}) = 1420.4057517667(9)\ \mathrm{MHz}$$ 1970th

- accuracy 10^{-12} - precise extraction of TPE

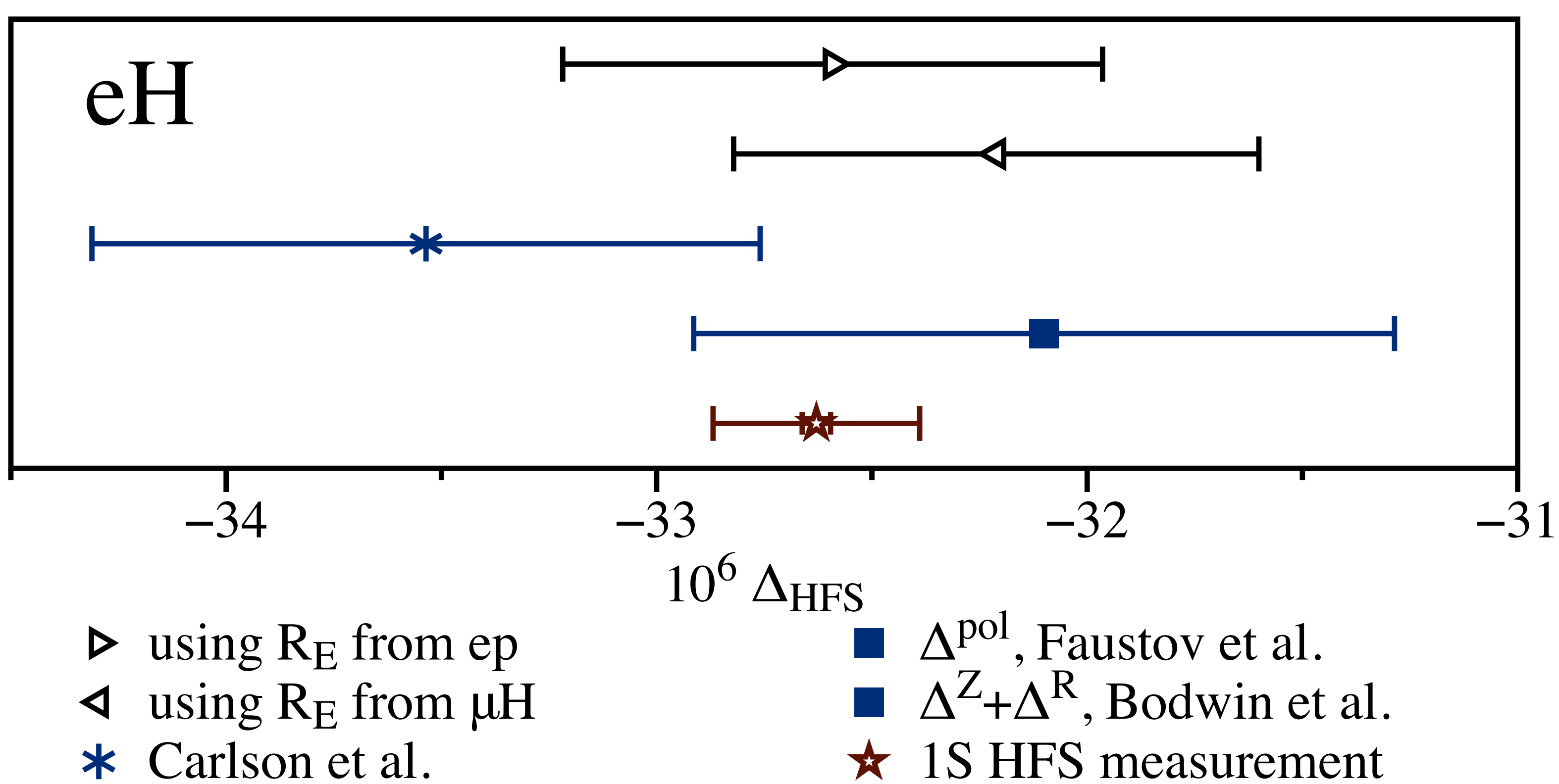

radiative corrections

Eides et al. (2008)
Martynenko et al.

error $\alpha\Delta_{\mathrm{HFS}}$

- dispersive evaluation and phenomenological extractions agree

Connection between eH and μH

- saturation of Q-integrals:

$$\mathrm{R^i} = \frac{\Delta^{\mathrm{i}}(\ Q_{\max})}{\Delta^{\mathrm{i}}} = \int\limits_0^{Q_{\max}} \mathrm{I^i}(Q)\mathrm{d}Q / \int\limits_0^{\infty} \mathrm{I^i}(Q)\mathrm{d}Q$$

Connection between eH and μH

- saturation of Q-integrals:

$$\mathrm{R}^{\mathrm{i}} = \frac{\Delta^{\mathrm{i}}(Q_{\max})}{\Delta^{\mathrm{i}}} = \int_0^{Q_{\max}} \mathrm{I}^{\mathrm{i}}(Q)\mathrm{d}Q \Big/ \int_0^{\infty} \mathrm{I}^{\mathrm{i}}(Q)\mathrm{d}Q$$

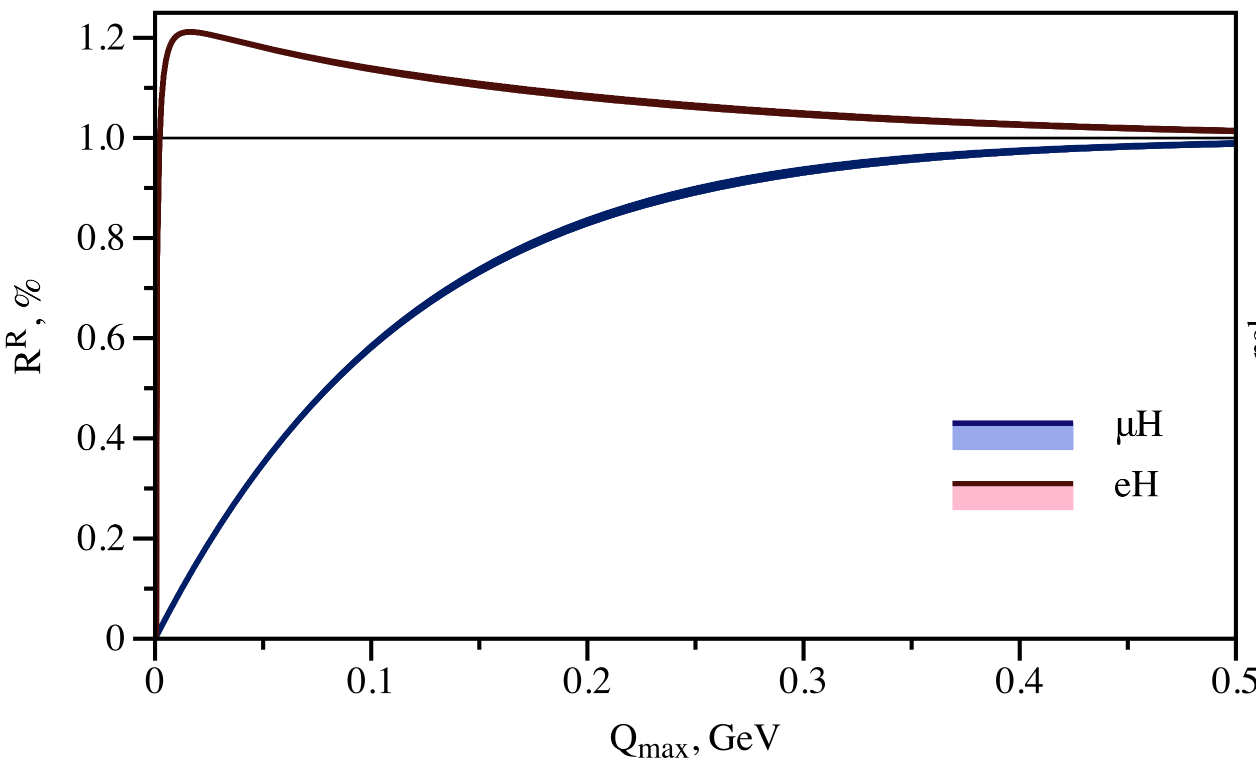

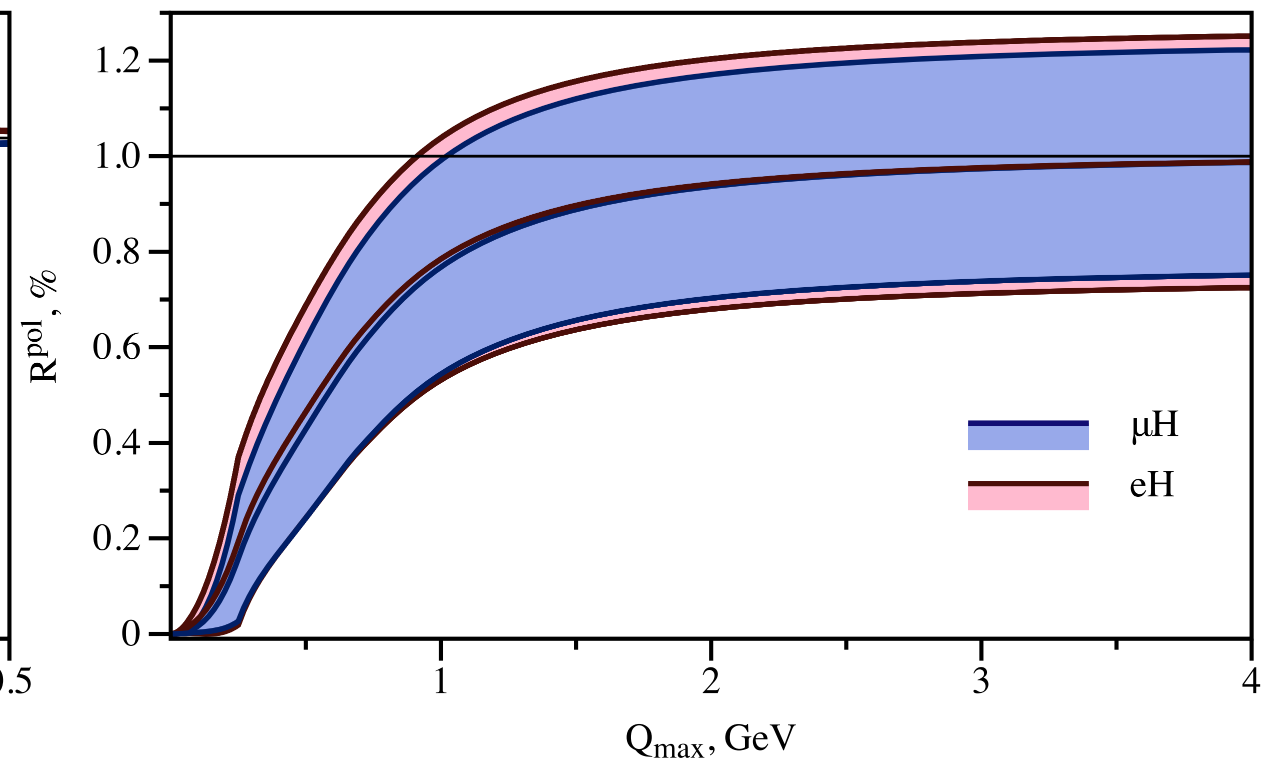

- Zemach correction: proportional to reduced mass

$$\Delta_{\mathrm{Z}} + \Delta^{\mathrm{pol}} \sim m_r$$

Connection between eH and μH

- saturation of Q-integrals:

$$\mathrm{R}^{\mathrm{i}} = \frac{\Delta^{\mathrm{i}}(\ Q_{\max})}{\Delta^{\mathrm{i}}} = \int_0^{Q_{\max}} \mathrm{I}^{\mathrm{i}}(Q)\mathrm{d}Q / \int_0^{\infty} \mathrm{I}^{\mathrm{i}}(Q)\mathrm{d}Q$$

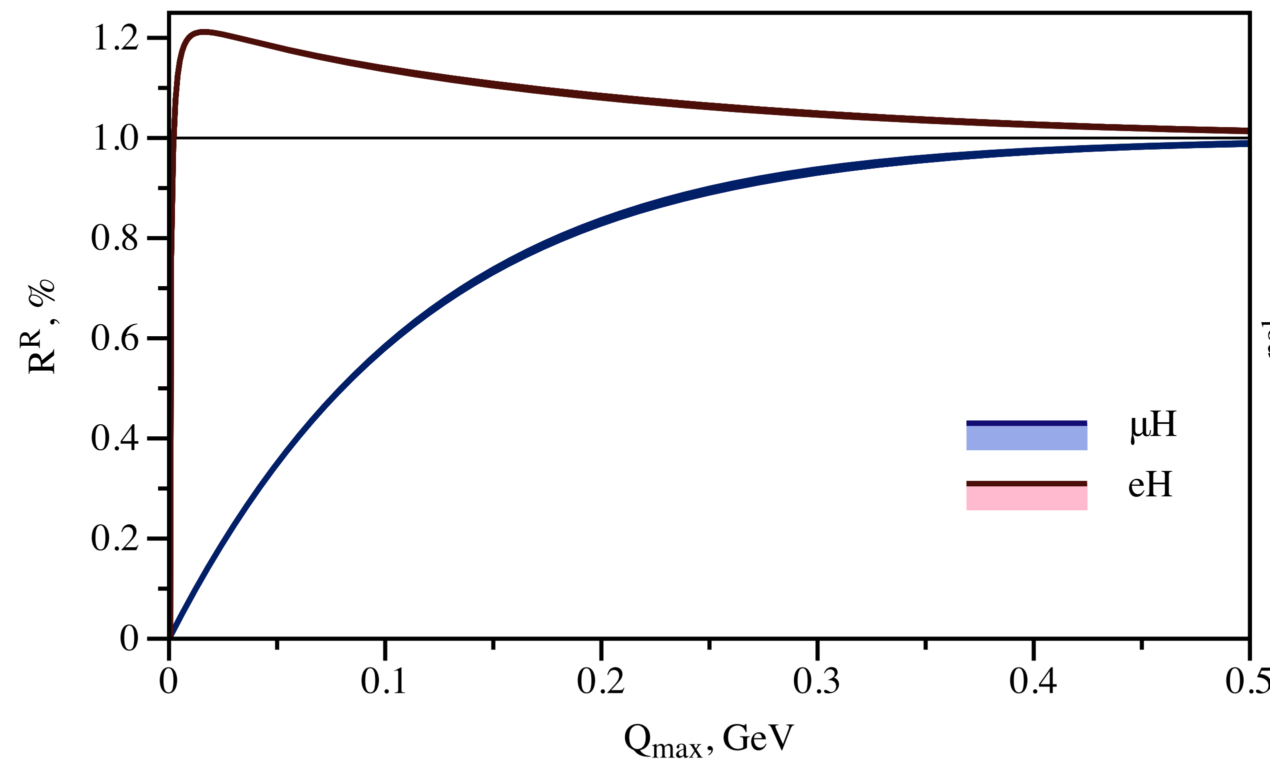

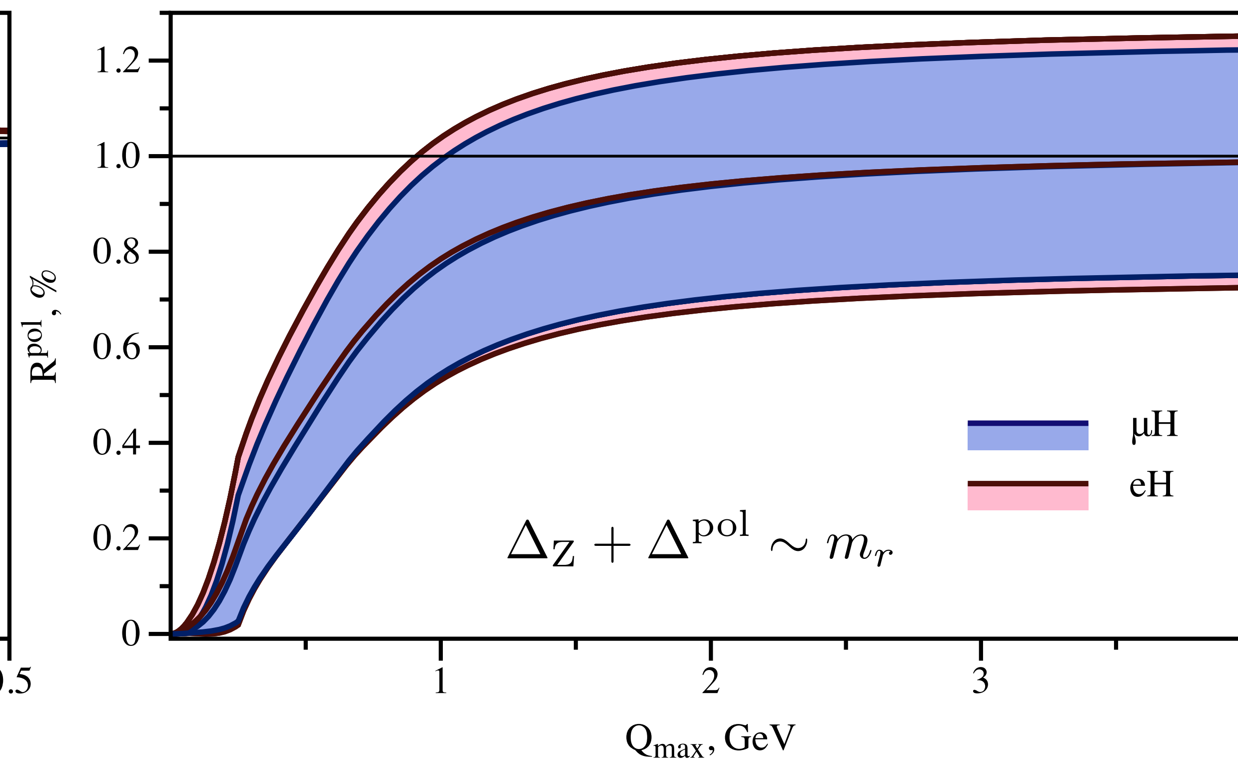

- Zemach correction: proportional to reduced mass

$$\Delta_{\mathrm{HFS}}(\mu\mathrm{H}) = \frac{m_{\mathrm{r}}(m_\mu)}{m_{\mathrm{r}}(m_e)}\Delta_{\mathrm{HFS}}\,(\mathrm{eH}) + \Delta^{\mathrm{th}}_{\mathrm{HFS}}\,(m_\mu) - \frac{m_{\mathrm{r}}(m_\mu)}{m_{\mathrm{r}}(m_e)}\Delta^{\mathrm{th}}_{\mathrm{HFS}}\,(m_e)$$

- Zemach correction vanishes and polarizability term is almost o

2γ correction in μH from eH HFS

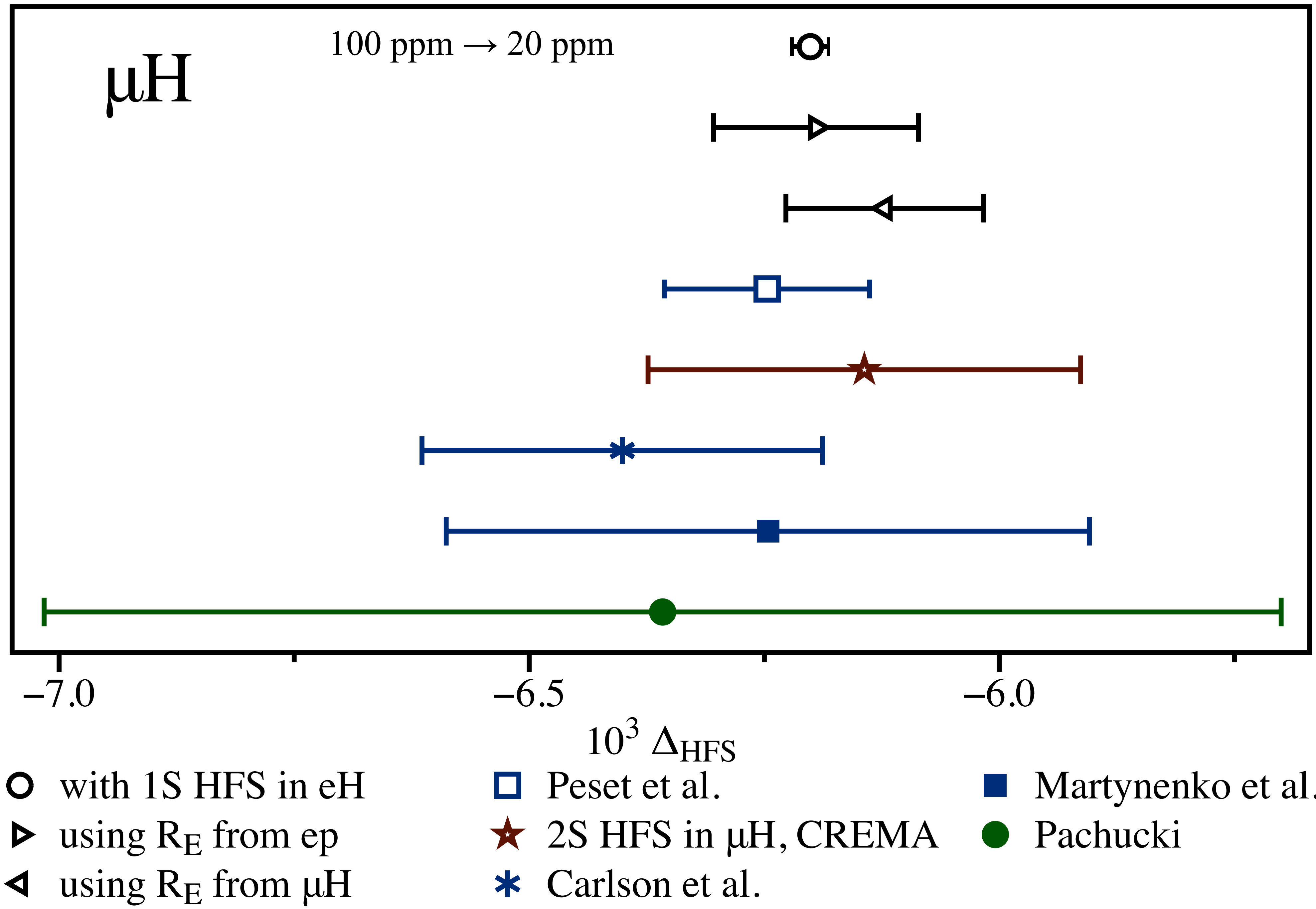

- error of TPE is significantly decreased

2γ correction in μH from eH HFS

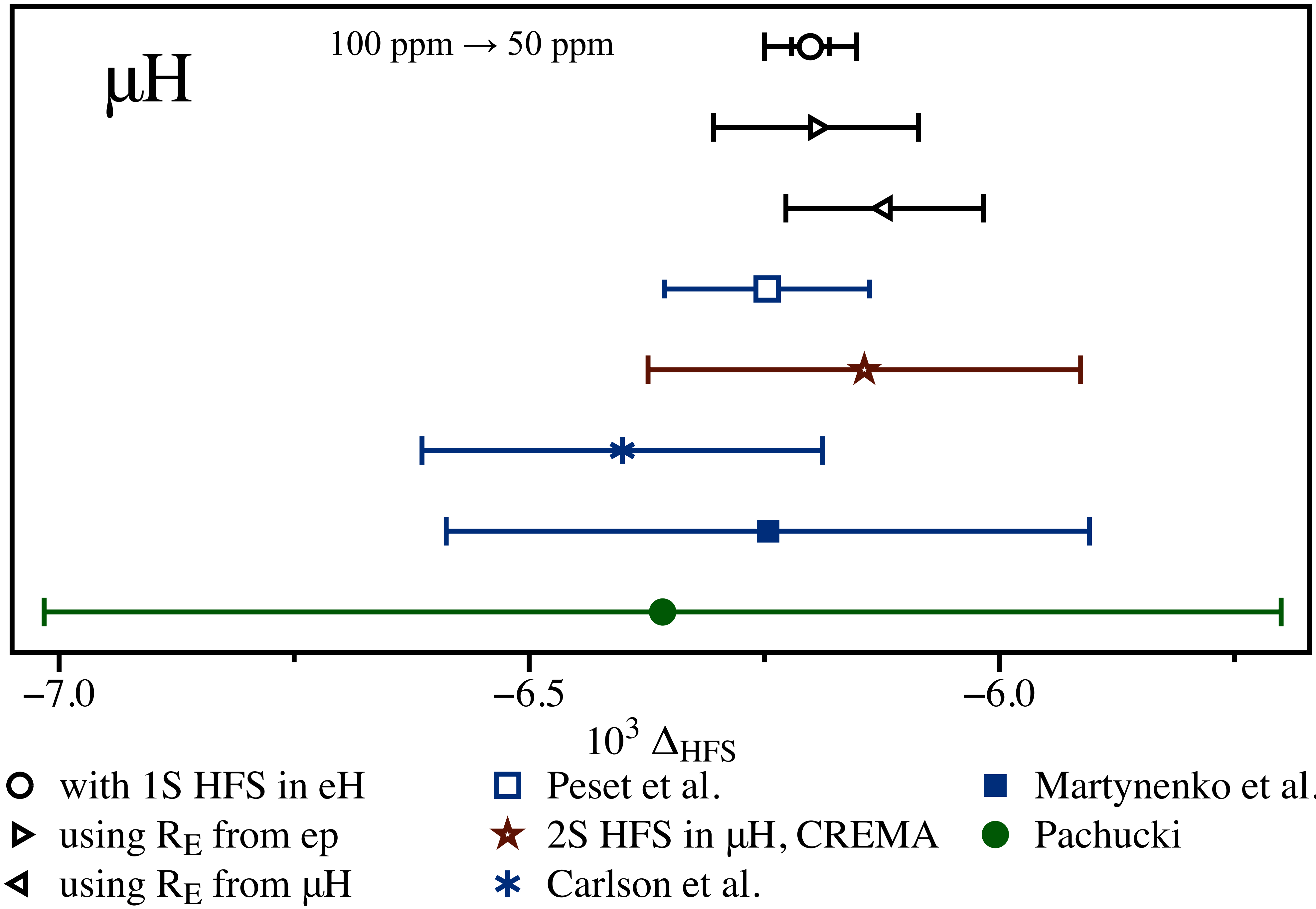

- precise 1S HFS prediction

$$E_{1S}^{HFS} = 182.601 \pm 0.013 \text{ meV}$$

Conclusions

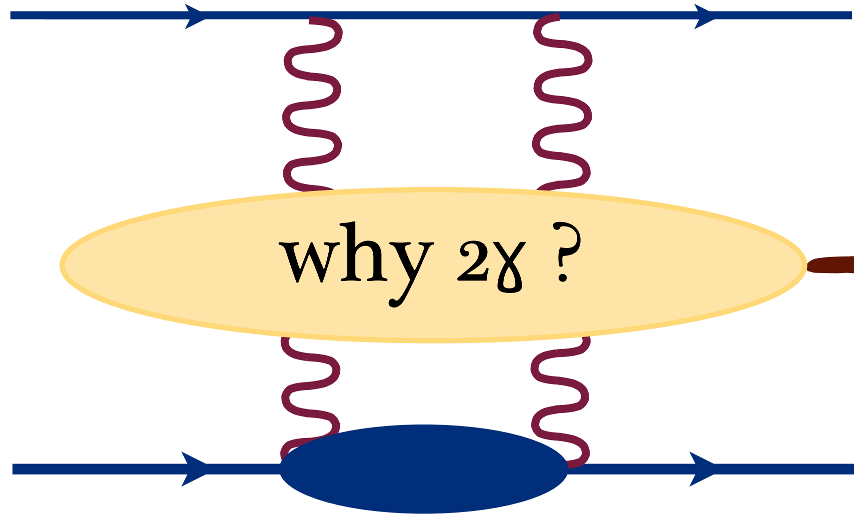

largest theoretical uncertainty in low-energy proton structure

Conclusions

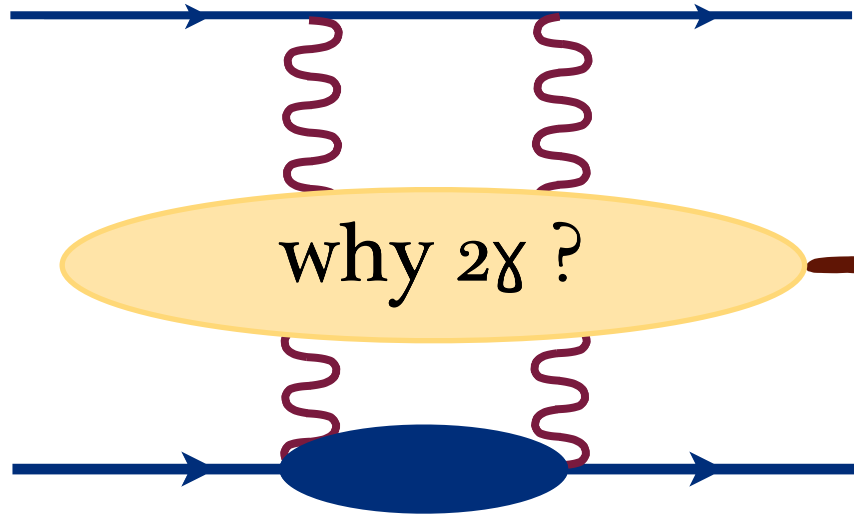

largest theoretical uncertainty in low-energy proton structure

what is achieved ?

- 2γ estimate for MUSE: proton+inelastic states
- dispersive framework and low-Q^2 limit for lp scattering
- scatt. observables and S-level HFS in terms of lp amplitudes
- Zemach radius: 2 times smaller uncertainty
- precise 2γ in μH from 1S HFS in eH

Thanks for your attention !!!